

**A STUDY BETWEEN SHORT- AND LONG-REACH FLOW SIMULATIONS WITH 1D
HYDRODYNAMIC MODEL IN A FLOODPLAIN ENVIRONMENT**

A Thesis by

Sabrina Rashid Sheonty

Roll No. 1018282079

In partial fulfillment of the requirement for the degree of
MASTER OF SCIENCE IN WATER RESOURCES DEVELOPMENT





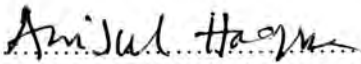

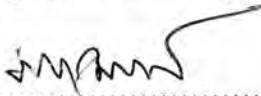
**INSTITUTE OF WATER AND FLOOD MANAGEMENT
BANGLADESH UNIVERSITY OF ENGINEERING AND TECHNOLOGY**

June, 2021

**INSTITUTE OF WATER AND FLOOD MANAGEMENT
BANGLADESH UNIVERSITY OF ENGINEERING AND TECHNOLOGY**

The thesis titled ‘**A Study between Short- and Long-Reach Flow Simulations with 1D Hydrodynamic Model in a Floodplain Environment**’ submitted by Sabrina Rashid Sheonty, Roll No. 1018282079 P, Session October, 2018, has been accepted as satisfactory in partial fulfillment of the requirement for the degree of M.Sc. in Water Resources Development on 19 June, 2021.

BOARD OF EXAMINERS

 Dr. Mohammad Shahjahan Mondal Professor Institute of Water and Flood Management Bangladesh University of Engineering and Technology	Chairman (Supervisor)
 Dr. Mohammad Shahjahan Mondal Director Institute of Water and Flood Management Bangladesh University of Engineering and Technology	Member (Ex-Officio)
 Dr. Mohammad Anisul Haque Professor Institute of Water and Flood Management Bangladesh University of Engineering and Technology	Member
 Dr. Shampa Assistant Professor Institute of Water and Flood Management Bangladesh University of Engineering and Technology	Member
 Dr. Md. Sabbir Mostafa Khan Professor Department of Water Resources Engineering Bangladesh University of Engineering and Technology	Member (External)

CANDIDATE'S DECLARATION

It is hereby declared that this thesis or any part of it has not been submitted elsewhere for the award of any degree or diploma.

.....

Sabrina Rashid Sheonty

Roll No. 1018282079 P

Dedicated to

My beloved parents, the source of all inspirations in my life

Acknowledgement

First of all, the author would like to express her heartfelt gratitude and devotion to the Almighty, who belongs to all admires and has given the chance to complete this study.

The author would like to express her sincere gratitude and regard to her honorable supervisor, Dr. Mohammad Shahjahan Mondal, Professor and Director, Institute of Water and Flood Management (IWFM), Bangladesh University of Engineering and Technology (BUET), for his constant guidance, valuable advice and comment, cordial cooperation, support and inspiration which have been very much beneficial and useful in carrying out this study successfully.

The author expresses her sincere appreciation and gratitude to Dr. Mohammad Anisul Haque, Professor, IWFM, BUET; Dr. Shampa, Assistant Professor, IWFM, BUET; and Dr. Md. Sabbir Mostafa Khan, Professor, Department of Water Resources Engineering, BUET, for their kind reviews, comments and suggestions, which helped to improve the quality this thesis.

The author would like to thank Mr. Md. Rashedul Islam, Assistant Professor, Institute of Water and Flood Management, BUET for his valuable suggestions to make the thesis work interesting.

The author would love to take this opportunity to express her heartfelt thanks to her parents and family members for their inspiration and moral support they provided during this study.

Abstract

Bangladesh is a floodplain deltaic country. There are around 700 rivers in the country with an extensive seasonally flooded floodplain. For proper management of these rivers and the natural resources of the floodplains, it is important to understand the hydrodynamic behavior of the rivers. The Atrai River is such a river where river-floodplain interaction is very prominent. Thus, in this study the Atrai River is chosen as the study river and the hydrodynamic parameters of this river are simulated with the HEC-RAS one-dimensional (1D) model. Moreover, in our country both long- and short-reach HEC-RAS models are being used extensively. However, there has been no study to compare the performances of these models. In this context, the main focus of this study was to setup two short- and one long-reach HEC-RAS 1D models for the Atrai River – the setup with 106 km reach of the river is regarded as the long-reach model and the two setups with 6 km reach each in the upstream and downstream of the river are regarded as the short-reach models. The main objective of this study was to compare the performance of these models with both steady and unsteady flow modules. For this study, all necessary data were collected from LGED, BWDB, USGS website and Google Earth. Hydrodynamic parameters were simulated for the flood season of the years 1998, 2006, 2014 and 2018 using different boundary conditions. The long-reach model was calibrated for 2013 and validated for 2016. The calibrated Manning's roughness coefficient 'n' was 0.025 for the main channel and 0.030 for the floodplain. The long-reach model results were evaluated based on six performance evaluation criteria (RMSE, MAE, RMAE, Relative bias, Co-efficient of determination, Efficiency index). The RMSE values for the unsteady flow module of the years 1998, 2006, 2014 and 2018, it was found that the long-reach model performed best at 2014. Finally, a comparative analysis of the model results was done to identify the suitability of the short- and long-reach models for hydrodynamic simulation in the floodplain environment. According to the results of the study for different boundary conditions, the performance of short-reach model was found better in the floodplain environment than the long-reach model. The possible reason behind it is that the fluctuation of water level due to river-floodplain interaction is more significant in the long-reach model, which cannot be captured well. Moreover, the unsteady flow module was found to produce better result than the steady flow module in both short- and long-reach models. Another finding was that the long-reach model with storage areas performed better in earlier years of 1998 and 2006, but the model without storage areas performed better in recent years of 2014 and 2018. The possible reason can be the increasing settlement or construction of embankments or roads surrounding the river. The study has broadened the understandings of hydrodynamic simulations with 1D model in floodplain environment. The results can help water development authorities, hydrodynamic modelers and water professionals in choosing model reach while quantifying flood parameters and designing hydraulic interventions at different locations of a river in floodplain environment.

Table of Contents

Content	Page no.
Acknowledgement	v
Abstract	vi
List of Tables	xi
List of Figures	xii
List of Abbreviations and Acronyms	xv
Chapter 1: Introduction	1
1.1 General	1
1.2 Background of the Study	4
1.3 Objectives of the Study	5
1.4 Importance and Limitations of the Thesis	5
1.5 Organization of the Thesis	6
Chapter 2: Literature Review	7
2.1 General	7
2.2 Studies on Hydrodynamic Modelling in the World	7
2.2.1. Studies using HEC-RAS	7
2.2.2. Studies using other software except HEC-RAS	12
2.3 Studies on Hydrodynamic Modelling in Bangladesh	16
2.3.1. Studies using HEC-RAS	16
2.3.2. Studies using other softwares except HEC-RAS	18
Chapter 3: Study Area and Model Description	21
3.1 General	21
3.2 Study Area	21
3.2.1 Location	21
3.2.2 Upazilas under study area	22
3.2.3 Navigability of the Atrai River	25
3.3 Hydrodynamic Modeling Approach	25
3.4 Hydrodynamic Modeling Using HEC-RAS	25
3.4.1 Analysis components of HEC-RAS	26

3.4.2 User interface and parameters of HEC-RAS	29
3.4.3 Steps for analysis in HEC-RAS	30
3.5 Basic Equations of Hydrodynamic Modelling	31
3.5.1 Steady flow equations	31
3.5.2 Unsteady flow equations	35
Chapter 4	38
Data Collection and Methodology	38
4.1 General	38
4.2 Data Collection	38
4.2.1 Cross-section data	38
4.2.2 Discharge and water level data	38
4.2.3 DEM data	39
4.3 Model Preparation	39
4.3.1 Drawing of the left and right banks in Google Earth	39
4.3.2 Georeferencing of the river-banks using ArcGIS	40
4.3.3 Marking of cross-section location from Google Earth	40
4.3.4 Estimation of reach lengths	41
4.3.5 River-bank data extraction from AutoCAD	41
4.3.6 Slope analysis	41
4.3.7 Rating curve development	41
4.3.8. Adjustment of DEM	44
4.3.9 Conversion of adjusted DEM to Triangulated Irregular Network	48
4.3.10 Storage area identification	50
4.4 Model Set Up	50
4.4.1 Geometric data input	51
4.4.2 Flow data input	51
4.5 Flow Simulation with Model	53
4.6 Model Calibration and Validation	54
Chapter 5: Results and Discussions	56
5.1 General	56
5.2 Long-Reach Model Simulation Results	56
5.2.1 Long-reach model result for 1998	56

5.2.2 Long-reach model result for 2006	58
5.2.3 Long-reach model result for 2014	60
5.2.4 Long-reach model result for 2018	62
5.2.5 Long-reach model performance evaluation	64
5.3 Comparison of Downstream Short-Reach Model and Long-Reach Model Using WL as Downstream Boundary Condition	70
5.3.1 Comparison for 1998	70
5.3.2 Comparison for 2006	70
5.3.3 Comparison for 2014	71
5.3.4 Comparison for 2018	71
5.4 Comparison of Upstream Short-Reach Model and Long-Reach Model Using WL as Downstream Boundary Condition	73
5.4.1 Comparison for 1998	73
5.4.2 Comparison for 2006	74
5.4.3 Comparison for 2014	74
5.4.4 Comparison for 2018	74
5.5 Comparison of Downstream Short-Reach Model and Long-Reach Model Using Normal Depth as Boundary Condition	77
5.5.1 Comparison for 1998	77
5.5.2 Comparison for 2006	78
5.5.3 Comparison for 2014	78
5.5.4 Comparison for 2018	78
5.6 Comparison of Upstream Short-Reach Model and Long-Reach Model Using Normal Depth as Downstream Boundary Condition	81
5.6.1 Comparison for 1998	81
5.6.2 Comparison for 2006	81
5.6.3 Comparison for 2014	81
5.6.4 Comparison for 2018	82
5.7 Comparison of Model Results with and without Storage Areas	85
5.7.1 Comparison for 1998	85
5.7.2 Comparison for 2006	87
5.7.3 Comparison for 2014	90
5.7.4 Comparison for 2018	92

Chapter 6: Conclusions and Recommendations	95
6.1 General	95
6.2 Conclusions	95
6.3 Recommendations	97
Reference	98

List of Tables

Table 5.1: Model evaluation for 1998 using RMSE value (m).....	65
Table 5.2: Model evaluation for 1998 using MAE value (m).....	65
Table 5.3: Model evaluation for 1998 using RMAE value (m).....	66
Table 5.4: Model evaluation for 1998 using R^2 value	66
Table 5.5: Model evaluation for 1998 using Relative Bias value.....	66
Table 5.6: Model evaluation for 1998 using Efficiency Index value	66
Table 5.7: Model evaluation for 2006 using RMSE value (m).....	66
Table 5.8: Model evaluation for 2006 using MAE value (m).....	67
Table 5.9: Model evaluation for 2006 using RMAE value (m).....	67
Table 5.10: Model evaluation for 2006 using R^2 value	67
Table 5.11: Model evaluation for 2006 using Relative Bias value.....	67
Table 5.12: Model evaluation for 2006 using Efficiency Index value	67
Table 5.13: Model evaluation for 2014 using RMSE value (m).....	67
Table 5.14: Model evaluation for 2014 using MAE value (m).....	68
Table 5.15: Model evaluation for 2014 using RMAE value (m).....	68
Table 5.16: Model evaluation for 2014 using R^2 value	68
Table 5.17: Model evaluation for 2014 using Relative Bias value.....	68
Table 5.18: Model evaluation for 2014 using Efficiency Index value	68
Table 5.19: Model evaluation for 2018 using RMSE value (m).....	69
Table 5.20: Model evaluation for 2018 using MAE value (m).....	69
Table 5.21: Model evaluation for 2018 using RMAE value (m).....	69
Table 5.22: Model evaluation for 2018 using R^2 value	69
Table 5.23: Model evaluation for 2018 using Relative Bias value.....	69
Table 5.24: Model evaluation for 2018 using Efficiency Index value	69

List of Figures

Figure 1.1: Flood inundation map of Bangladesh at October 4, 2020 (FFWC, 2020)	2
Figure 3.1: The study area	22
Figure 3.2: Upazilas of the study area	23
Figure 3.3: Schematic diagram of the models for the study river.....	24
Figure 3.4: Diagram showing the energy equations terms	32
Figure 3.5: HEC-RAS default conveyance subdivision method for the left and the right overbank	33
Figure 3.6: Example of how mean energy is obtained weighting coefficient alpha.....	34
Figure 3.7: Elementary control volume for derivation of continuity and momentum equations .	36
Figure 3.8: Illustration of terms associated with definition of pressure force	37
Figure 4.1: River-banks of the Atrai River from Google Earth.....	39
Figure 4.2 : Georeferencing of study area using ArcMap 10.2.2	40
Figure 4.3: Rating curve for station 144	42
Figure 4.4: Rating Curve for station 145	42
Figure 4.5: Rating Curve for station 147	43
Figure 4.6: Rating Curve for station 147.5	43
Figure 4.7: DEM of the study area.....	45
Figure 4.8: Modified DEM of the study area.....	47
Figure 4.9: TIN of the study area.....	49
Figure 4.10: Identification of storage areas from Google Earth	50
Figure 4.11: Flow hydrograph in unsteady flow simulation for 2016	52
Figure 4.12: Stage hydrograph in unsteady flow simulation of 2016.....	53
Figure 4.13: Calibration using 2013 flood year	54
Figure 4.14: Validation using 2016 flood year	55
Figure 5.1: Comparison of WL of 1998 for station 144	57
Figure 5.2: Comparison of WL of 1998 for station 145	57
Figure 5.3: Comparison of WL of 1998 for station 147	58
Figure 5.4: Comparison of WL of 2006 for station 144	59
Figure 5.5: Comparison of WL of 2006 for station 145	59
Figure 5.6: Comparison of WL of 2006 for station 147	60
Figure 5.7: Comparison of WL of 2014 for station 144	61
Figure 5.8: Comparison of WL of 2014 for station 145	61
Figure 5.9: Comparison of WL of 2014 for station 147	62
Figure 5.10: Comparison of WL of 2018 for station 144	63
Figure 5.11: Comparison of WL of 2018 for station 145	63
Figure 5.12: Comparison of WL of 2018 for station 147	64
Figure 5.13: Comparison of WL of short- and long-reach model at station 147 for 1998 using downstream WL as boundary condition.....	71
Figure 5.14: Comparison of WL of short- and long-reach model at station 147 for 2006 using downstream WL as boundary condition.....	72

Figure 5.15: Comparison of WL of short- and long-reach model at station 147 for 2014 using downstream WL as boundary condition.....	72
Figure 5.16: Comparison of WL of short- and long-reach model at station 147 for 2018 using downstream WL as boundary condition.....	73
Figure 5.17: Comparison of WL of short- and long-reach model at station 144 for 1998 using downstream WL as boundary condition.....	75
Figure 5.18: Comparison of WL of short- and long-reach model at station 144 for 2006 using downstream WL as boundary condition.....	76
Figure 5.19: Comparison of WL of short- and long-reach model at station 144 for 2014 using downstream WL as boundary condition.....	76
Figure 5.20: Comparison of WL of short- and long-reach model at station 144 for 2018 using downstream WL as boundary condition.....	77
Figure 5.21: Comparison of WL of short- and long-reach model at station 147 for 1998 using normal depth as boundary condition	79
Figure 5.22: Comparison of WL of short- and long-reach model at station 147 for 2006 using normal depth as boundary condition	79
Figure 5.23: Comparison of WL of short- and long-reach model at station 147 for 2014 using normal depth as boundary condition	80
Figure 5.24: Comparison of WL of short- and long-reach model at station 147 for 2018 using normal depth as boundary condition	80
Figure 5.25: Comparison of WL of short- and long-reach model at station 144 for 1998 using normal depth as boundary condition	82
Figure 5.26: Comparison of WL of short- and long-reach model at station 144 for 2006 using normal depth as boundary condition	83
Figure 5.27: Comparison of WL of short- and long-reach model at station 144 for 2014 using normal depth as boundary condition	83
Figure 5.28: Comparison of WL of short- and long-reach model at station 144 for 2018 using normal depth as boundary condition	84
Figure 5.29: Comparison of model with and without storage area for station 144 in 1998	85
Figure 5.30: Comparison of model with and without storage area for station 145 in 1998	86
Figure 5.31: Comparison of model with and without storage area for station 147 in 1998	86
Figure 5.32: Comparison of model with and without storage area for station 147.5 in 1998	87
Figure 5.33: Comparison of model with and without storage area for station 144 in 2006	88
Figure 5.34: Comparison of model with and without storage area for station 145 in 2006	88
Figure 5.35: Comparison of model with and without storage area for station 147 in 2006	89
Figure 5.36: Comparison of model with and without storage area for station 147.5 in 2006	89
Figure 5.37: Comparison of model with and without storage area for station 144 in 2014	90
Figure 5.38: Comparison of model with and without storage area for station 145 in 2014	91
Figure 5.39: Comparison of model with and without storage area for station 147 in 2014	91
Figure 5.40: Comparison of model with and without storage area for station 147.5 in 2014	92
Figure 5.41: Comparison of model with and without storage area for station 144 in 2018	93
Figure 5.42: Comparison of model with and without storage area for station 145 in 2018	93
Figure 5.43: Comparison of model with and without storage area for station 147 in 2018	94

Figure 5.44: Comparison of model with and without storage area for station 147.5 in 2018 94

List of Abbreviations and Acronyms

1D	One-Dimensional
2D	Two-Dimensional
ArcGIS	Arc Geographic Information System
BDP	Bangladesh Delta Plan
BWDB	Bangladesh Water Development Board
BUET	Bangladesh University of Engineering and Technology
CEGIS	Center for Environmental and Geographic Information Services
DDM	Department of Disaster Management
DEM	Digital Elevation Model
DL	Danger Level
DM&RD	Disaster Management and Relief Division
FAP	Flood Action Plan
FCDI	Flood Control, Drainage and Irrigation
FFWC	Flood Forecasting and Warning Centre
FRERMIP	Flood and Riverbank Erosion Risk Management Investment Program
GBM	Ganges- Brahmaputra- Meghna
GED	General Economics Division
GIS	Geographic Information System
GoB	Government of Bangladesh
GUI	Graphical User Interface
HD	Height of the Embankment
HEC	Hydrologic Engineering Center
HEC-RAS	Hydrologic Engineering Centre-River Analysis System
IPCC	Intergovernmental Panel on Climate Change
IWFM	Institute of Water and Flood Management
IWM	Institute of Water Modelling
m ³ /s	Cubic meter per second
MDD	Mean Daily Discharge
MODIS	Moderate Resolution Imaging Spectroradiometer

NASA	National Aeronautics and Space Administration
NHC	Northwest Hydraulic Consultants
NSE	Nash-Sutcliffe Efficiency
PWD	Public Works Datum
R^2	Coefficient of Determination
RAS	River Analysis System
RMSE	Root Mean Square Error
RS	Remote Sensing
SI	International System of Units
SW	South-West
TIN	Triangular Irregular Networks
UNDRO	United Nations Disaster Relief Organization
USACE	United States Army Corps of Engineers
WARPO	Water Resources Planning Organization

Chapter 1: Introduction

1.1 General

Bangladesh is a floodplain deltaic country formed by the deposits of the three major river systems of the Ganges, Brahmaputra-Jamuna, and Meghna Rivers. It is one of the most floodplain-dominated countries in the world with a population density of 1265 per km² (Worlometer, 2020). Including tributaries and distributaries there are around 700 rivers in Bangladesh stretching over 24,140 km, thousands of smaller channels, floodplain depressions (known as beels), and extensive seasonally flooded lands that collectively form the floodplain ecosystems (Akonda, 1989). Estimates of the area of floodplain in Bangladesh range up to 80% (Brammer, 1990). About 25% to 33% of the country remains under water every year for four to six months during the monsoon (Sultana et al, 2017).

In the year 2017, major flooding hit Bangladesh. Almost half (42%) of the country was under water (FFWC, 2018). In 2020, the monsoon flood had a significant impact on the Northern, North-Eastern and South-Eastern region of Bangladesh. Figure 1.1 shows the recent flood inundation map of the year of 2020 prepared by FFWC, BWDB. Riverine floods in northern part of Bangladesh creates infrastructures damages, including physical damages to agricultural crops, buildings and other infrastructures, social disruptions in vulnerable groups, livelihoods and local institutions, and direct and indirect economic losses. The majority of flood disaster's victims are poor people, who suffer most and are the first casualty of such incidents (WWAP, 2006). The floods have impacted 30 districts of Bangladesh with moderate to severe impact on 15 Districts. 1022 unions from 158 upazila have been inundated by flood water, affecting 5.4 million people and leaving 1,059,295 families water logged. The Monsoon floods coupled with prolonged inundation and the COVID-19 pandemic has an exacerbating effect on the flood affected people. As per DGHS control room, 135 people has already lost their life, mostly as a result of drowning is the major cause of the death and among drowned death about 70% are child since 30th June 2020 (Humanitarian Response, 2020).

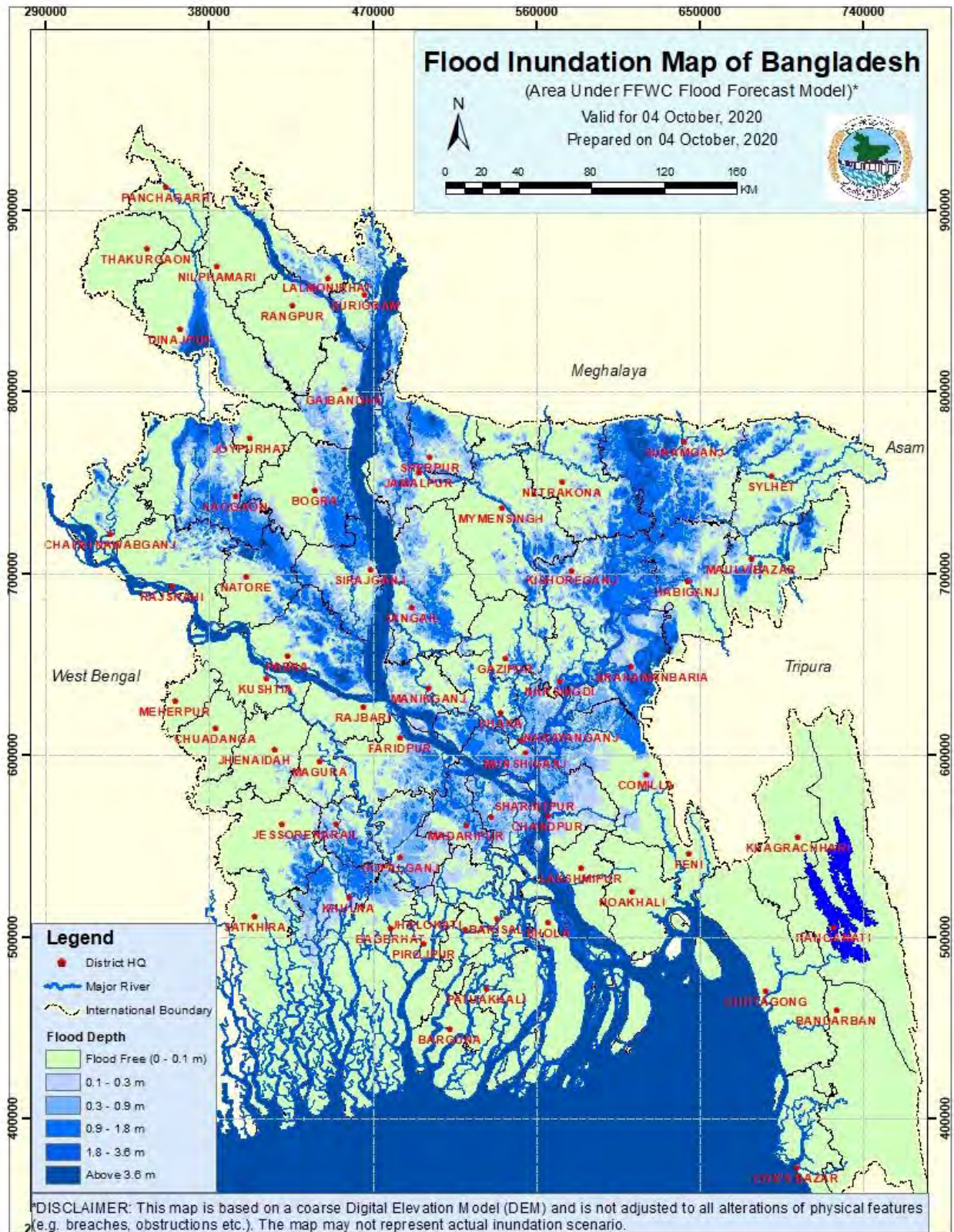


Figure 1.1: Flood inundation map of Bangladesh at October 4, 2020 (FFWC, 2020)

Several structural interventions such as embankments, revetments, bridges, levee, regulator, groyne are frequently constructed on the river to control the flood and other purposes. For construction and management of these structural interventions, understanding the hydrodynamic behavior of rivers is really important. Without assessment of proper hydrodynamic parameters of river, these flood protection structures can be damaged or failed. It can cause significant economic losses. For example, in 2020, many flood protection infrastructures such as dykes and embankments were damaged from previous monsoon floods along with the current floods. 220 unions reported having their embankments damaged during this time. The normal recovery cycle after a disaster is 3-5 years but due to back-to-back floods (2016, 2017, 2019) in affected areas this recovery cycle is hampered. This also compromises the repair and reconstruction of the infrastructures, which is further constrained by the COVID-19 pandemic. These unrepaired and unmaintained infrastructures can be dangerous in future (Humanitarian Response, 2020).

For reducing the huge cost associated with the damage of these structural interventions, hydrodynamic modelling of rivers is really important. Hydrodynamic modelling approach has become popular in recent years for estimating the flood levels and damage estimation as it provides the basis for the decision making of flood risk management. So hydrodynamic models are used in different rivers to simulate flood inundation extent and depths at different sections of the studied flood rivers. From the model simulation results, flood phenomenon can be studied and analyzed well. (UKEssays, 2018). Hydrodynamic modelling approach is very important for assessing the actual condition of various river processes and for reliable prediction of complex situation found in nature. These hydrodynamic models are also necessary to manage the floodplain resources properly. There are several modeling software which can be used for hydrodynamic modelling of a river reach. Some of them are: HEC-RAS, MIKE 11, MIKE 21C, MIKE SHE, MIKE Flood, Delf 3D etc. Among these software, HEC-RAS is comparatively easy to operate and also provides good results.

1.2 Background of the Study

There are many important rivers in Northern part of Bangladesh which are really important in the context of agriculture and industry. There are several important structures in this region of Bangladesh such as Teesta barrage, Hardinge bridge, Bangabandhu bridge etc. Apart from that, there are several embankments, levees, dykes over the rivers of the region which are under construction to control flood. But for proper design of these structures, the hydrodynamic parameters are must. Without the proper assessment of these parameters and flood levels, the design of the structures will be faulty. If they are damaged or failed for such reasons, it will cause significant social and economic loss. As these rivers are very important in the socio-economic context of the country and this zone is very vulnerable in terms of flood hazard, there is no alternative of proper hydrodynamic study of the rivers. Hydrodynamic modelling approach is a popular method for conducting this type of studies.

As mentioned earlier, the 2017 and 2020 floods created catastrophic effects on North-eastern part of Bangladesh. In 2017 at Northern zone, the historic record was broken by crossing the danger levels in several stations of many tributaries of the Brahmaputra-Jamuna river systems such as Bahdurabad in Jamuna, Mohadevepur in Atrai, Badarganj in Jamuneswari, Kurigram in Dharala and Dalia in the Teesta. (Rahman, 2017). During middle of August, water in the Atrai River was currently 214 cm above the danger level. Dams are breached in more than 100 villages across the district. Ten villages were flooded near the Dhamirhat border after the Atrai River broke through dams in the area (Islam, 2017). In order to analyze the flood level on different stations of the Atrai River and construct structures on it to control flood, proper hydrodynamic study of this river is a prerequisite.

In this context, for flood protection and proper construction of structural interventions, study regarding hydrodynamic behavior of the Atrai River is extremely important. Thus, this study attempts to assess the hydrodynamic behavior of the Atrai River. This river is one of the most important rivers in Northern part of Bangladesh where river-floodplain interaction is significant as well. Thus, the Atrai River reach is chosen as the study area to model with several one dimensional (1D) hydrodynamic models using HEC-RAS software. The Atrai River floodplain environment is modelled with both short- and long-reach flow models to understand the best suited hydrodynamic model that can precisely estimate the hydrodynamic parameters of the river. Finally, a comparison between the results of short- and long-reach flow simulations is shown and more suitable model is identified for such river system. The outcome of the study will be helpful to select better suited model to analyze hydrodynamic parameter in a floodplain environment.

1.3 Objectives of the Study

This study mainly focuses to set up three 1D short- and long-reach hydrodynamic models for the Atrai River reach and identify the better suited model set up for this river system. In another words, this study is divided into two specific parts or objectives.

The two objectives of this study are stated in the following.

- i. To setup long- and short-reach hydrodynamic models of the Atrai River and to estimate hydraulic parameters along the river for different years using both steady and unsteady flow modules and compare them with standard criteria;
- ii. To compare the short- and long-reach model performances under steady and unsteady flow conditions and different types of boundary conditions.

1.4 Importance and Limitations of the Thesis

The importance of the study is significant in terms of the socio-economic important associated with the Atrai River or the study area. Firstly, this study estimates the hydraulic parameters like water levels of the Atrai River in floodplain environment by analysing the hydrodynamic behavior of the river in four different flood years such as 1998, 2006, 2014 and 2018.

Secondly, the models are calibrated and validated for the year of 2016. This calibrated model can help water development authorities to quantify flood parameters at different locations of the Atrai River for flood forecasting. The estimation of hydraulic parameters will also help to design and maintain different structural interventions in this floodplain environment in an efficient way.

Finally, this study also identifies the suitability of the short- and long-reach models for hydrodynamic analysis in floodplain environment of Bangladesh. It will help to select the better suited model set up for precise analysis of hydrodynamic behavior of such rivers in the future studies.

Moreover, there are some limitations of the study as well. Firstly, the rating curves used in this study were assumed as linear. Non-linear curves can be assumed for more accuracy in this case.

Secondly, the model didn't consider any contribution of rainfall. Along with this hydrodynamic model, a hydrologic rainfall runoff model could have been done for achieving more accuracy in predicting water levels.

1.5 Organization of the Thesis

Chapter 1 is the introduction, background and objectives of the thesis work of the study.

Chapter 2 provides detail literature review with the background of previous studies on similar topic.

Chapter 3 explains the study area and theory and background of models.

Chapter 4 explains the methodology of the study.

Chapter 5 presents the summary of results and discussions. These results are being discussed in such a way that the reader can more easily follow the discussion related to each part of the results.

Chapter 6 presents some conclusions of the study and provide some necessary recommendations for future studies.

Chapter 2: Literature Review

2.1 General

There are many studies regarding hydrodynamic modelling of rivers in different parts of the world. Bangladesh, being a riverine country, numerous studies on different rivers were conducted here. Many investigations and researches have been done on this topic by adopting modern technology. In recent years, hydrodynamic modelling approach has gained much popularity in this context. Apart from Bangladesh, huge number of studies have been carried out all through the world with the method of hydrodynamic modelling. Some of these researches have been summarized in this chapter on various river of the world. Special focus has been given on the studies where HEC-RAS model was used.

2.2 Studies on Hydrodynamic Modelling in the World

Different models were used to study the hydrodynamic behaviour of different rivers in different parts of the world. In recent years, hydrodynamic models have gained popularity among the researchers in both flood forecasting and damage estimation as it provides the basis for the decision making of flood risk management. These models are mainly used to simulate flood inundation extent and depths at different sections of the studied flood rivers. Modelling approach is very necessary for assessing the actual condition of various river processes and for reliable prediction of complex situation found in nature. There can be many modeling software to simulate a river model. Some of them are HEC-HMS, MIKE 11, MIKE 21C, MIKE SHE, MIKE Flood, Delf 3D, HEC-RAS, HEC-GeoRAS.

2.2.1. Studies using HEC-RAS

Among all the software used for hydrodynamic modelling, HEC-RAS is one of the most frequently used software for hydrodynamic analysis. One of the main causes of its high usage is that it is comparatively easy to operate. Moreover, it is available at no cost where some of the other software like MIKE 11, MIKE 21C etc. are quite expensive. HEC-RAS model can be used to simulate floodplain, sediment and sediment transport, water quality, dam break, blocking bridges, scour phenomenon, and ice-covered river. Thus, different studies are conducted using HEC-RAS around the globe. In this section, some of the studies are explained.

In this study, the Atrai River of Bangladesh is modelled in 1D HEC-RAS model. A similar study has been conducted in Malaysia where 1D hydrodynamic model was developed for Pahang River

using HEC-RAS 5.0. Combinations of surveyed data with spatial-extracted cross sections and recorded stream flow were used in this study. The study area had been hit by several extreme floods that caused substantial property damages and loss of lives. This study focused on the 2007 and 2014 flood events. Analyses of water levels, stream discharges and river cross sections were carried out based on the data gathered. A set of flood levels were obtained as the outputs of the hydraulic model and the accuracy of the simulated flood levels were validated. It was found that the model predicts a good output agreement with $R^2 = 0.96$ and $R^2 = 0.82$ for the 2007 and 2014 flood events respectively (Zainalfikry et al, 2020).

In another study, some different approach was seen in 1D hydrodynamic flood modelling of Purna river in Navasari city of Gujarat, India. This study was conducted using HEC-RAS with special reference to geospatial techniques. This study aimed to demonstrate the geospatial analyzing capabilities of HEC-RAS version 5. For the purpose of flood modeling, the river data such as bank lines, flow path lines, cross-section cut lines are extracted from Cartosat-1 DEM. Steady flow analysis was carried out for the simulation of a 1D hydrodynamic model. The outcome obtained from the model was in the form of water depth, which can be observed in the geospatial HEC-RAS mapper window. The flood depth maps for the 2002 and 2004 flood events were generated, which indicated that the low-lying areas of Navsari city near Jalalpore and Viraval were susceptible to flooding when the discharge in the river exceeds $8836 \text{ m}^3/\text{s}$. The accuracy of the model was calculated by comparing the simulated data with the observed data for the above-mentioned flood events. The results obtained from the 1D models were found promising and accurate (Pathan et al, 2020).

Some 2D HEC-RAS models have been also developed in recent studies with some other objectives where this study of Atrai River focused mainly on the comparison of one-dimensional short- and long-reach model types. But in future, 2D modelling approach can be adopted as well with other sets of objectives. Some examples of 2D modelling approach are discussed here. In a study at Italy, the main purpose of the work was set to assess the potential and the capabilities of the 2D HEC-RAS model in rainfall-runoff simulations at the basin scale, comparing the results obtained using both fully dynamic equations and diffusion wave equations to the simulations obtained by using a 2D fully dynamic model with version 5.0.7. The HEC-RAS model had been enriched with novel modules, performing fully 2D computations based on the 2D fully dynamic equations as well as the 2D diffusion wave equations. So, in this study, two models were prepared and both models were tested in a small basin in Northern Italy to analyze the differences in terms of discharge hydrographs and flooded areas. The application of a criterion for hazard class mapping showed significant variations between the two models (Costabile et al, 2020).

In a study in Ghana, the impacts of dam releases from reoperation scenarios of the Akosombo and Kpong hydropower facilities on downstream communities along the Lower Volta River were examined through hydrodynamic modelling using the HEC-RAS software. The model was used

to simulate surface water elevation along the river reach for specified discharge hydrographs from proposed re-operation dam release scenarios. The morphology of the river and its flood plains together with cross-sectional profiles at selected river sections were mapped and used in the hydrodynamic modelling. In addition, both suspended and bed-load sediment were sampled and analyzed to determine the current sediment load of the river and its potential to carry more sediment. The modelling results indicated that large areas downstream of the dam including its flood plains would be inundated if dam releases came close to or exceeded 2300 m³/s. It was therefore recommended to relocate communities along the banks and in the flood plains of the Lower Volta River when dam releases were to exceed 2300 m³/s. From the analysis, suspended sediment transport was found to be very low in the Lower Volta River and the predominant soil type in the river-banks and bed is sandy soil. (Logah et al, 2017). Though in this study similar hydrodynamic modelling approach with HEC-RAS software was used, still the basic objectives were different. Here, the water surface was simulated for specified discharge hydrographs and the sediment load of the river was also estimated.

In a study in the Bolivian Amazonia, February 2014 flood water levels was simulated using HEC-RAS. Here, satellite images were used to compare the results which was different than other studies. The flood simulation showed good performance when compared with satellite image of the flood event. In addition, the simulation provided information like water depth, flow velocity and a temporal variation of the flood. Specific locations where water began to overflow were identified. Over most of the flooded area the water velocity was found lower than 0.25 m/s. From the analysis it was found that during first ten days of the flood the flood extent increased rapidly and the flood depth allowed identifying areas exposed to different hazard levels. The west plain of the Mamore River was found as the most exposed to the flood and it showed bigger flood extent, longer flood duration and deeper water depth (Quiroga et al, 2016).

In a study in India, river reach in the Mahanadi system extending over a length of 200 km from Khairmal to Munduli was considered for analysis to calibrate the channel roughness coefficient along the river Mahanadi, Odisha through simulation of floods using HEC-RAS. For calibration of Manning's "n" value the flood of year 2003 was considered. The calibrated model, in terms of channel roughness, was used to simulate the flood for year 2006 in the same river reach. The performance of the calibrated and validated HEC-RAS based model was tested using Nash and Sutcliffe efficiency. It was concluded from the simulation study that Mannnig's "n" value of 0.032 gives best result for Khairmal to Munduli reach of Mahanadi River (Parhi et al, 2012). The calibration process of this study is quite similar with the study with the Atrai River. In both cases, Manning's "n" was adjusted and as both the Mahanandi River and Atrai River have similar characteristics, the "n" values got from both of the studies were quite similar.

Another similar study was conducted in lower Tapi river, India where for years 1998 and 2003 floods were simulated using HEC-RAS. The calibrated model, in terms of channel roughness, was used to simulate the flood for year 2006 in the river. The performance of the calibrated HEC-RAS based model was assessed by capturing the flood peaks of observed and simulated floods; and computation of RMSE for the intermediated gauging stations on the lower Tapi River (Timbadiya et al, 2011). This study was also similar with the study of Atrai River where standard criteria like RMSE was used to determine the model performance.

1D HEC-RAS and CCHE2D was applied to assess and predict the flood depth and spatial extent of flood in the Sungai Maka floodplain, Kelantan state, Malaysia. The results of the study showed that the maximum difference between the 1D and 2D models was 6% in the meander's part of the river. The results of these two models in most sections approximately matched. Most differences in the results were in the shape of the river. (ShahiriParsa et al, 2016). The uniqueness of this study was to compare the results of 1D and 2D models where in the study of Atrai River the objective was set to compare the results of two types of one-dimensional model.

Some researchers showed an application of HEC-RAS in combination with ArcGIS to develop floodplain maps for part of Kabul River in Pakistan. The researchers described the application of HEC-RAS model to the development of floodplain maps for the part of Kabul River that lies in Pakistan. The intent was to assist policy makers and planners in the development of flood mitigation measures for the Khyber Pakhtunkhwa Province, which experienced unprecedented floods in July/August 2010 exposing the vulnerability of the province to this natural catastrophe. Owing to its reasonable accuracy and free availability, shuttle radar topography mission digital elevation model was chosen for the extraction of geometrical data for the river. Conventional flood frequency analysis, involving log-normal, Gumbel's, and log-Pearson type III distributions, was used to calculate extreme flows with different return periods. Using Kolmogorov–Smirnov test, LP3 was found to be the best distribution for the Kabul River. The peak floods from frequency analysis were input into HEC-RAS model to find the corresponding flood levels expected along river reaches extending through Warsak dam to Attock. Results obtained with HEC-RAS model were used in combination with ArcGIS to prepare floodplain maps for different return periods. Through floodplain maps, areas that are vulnerable to flooding hazards have been identified. Analysis of floodplain maps indicated that more than 400 % area is likely to be inundated as compared to the normal flow of the river. Most of the area found to be vulnerable to flooding is currently used for agriculture (Khattak et al, 2016). There were some differences between the methodology of this study at Pakistan and our study of Bangladesh. There the geometric data were extracted from shuttle radar topography mission digital elevation model where in our study survey data were used.

In some studies, 1D and 2D coupled model were used where in our study only 1D model was taken into account as the objectives of the study was different. At Surat city in India, simulation work

was carried out under the 1D and 2D couple hydrodynamic modeling to assess the flood and find inundation in low-lying areas in 2006. Two hundred ninety-nine cross sections, two hydraulic structures and five major bridges across the river were considered for 1D modeling, whereas a topographic map at 0.5 m contour interval was used to produce a 5 m grid, and SRTM 30 m and 90 m grid was considered for Surat and the Lower Tapi Basin. The tidal level at the river mouth and the release from the Ukai Dam during 2006 flood were considered as the downstream and upstream boundaries, respectively. The flood water levels were simulated under the unsteady flow condition and validated for the year 2006. The simulated result showed that 9th August was the worst day in terms of flooding for Surat city and a maximum 75–77% area was under inundation. Out of seven zones, the west zone had the deepest flood and inundated under 4–5 m. Furthermore, inundation was simulated under the bank protection work constructed after the 2006 flood. The simulated results showed that the major zones are safe against the inundation under 14,430 m³/s water releases from Ukai Dam except for the west zone (Patel et al, 2017).

A study was conducted on the Ichamati river at the part of the river that remains in West Bengal, India. A 1D HEC-RAS model over the stream network of the Ichamati river basins was set up. Good quality in situ measurements of river hydraulics including cross section, slope, flow were available only for the upstream and middle stream flood prone region of the basin. The de-siltation of the stretch of Ichamati river under survey i.e., middle part showed impacts which were positive in ways more than one. The river velocity in the top strata is 0.3 m/s from model and the river regained its ecological flow. Also, the increased salinity of the river helped in cultivation of different species of fishes, which are socio economically relevant in the adjoining areas. Due to the increased capacity of the channel in the middle part possibility of flood has also decreased. The total volume of silt accumulated has been estimated 277,589.92 m³. The rate of sedimentation was then calculated and found to be 16,328.82 m³/month silt deposition during monsoon and 11,109 m³ silt deposition during non-monsoon period. It may be concluded that out of 6 % annual silt deposition, 5 % silt deposition took place during the month between June and October and 1 % silt deposition during the month between November and May. Silt excavation along 20 km stretch of Ichamati river showed distinct rejuvenation of the river stretch (Mondal et al, 2016).

A flood inundation map was developed for the Blue River and Selected Tributaries in Kansas City, Missouri. In this study flood inundation map were created in a geographic information system by combining simulated water-surface profiles and terrain elevation data. The terrain model data were derived from lidar data and stream channel and bridge surveys at selected locations. Estimated flood-inundation boundaries for each simulated profile in HEC-RAS were developed with HEC-GeoRAS software which allows the preparation of geometric data for import into HEC-RAS and processes simulation results exported from HEC-RAS. These maps give detailed information on flood extents and depths for modeled sites (Heimann et al, 2012).

A study was conducted showing 2D flow routing capabilities of HEC-RAS for flood inundation mapping in lower region of Brazo River watershed subjected to frequent flooding. River reach length of 20 km located at Richmond, Texas was considered for this study. Detailed underlying terrain information available from digital elevation model of 1/9-arc second resolution was used to generate the 2D flow area and flow geometrics. Stream flow data available from gauging station USGS08114000 were used for the full unsteady flow hydraulic modeling along the reach. Developed hydraulic model was calibrated based on the Manning's roughness coefficient for the river reach by comparison with the downstream rating curve. Water surface elevation and velocity distribution obtained after 2D hydraulic simulation were used to determine the extent of flooding. For this, RAS mapper's capabilities of inundation mapping in HEC-RAS itself were used. Mapping of the flooded areas based on inflow hydrograph on each time step were done in RAS mapper, which provided the spatial distribution of flow. The results from their study can be used for flood management as well as for making land use and infrastructure development decisions (Kalra et al, 2012).

2.2.2. Studies using other software except HEC-RAS

A hydrodynamic river model was developed and calibrated for a flood-prone tidal river located in South East Queensland, Australia using MIKE HYDRO River. The model was calibrated using Manning's roughness coefficient for the normal dry and flood periods. The model performance was assessed by comparing observed and simulated water level, and estimating performance indices. Results indicated a satisfactory agreement between the observed and simulated results. The hydrodynamic modelling results revealed that the calibrated Manning's roughness coefficient ranged between 0.011 and 0.013. The impacts of tidal variation at the river mouth and the river discharge from upstream are the major driving force for the hydrodynamic process. To investigate the impacts of the boundary conditions, a new sensitivity analysis approach, based on adding stochastic terms to the time series of boundary conditions, was conducted. The sensitivity analysis results revealed that in the river under study, the middle parts of the river were shown to be more sensitive to downstream boundary condition as maximum water level variations can reach 8%, 12%, and 15% under 5%, 10%, and 15% changes in the downstream boundary, respectively (Jahandideh-Tehrani et al, 2020).

In order to improve the understanding of the hydrodynamics and morphodynamics of Tidally-Influenced Fluvial Zone (TIFZ) a combined field and numerical modelling study was conducted at the Columbia River Estuary, USA using Delft3D. A shallow water model was applied in both 2D and 3D configurations and model sensitivity to the key process parameterizations was investigated. The results indicate that a 2D model constrained within the estuary can sufficiently reproduce depth-averaged flow within the TIFZ of a stratified estuary. Model results highlighted the interactions between tidal-, fluvial- and topographic-forcing that result in depth dependent tidal rectification. Analysis of the model data revealed flood-directed sediment transport is due to both

tidal variability and mean flow. These results highlighted the need to include the mean flow component when considering the long-term morphodynamic evolution in a TIFZ (Sandbach, 2018).

In lower Tapi River in India, a one-dimensional hydrodynamic model was set up using MIKE 11. flood seasons were simulated for the years 2003 and 2006 and the development of stage–discharge relationship along the river. The river network and cross-sections were extracted from the field-surveyed contours of the Tapi River for the study. Using the aforesaid geometry and hydrological data, supplied by the stakeholders, the MIKE 11 hydrodynamic model was calibrated for the 1998 flood using releases from the Ukai Dam. The time series of the simulated flood levels were compared with the corresponding observed values at four intermediate gauging stations: Kakrapar Weir, Mandavi Bridge, Ghala village and the Surat city. The rating curves and stage–discharge relationship were also developed from the aforesaid calibrated model which would be useful in flood forecasting and development of flood protection measures along the lower Tapi River (Timbadiya et al, 2014).

In another study at Hau River, Vietnamese Mekong Delta, both 1D and 2D models were set up. In this study, 1D-MIKE 11 and 2D-MIKE 21 hydrodynamic models were combined to simulate future flows, water level and salinity intrusion in the Hau River which is one main river branch in the Mekong Delta. Future hydrological changes were simulated under multiple scenarios of upstream inflow changes, climate change and sea level rise for the 2036–2065 period. The main focus of the study was to simulate future flows and salinity intrusion using combined one- and two-dimensional hydrodynamic modelling. Simulation results showed that salinization will increase substantially, characterized by higher salinity intrusion length under spring tide from 6.78% to 7.97%, and 8.62% to 10.89% under neap tide; and progression of the salinity isohalines towards the upper Mekong Delta, from 3.29 km to 3.92 km for 1 practical salinity unit (PSU) under spring tide, and 4.36 km to 4.65 km for 1 PSU concentration under neap tide (Tran et al, 2018).

In a study, Delft3D model was used to simulate flood extent and inundation depth due to a storm event that occurred in June 2016 in the Shoalhaven Estuary, south-eastern Australia. This study investigated compound flooding by quantifying horizontal and vertical differences in coastal flood risk estimates resulting from a separation of storm-tide and riverine flooding processes. Time series of observed water levels and discharge measurements were used to force model boundaries, whereas observational data such as satellite imagery, aerial photographs, tidal gauges and water level logger measurements are used to validate modelling results. The comparison of simulation results including and excluding riverine discharge demonstrated large differences in modelled flood extents and inundation depths. From the analysis, comparison of different boundary set-ups at the intermittent entrance in Shoalhaven Heads indicated that a permanent opening, in order to reduce exposure to riverine flooding, would increase tidal range and exposure to both storm-tide flooding and wave action (Kumbier et al, 2018).

In the delta region of Mahanadi River basin in India, a 1D hydrodynamic model was used to simulate the river flows with limited available data. The SRTM DEM were analyzed in this study and compared with the elevations derived from available topographic maps and measured river cross-sections. The 1D hydrodynamic model was set up and calibrated using the refined cross-sections derived from SRTM DEM along with the measured ones and all available river discharge as well as water-level data at different gauging sites for the monsoon period (June–September) of the year 2004. The study demonstrated the usefulness of using the SRTM DEM to derive river cross-sections for use in hydrodynamic modelling studies (Patro et al, 2009).

A hydrodynamic model was used to simulate three flood events along a 200 km stretch of the low-gradient Thompson River in arid Australia using five metrics: peak discharge, peak height, travel time, terminal water storage and flood extent. This study highlights the important impact that the quality of the underlying DEM has, and in particular how sensitive hydrodynamic models are to preparation methods and how important vegetation smoothing and hydrological correction of the base topographic data for modelling floods in low-gradient and multi-channel environments (Jarihani et al, 2015).

In a study, a 2D hydrodynamic model was applied along a 7 km stretch of the River Ciliwung in central Jakarta. This study examined the developments in the field of collecting cost-effective high resolution terrain data that can contribute in the growing area of urban hydrodynamic modelling. The scope of providing coverage for large segments of the city was also evaluated in this research. In the context of this urban and densely settled river corridor, the challenge of obtaining “hydraulically representative” ground description and influence of representation of structures in hydrodynamic models was explored, alongside identifying the future work required to allow scaling of the methods and acquired datasets beyond the limits of the test site (Shaad et al, 2016).

The performance of hydrostatic versus nonhydrostatic pressure assumption in the 3D hydrodynamic modelling of a tortuously meandering river was studied in Canada. Both hydrostatic and nonhydrostatic numerical models were developed using Delft3D-Flow to predict the 3D flow field in a reach of Stillwater Creek in Ottawa, Canada. This study illustrated the superior performance of the hydrostatic over nonhydrostatic 3D modelling of the secondary flow using Delft3D. Several possible reasons were identified in this study for unfavourable performance of the nonhydrostatic version of Delft3D including the pressure correction technique employed in Delft3D (Parsapour-Moghaddam et al, 2017).

A full-scale fluvial flood modelling framework based on a high-performance integrated hydrodynamic modelling system (HiPIMS) was applied to reproduce the flood event caused by the 2015 Storm Desmond in the 2500 km² Eden Catchment at 5 m resolution. Without intensive model calibration, the predicted results compare well with field observations in terms of inundation

extent and gauged water levels across the catchment. Sensitivity tests of this research revealed that high-resolution grid is essential for accurate simulation of fluvial flood events using a 2D hydrodynamic model. Accelerated by multiple modern GPUs, the simulation of the study was more than 2.5 times faster than real time although it involved 100 million computational cells inside the computational domain (Xia et al, 2019).

Hydrodynamic modelling of a tidal delta wetland was done using an enhanced quasi-2D model to demonstrate the application of the quasi-2D CTSS8 model to a complex estuarine delta. This study proposed an enhanced quasi-2D modelling strategy that captures the interaction between river discharge and moon tides and the resulting hydrodynamics, while using the scarce data available. The water flow equations were discretized with an interconnected irregular cell scheme, in which a simplification of the 1D Saint-Venant equations is used to define the water flow between cells. The spatial structure of wetlands was based on the ecogeomorphology in complex estuarine deltas. The model was calibrated for an average year and the model performance was evaluated for another average year and additionally an extreme dry three-month period and an extreme wet three-month period. The calibration and evaluation were done based on two water level measurement stations and two discharge measurement stations, all located in the main rivers (Wester et al, 2018).

A methodology was demonstrated to determine the spatial and temporal evolution of stratification in estuaries driven by astronomical tides and river discharges in a study at Suances Estuary using a 3D hydrodynamic model. The variation of estuarine currents, water levels and densities was investigated in this study under different realistic forcing conditions. These conditions were classified from a long-term period (>30 years) of river flows and tidal water levels by a K-means clustering approach. The methodology allowed computing the location of mixed, partially mixed/stratified and stratified areas in tidal river estuaries along a continuum by means of Richardson's Layer number and the frequency of every model scenario. The results showed the Suances Estuary was vertically mixed at its innermost part due to riverine influence and at the outer part, it was also vertically mixed due to the turbulence caused by tidal action (Bárcena et al, 2016).

A study presented the development of a 2D hydrodynamic model based on TELEMAC-2D for the flood simulation of the river from Kratie to Kampong Cham in Cambodia, a part of the Mekong River. The focus of the research was to study the feasibility of TELEMAC-2D in flood forecasting, and specifically to determine its adequacy in flood simulations with a focus on the reduction in model run-time through parallelization. An actual flood event was simulated which occurred between June to November in 2001 for the stretch of the Mekong River from Kratie to Kampong Cham and compared the model simulations with MODIS satellite Images for specific days in the pre-, peak- and post-flood period. It was found from the analysis that during the peak-flood period, there was high percentage (>90%) match between the simulation results and observation obtained

from satellite images while the match was below 50% for the pre- and post-flood periods (Vu et al, 2015).

2.3 Studies on Hydrodynamic Modelling in Bangladesh

As a riverine country, numerous studies have been done of different rivers of Bangladesh using Different software like: MIKE, Delft3D, HEC-RAS etc. Some of these studies are explained in this section.

2.3.1. Studies using HEC-RAS

A study on Dharala river was conducted to identify the low-lying areas prone to inundation and to reduce the uncertainty in flood mitigation measures, HEC-RAS based 1D and 2D Coupled hydrodynamic model had been carried out for Dharla River. Boundary conditions for upstream and downstream had been defined by discharge of Taluk-Simulbari station and water level of Kurigram station respectively. Flow had been simulated under unsteady conditions, calibrated for the year 2013 and validated for the year 2014. Flood Inundation maps had been generated in the RAS mapper for the years 2010, 2013 and 2014 from the month June to October for highest water levels of each month. The validation of the generated flood map of 2010 had been performed using the MODIS flood map of 2010. A comparative analysis was carried out between the maps generated by using HEC-RAS 1D and 2D coupled model and using HEC-RAS 1D model and Arc-GIS. Also, a correlation was developed from the comparison (Bose et al, 2018).

Some researchers conducted a study to develop inundation maps of the Surma and the Kushiya River using combined 1D and 2D HEC-RAS model. The model needed cooperation of GIS and HEC-GeoRAS. Calibration and validation showed result much closer to the actual scenario. After calibration and validation flood inundation map were generated using RAS Mapper. Changing the actual discharge different scenario were generated using RAS Mapper. Those scenarios were calculated in GIS by exporting data from HEC-RAS to GIS. Levee was constructed in HEC-RAS 2D. The average levee height was found about 1.8 m which showed significant amount of resistance against flood (Khan et al, 2018).

A study was carried out to develop floodplain extend maps and inundation maps of the Jamuna River (Rahman, 2015). The study also focused on the flood pattern change with time and impact of levee on flood inundation area. 1D hydraulic model HEC-RAS with HEC-GeoRAS interface in coordination with ArcView was applied for the analysis. Thus, findings of the study helped in planning and management of flood plain area of the Jamuna River to mitigate future probable

disaster through technical approach. In future study, this model results can be compared with the studies with SOBEK or HEC-RAS 1D and 2D model results. Flood risk maps, others structures like flood control dam, reservoir impact on flood can be studied in future studies.

Rahman (2012) studied an unsteady flow analysis of the Shitalakhya and the Dhaleswari to assess the availability of flow in these rivers during dry season for Dhaka city water supply. He used HEC-RAS to analyze the low flow of the Shitalakhya and the Dhaleswari River. The study assessed whether the flows in these rivers are adequate enough during the dry season to be used for Dhaka city water supply. The study concluded that the flow varied from moderate to low in both the rivers. He recommended that the flow in both of these rivers has to be increased by means of dredging or by means of suitable hydraulic structures whichever is technologically and economically suitable.

In Bangladesh, in a study HEC-RAS coupled model was used for Jamuna Basin floodplain to generate the flood inundation map of the study area. The study was based upon a combined 1D and 2D model which needs cooperation of GIS and HEC-GeoRAS. In HEC-RAS, boundary conditions for upstream and downstream are defined by discharge and water level for running the 1D river, while for 2D floodplain discharge data was used in upstream side and rating curve was used in downstream portion. For floodplain calibration about 1% discharge flowing through the channel was used only when the channel discharge was more than bank full discharge. Finally, the establishment of Hydrodynamic model through coupling of 1D river and 2D floodplain was made for the Jamuna River in this study. Calibration and validation of the model showed good correlation between the observed and simulated data. The value of correlation coefficient, R was found 0.93 and 0.83 for calibration and validation respectively (Ali et al, 2016).

The flood hazard of mid-eastern part of Greater Dhaka was assessed in another study by developing a flood hazard map through 1D hydrodynamic simulation on the basis of a DEM data and hydrological field observations. In this study, flood hazard was assessed by developing a flood hazard map for mid-eastern Dhaka (37.16 km²) by 1D hydrodynamic simulation on the basis of DEM data from Shuttle Radar Topography Mission and the hydrologic field-observed data for 32 years (1972–2004). As the topography of the area has been considerably changed due to rapid land-filling by land developers which was observed in recent satellite image, the acquired DEM data were modified to represent the current topography. The inundation simulation was conducted using hydrodynamic program HEC-RAS for flood of 100-year return period. The simulation revealed that the maximum depth is 7.55 m at the southeastern part of that area and affected area was more than 50% (Masood et al, 2012).

2.3.2. Studies using other softwares except HEC-RAS

The Flood Forecasting and Warning Centre, under the Processing and Flood Forecasting Circle, Hydrology, BWDB use hydrodynamic model to forecast flood levels at different points of major rivers of the country. It takes hydrological monitoring data of 94 representative water level stations and 70 rainfall stations throughout the country. The principal outputs are the daily statistical bulletin of floods, river situations, a descriptive flood bulletin, forecast for 24, 48, 72, 96 and 120 hours at 54 monitoring points on the major rivers, special flood report along with different graphical and statistical presentations during the monsoon season. Before 1990, forecast for six locations viz. Bahadurabad, Serajgonj, Aricha, Goalondo, Bhagyakul and Hardinge Bridge on the Padma –Brahmaputra –Jamuna river system were issued by Co-axial correlation, Gauge to Gauge relation and Muskingum-Cunge Routing Model. After the devastating flood of 1987 and catastrophic flood of 1988, it was deeply realized by the organization that the forecast formulation should be introduced in the process of river modelling. In this context, the simulation model MIKE11 developed by Danish Hydraulic Institute (DHI) was installed at FFWC and a special version of MIKE11 FF conceptual Hydrodynamic model is in operation for forecast formulation.

The dynamics of bar in the braided river Jamuna was analyzed in a study. This study focused to understand the dynamics of the braided bar or island development process of braided river, Jamuna which is the downstream continuation of Brahmaputra River in Bangladesh. This study recommended that before any interventions in the river, it should be considered that the river may not behave as the same as it do now. A two-dimensional morphological model had been developed for simulating the hydraulic and morphological processes in the Gorai off take to study the feasibility of undertaking Gorai river restoration work. A quasi-steady flow calculation was carried out for the morphological calculation using MIKE-21C of DHI Water and Environment. A helical flow module was used to calculate the streamline curvature generated secondary flows. The sediment transport computed are composed of bed-load and suspended load. For the bed load calculation, the effects of the helical flow and bed slope were accounted through the direction of bed-shear stress and direction of the bed-slope. The model was calibrated and validated at the off take with extensive data collected for three consecutive monsoons from 1998 to 2000. Both Chezy's roughness and depth variant roughness were used in the study (Shampa, 2015).

Islam (2016) studied the hydrodynamic modeling of Dhaleswari River for dry period flow augmentation. He analyzed whether the flows in this river is adequate enough during the dry season. He suggested a channel modification to increase the carrying capacity and navigability of the river. Flow condition at offtake of Dhaleswari is analyzed in this study. Minimum historical water level was found 3.0 m PWD approximately at downstream and 5.8 m PWD at upstream of the river. He performed calibration and validation for the year 2014 and 2013. And calibrated parameter was set to be 0.018. The study shows that before modification the maximum channel depth is found 0.6m to 1.0m approximately. The estimated dredged volume was 56.4 Mm³.

BWDB initiated a project in 2011 for protection of the left bank of the Padma River from erosion at Bhagyakul Bazar, Baghra Bazar and Kobutorkhola under Sreenagar Upazila of Munshigonj district. Institute of Water Modelling (IWM) carried out a study using Mathematical Modelling tool MIKE-21C in 2011 to ascertain hydro morphological design parameters of protection works of this project. The study provided the identification of erosion trend of the vulnerable areas, devising suitable options of river-bank protection works, determination of maximum expected scour level around river-bank protection works, assessment of morphological changes in the vicinity of the river-bank protection works, assessment of river-bank protection induced morphological changes, providing outline design of river-bank protection works, formulation of monitoring program for the river-bank protection works.

Jagers (2003) focused on Modelling techniques to predict plan form changes of braided rivers and their relation with state-of-the-art knowledge on the physical processes and the availability of model input data. Three Modelling techniques were analyzed with respect to their suitability for predicting plan form changes of braided rivers: a neural network, a cellular model and an object-oriented approach. Two-dimensional depth-averaged morphological simulations of sharp bends have been carried out to improve the understanding of the processes involved. The results of those simulations indicated that cutoff formation of Jamuna is accelerated by a low water level downstream, a large roughness, a low threshold for sediment transport, and a small value for the exponent c of the Shields parameter q or of the velocity u in the sediment transport relation if the average sediment transport rate remains constant. A simple model concept for simulating head ward erosion was presented and tested. Finally, an algorithm for formation of new channels was presented that can be implemented as a new module in the branches model.

A study had been conducted to determine the braiding indices of the lower Brahmaputra-Jamuna River lying within Bangladesh for the different years using different approaches. The researcher concluded that any large-scale water resources development projects on the Brahmaputra-Jamuna deserve the highest technological considerations and remedial measures for arresting such trends. The Braiding indices calculated in this study are broadly consistent with those found in the previous studies (Mamun et al, 1997).

2D hydraulic model and morpho-dynamic model were developed by IWM in 1998 under the Meghna Estuary Study. The Meghna Estuary Study covered an area of the lower Meghna from Chandpur town up to the Bay of Bengal. The model was developed using MIKE-21. The dominant hydraulic and morphologic conditions and processes in the study area are studied through regional and detailed local 2D models. Computations are carried out under different hydrodynamic conditions during low and monsoon seasons to determine the dynamic behaviour of the entire estuary system.

The morphological processes of the Jamuna River at Pabna Irrigation Rural Development Project (PIRDP) were reviewed in a study (Halcrow, 2002). Halcrow et al. proposed riverbank protection based on the morphological studies of the area. Three reaches of the bank were identified as susceptible to different degrees of erosion, and then the sites were being prioritized to allow the introduction of a staged intervention program for protecting the vulnerable bank reaches. A 4 km reach of bank line within PIRDP showed immediate need for protection.

The morphological behavior of Brahmaputra-Jamuna River was also analyzed in a study. The study focused on the Morphological behavior of Brahmaputra-Jamuna River within the territory of Bangladesh. The analysis had been carried out mainly based on cross-sectional data for 17 selected stations, Study of variation of cross-sectional area with elevation from bottom to high water level shows that at first the area increases slowly, and then increases very fast with faster increase of width with elevation. No systematic change in the variation of cross-sectional area, total width and effective width has been observed at any station over the years (Mukherjee, 1995).

In a nutshell, in this chapter different studies on hydrodynamic modelling using different software at different parts of the world were discussed. HEC-RAS 1D, 2D and 1D-2D coupled models were reviewed in this literature. There were some significant similarities of our study with the methodology of some studies using 1D model where some differences were also identified. 2D and 1D-2D coupled models and their objectives were also reviewed to discuss the future scopes of studies on the Atrai River.

Chapter 3: Study Area and Model Description

3.1 General

The Atrai River reach was selected as the study area for this study which is an important floodplain area of north-western part of Bangladesh. To set up the short-and long-reach hydrodynamic models of this river, HEC-RAS 1D model was used. The simulation analysis was mainly conducted by HEC-RAS 5.0.3 version. For extracting some information regarding geometric data, Google Earth was used. Some other software had been also used such as ArcGIS to view, edit, analyze geospatial data and produce maps. HEC-RAS, an open-source model which have excellent Graphical User Interfaces, was developed by US Army Corps of Engineers. Theoretical concept used for this hydrodynamic modelling approach and details of the study area are described in this chapter.

3.2 Study Area

The Atrai River is selected as the study area for this study. This river reach is one of the ideal locations where river floodplain interaction is really prominent. At the rising phase of flood, the river loses water and the floodplain gains it where in the falling phase water goes from floodplain to the river. This feature is quite prominent in this river in comparison to other rivers of the country. The details of study area is explained in this section.

3.2.1 Location

The study river for this study is the Atrai River which is considered one of the most important rivers in Northern part of Bangladesh. It is a transboundary river which flows in West Bengal and northern parts of Bangladesh. It originates in Siliguri ward no 40, near Baikantapur forest West Bengal. After flowing through Dinajpur District of Bangladesh, it enters into India again. It passes through Kumarganj and Balurghat community development blocks in Dakshin Dinajpur district. After that, the river then reenters Bangladesh through Naogaon district and falls into Hurasagar which is in Sirajgonj district. It crosses the Barind Tract and flows into Chalan Beel. The offtake of Atari is Karatoya River and outfall is Hurasagar. It has some tributary, distributary and branch rivers. It splits into two rivers: the Gabura and the Kankra in Dinajpur district. Total length of the river is approximately 390 kilometers. The average width is 177 m where the maximum width is found 285 m and minimum is 127 m. The maximum depth of the river is 30m (Wikipedia, 2021). The study area of this study is 106 km reach of the Atrai River which is shown in Figure 3.1.

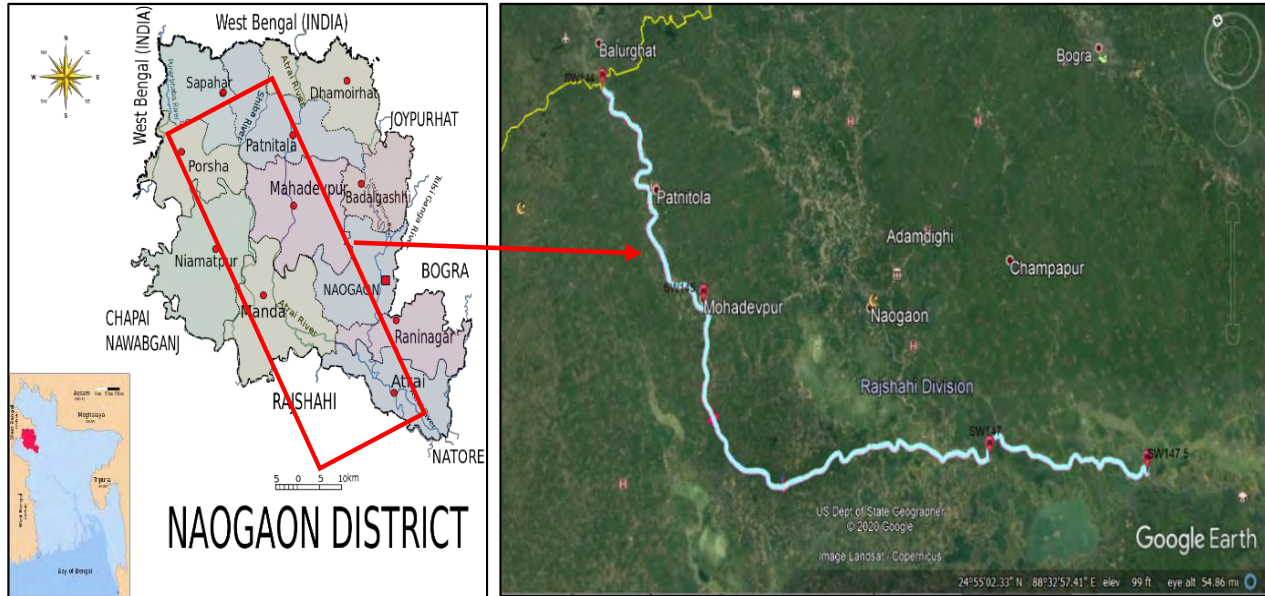


Figure 3.1: The study area

3.2.2 Upazilas under study area

The study area includes four upazilas from the upstream to downstream. They are:

- Patnitola,
- Mohadebpur,
- Manda and
- Atrai upazila

These upazilas are under the administrative boundary of Naogaon district. The upazilas are shown in Figure 3.2.

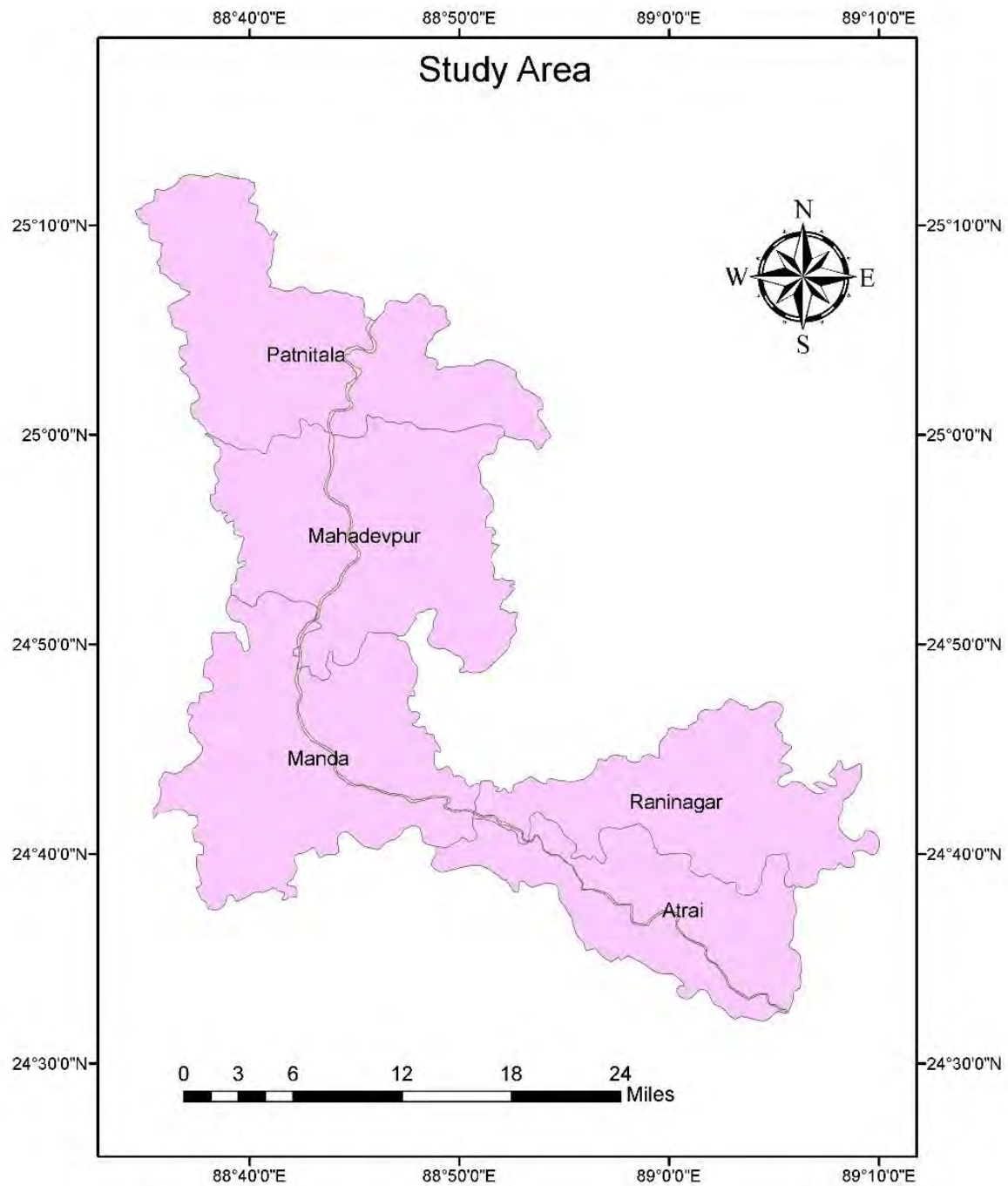


Figure 3.2: Upazilas of the study area

A total of three 1D models were developed in this study river. Two of them were short-reach models and one was long-reach model.

1. Upstream short-reach model having 6 km reach starting from station 144
2. Downstream short-reach model having 6 km reach starting from station 147
3. One long-reach model having 106 km reach starting from station 144

For the upstream short-reach model, station 144 was the discharge boundary station and after 6 km from it, the water level boundary station was selected. Observed discharge of station 144 and interpolated water level from station 144 and 145 was used as the boundary conditions in this model. On the other hand, discharge boundary station of downstream short-reach model was chosen at station 147 and after 6 km from it, the water level boundary station was selected. Observed water level of station 147 and interpolated water level from station 147 and 147.5 was used as the boundary conditions in this model. The discharge boundary station for long-reach model was station 144 and after 106 km, the water level boundary station was selected and interpolated water level from station 147 and 147.5 was used for long-reach model. This boundary for long-reach model was selected as the bathymetry data was available up to this point.

A schematic diagram of the whole scenario is shown in Figure 3.3.

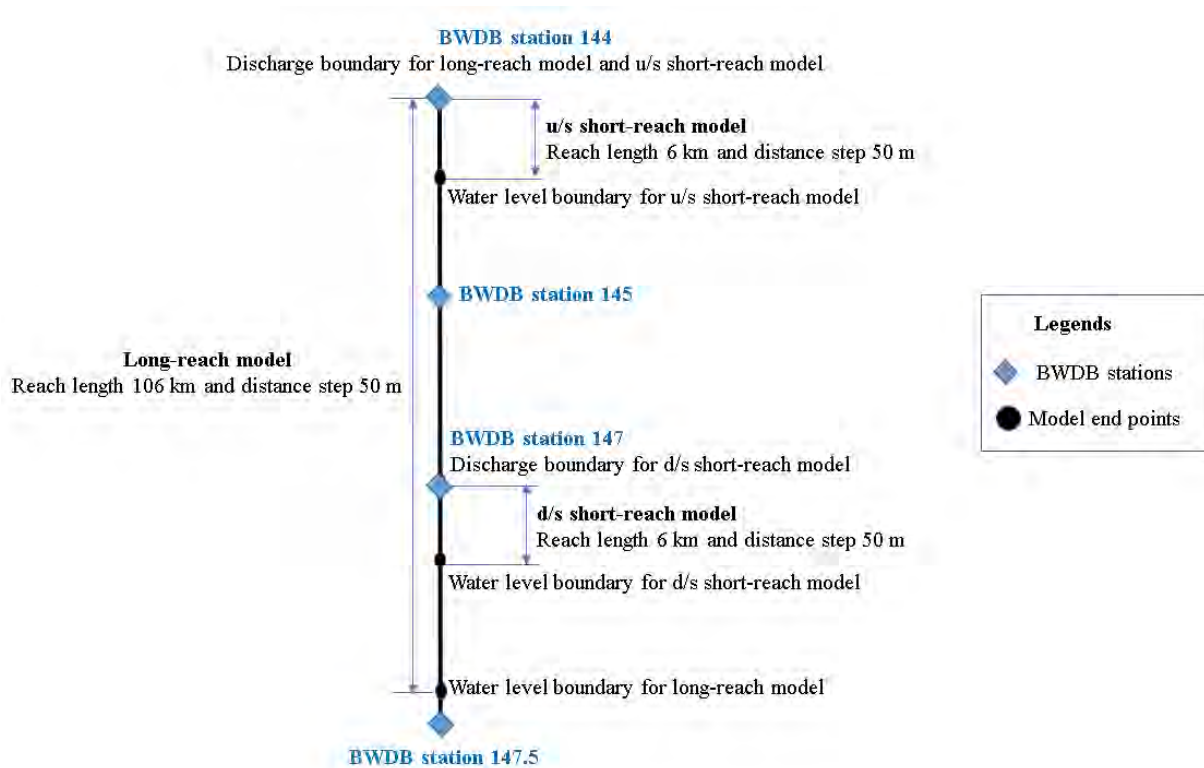


Figure 3.3: Schematic diagram of the models used for the study river

3.2.3 Navigability of the Atrai River

At the dry season means during January to April, the discharge of the river remains very low. This little amount of water is not sufficient for irrigation purpose. So, some earthen dams were built in some portion of the river in order to use that water for irrigation purpose. A rubber dam was also constructed on Atrai River in Sadar upazila which was about 18 km away from the district town. It was 135 m in length and 4 m in height. During rainy season discharge becomes higher and flood occurs due to overflow of the river water along the riverbanks. Atrai is navigable for whole year and serves as a perennial source of fishing, even though it is often the cause of flooding in many areas during monsoons (Wikipedia, 2021).

3.3 Hydrodynamic Modeling Approach

Mathematical models are mathematical representations of actual physical processes. Depending upon the type and application of the model, it requires a large volume of high-quality data including river channel bathymetry, hydrological and environmental data. After a model has been developed, it requires to be calibrated. This is done to determine its ability to reproduce phenomena actually observed in the field. This is a trial-and-error process in which any deficiencies in the model setup and input data are rectified and model elements fine-tuned until a reasonable agreement between simulations and observations is reached. A calibrated and validated model is a very useful tool for planning purpose that can be used confidently for impact assessment and performance evaluation of different alternative plans prior to implementation.

Rivers and estuaries are generally many times longer than they are wide or deep. As a result, inputs from external sources rapidly mix over the entire cross section and a 1-dimensional approach is often justified.

3.4 Hydrodynamic Modeling Using HEC-RAS

HEC-RAS is a computer program that models the hydraulics of water flow through natural rivers and other channels. The latest version HEC-RAS 5.0.7 was released at 2019. Prior to the 2016 update to Version 5.0, the program was one-dimensional, meaning that there is no direct modeling of the hydraulic effect of cross section shape changes, bends, and other 2D and 3D aspects of flow. The release of Version 5.0. introduced two-dimensional modeling of flow as well as sediment transfer modeling capabilities. The program was developed by the United States Army Corps of Engineers in order to manage the rivers, harbors, and other public works under their jurisdiction;

it has found wide acceptance by many others since its public release in 1995. Hydrologic Engineering Centers in Davis, California, developed the River Analysis System to aid hydraulic engineers in channel flow analysis and floodplain determination. It includes numerous data entry capabilities, hydraulic analysis components, data storage and management capabilities, and graphing and reporting capabilities (Wikipedia, 2021).

In other words, HEC-RAS is an integrated package of hydraulic analysis programs, in which the user interacts with the system through the use of a graphical user interface. The system is capable of performing steady flow water surface profile calculations and includes unsteady flow, sediment transport, and several hydraulic design calculations (ShahiriParsa et al, 2016). The results of the model can be applied to floodplain management and flood insurance studies (Othman et al, 2014).

HEC-RAS program is capable of carrying out a steady flow modeling and dynamic routing of flood hydrograph. It is also completely compatible with Windows operating system. Various river features, such as storages, diversions, bridges, and any hydraulic structures in the river can be defined easily in this model. Simulating steady flow is one of the previous capabilities of the model, in which Manning's roughness coefficient could be defined and calibrated in various ways. HEC-RAS software is used frequently in the 1D hydraulic analysis of both the steady and unsteady flows in natural rivers or canals.

3.4.1 Analysis components of HEC-RAS

HEC-RAS is an integrated system of software, designed for interactive use in a multi-tasking environment. The system is comprised of a graphical user interface, separate analysis components, data storage and management capabilities, graphics, mapping and reporting facilities. The HEC-RAS system contains the following river analysis components for:

- (1) one dimensional steady flow water surface profile computations;
- (2) one-dimensional and/or two-dimensional unsteady flow simulation;
- (3) quasi unsteady or fully unsteady flow movable boundary sediment transport computations (1D and 2D); and
- (4) one dimensional water quality analysis.

A key element is that all four components use a common geometric data representation and common geometric and hydraulic computation routines.

The first two components are used in this study.

(i) Steady flow water surface profile computations:

In this study, for four flood seasons, one dimensional steady flow has been simulated for consecutive 30 days to compare the performances with unsteady flow simulation for the same flood seasons. This steady component of the modeling system is intended for calculating water surface profiles for steady gradually varied flow. It is capable of modeling subcritical, supercritical, and mixed flow regime water surface profiles. The basic computational procedure is based on the solution of the one-dimensional energy equation. Energy losses are evaluated by friction using Manning's equation and contraction or expansion with coefficient multiplied by the change in velocity head. The momentum equation is utilized in situations where the water surface profile is rapidly varied. These situations include mixed flow regime calculations (i.e., hydraulic jumps), hydraulics of bridges, and evaluating profiles at river confluences. The system can handle a full network of channels, a dendritic system, or a single river reach.

The steady flow system is designed for application in flood plain management and flood insurance studies to evaluate floodway encroachments. There are some special features of the steady flow component such as: multiple plan analyses, multiple profile computations, multiple bridge or culvert opening analysis, bridge scour analysis, split flow optimization, and stable channel design and analysis. In this study, using steady component the flood parameters such as water surface elevations were evaluated using this module.

(ii) Unsteady flow simulation:

Though both 1D and 2D flow simulation model is available in HEC-RAS, in this study, two types of 1D model performances were compared. HEC-RAS modeling system is capable of simulating 1D, 2D or combined 1D and 2D unsteady flow through a full network of open channels, floodplains, and alluvial fans. The unsteady flow component can be used to performed subcritical, supercritical, and mixed flow regime (subcritical, supercritical, hydraulic jumps, and drawdowns) calculations in the unsteady flow computations module. The hydraulic calculations for cross-sections, bridges, culverts, and other hydraulic structures that were developed for the steady flow component were incorporated into the unsteady flow module.

There are some special features of the unsteady flow component such as: hydraulic structure capabilities, dam break analysis, levee breaching and overtopping, navigation dam operations, pressurized pipe systems, automated calibration features, user defined rules, and combined 1D and 2D unsteady flow modeling. In this study, unsteady component was used for simulating the flood parameters such as water surface elevations for different flood seasons using different boundary conditions.

Boundary Conditions

There are several different types of boundary conditions available to the user. The following is a short discussion of each type:

1. Flow Hydrograph

A flow hydrograph of discharge versus time can be used as either an upstream or downstream boundary condition, but it is most commonly used as an upstream boundary condition.

2. Stage Hydrograph

A stage hydrograph of water surface elevation versus time can be used as either an upstream or downstream boundary condition.

3. Stage and Flow Hydrograph

Stage and flow hydrograph can be used together as either an upstream or downstream boundary condition. The upstream stage and flow hydrograph is a mixed boundary condition where the stage hydrograph is inserted as the upstream boundary until the stage hydrograph runs out of data, at this point the program automatically switches to using the flow hydrograph as the boundary condition. This type of boundary condition is primarily used for forecast models where the stage is observed data up to the time of forecast, and the flow data is a forecasted hydrograph.

4. Rating Curve

Rating curve is a graph of discharge versus stage. The rating curve option can be used as a downstream boundary condition.

5. Normal Depth

The normal depth option can be used as a downstream boundary condition for an open-ended reach. Manning's equation with a user entered friction slope produces a stage is considered to be normal depth if uniform flow conditions exist.

3.4.2 User interface and parameters of HEC-RAS

The user interacts with HEC-RAS through a graphical user interface. The main focus in the design of the interface was to make it easy to use the software, while still maintaining a high level of efficiency for the user. The interface provides for the following functions:

- i. File management
- ii. Data entry and editing
- iii. River analyses
- iv. Tabulation and graphical displays of input and output data
- v. Reporting facilities
- vi. Online help

HEC-RAS uses a number of input parameters for hydraulic analysis of the stream channel geometry and water flow. These parameters are used to establish a series of cross-sections along the stream. In each cross-section, the locations of the stream banks are identified and used to divide into segments of left floodway, main channel, and right floodway. At each cross-section, HEC-RAS uses several input parameters to describe shape, elevation, and relative location along the stream such as:

- i. River station (cross-section) number.
- ii. Lateral and elevation coordinates for each terrain point.
- iii. Left and right bank station locations.
- iv. Reach lengths between the left floodway, stream centerline and right floodway of adjacent cross-sections.
- v. Manning's roughness coefficients.
- vi. Channel contraction and expansion coefficients.
- vii. Geometric description of any hydraulic structures, such as bridges, culverts, and weirs.

HEC-RAS assumes that the energy head is constant across the cross-section and the velocity vector is perpendicular to the cross-section. After defining the stream geometry, flow values for each reach within the river system. The channel geometric description and flow rate values are the primary model inputs for the hydraulic computations (Islam et al, 2000).

The basic computational procedure is based on the iterative solution of the energy equation. Given the flow and water surface elevation at one cross-section, the goal of the standard step method is to compute the water surface elevation at the adjacent cross-section (Hicks et al, 2005).

3.4.3 Steps for analysis in HEC-RAS

Some steps need to be followed for analysis in HEC-RAS. The process is summarized as follows:

- i. Starting a new project
- ii. Entering geometric data
- iii. Entering steady flow data
- iv. Performing the hydraulic calculation
- v. Viewing results
- vi. Printing graphics and tables
- vii. Exiting the program

Performing analysis may be subdivided as performing a steady flow analysis and unsteady flow analysis. Performing a steady flow analysis consists of entering and editing steady flow data and performing steady flow calculations. Performing an unsteady flow analysis consists of entering and editing unsteady flow data, performing unsteady flow calculations, calibration of unsteady flow models, model accuracy, stability, and sensitivity and viewing results. After the model has finished the steady or unsteady flow computations the user can begin to view the output. Output is available in a graphical and tabular format. The current version of the program allows the user to view cross sections, water surface profiles, general profiles, rating curves, hydrographs, X-Y-Z perspective plots, detailed tabular output at a single location, and summary tabular output at many cross sections. Users also have the ability to develop their own output tables.

Contents of the output results of the HEC-RAS model are as follows:

- i. Cross section, profiles, and rating curves
- ii. X-Y-Z perspective plots
- iii. Tabular output
- iv. Viewing results from the river system schematic
- v. Stage and flow hydrographs
- vi. Viewing computational level output for unsteady flow
- vii. Viewing ice information
- viii. Viewing data contained in an HEC-DSS file
- ix. Exporting results to HEC-DSS.3

3.5 Basic Equations of Hydrodynamic Modelling

In steady modeling, the flows are prescribed by the user and the model calculates water levels at discrete cross-sections. There is essentially one unknown variable (stage) and therefore, one equation is needed - the energy equation. In unsteady flow modeling, two variables are calculated (stage and flow), so two equations are needed. Unsteady modeling is also concerned with how these parameters change with time and distance downstream. This is reflected in the partial differential terms in the equations.

3.5.1 Steady flow equations

Different fundamental equations used for HEC-RAS algorithm to compute water surface elevations using the standard step method for steady flow analysis are discussed in the following section.

Energy equations

Water surface profiles are computed from one cross-section to the next by solving the Energy Equation with an iterative procedure. Energy equation is based on Principle of conservation of the energy and it states that the sum of the kinetic energy and potential energy at a particular cross-section is equal to the sum of the potential and kinetic energy at any other cross section plus or minus energy loss or gains between the sections. The energy equation can be written in the following form.

$$z_1 + Y_1 + \frac{a_1 v_1^2}{2g} = z_2 + Y_2 + \frac{a_2 v_2^2}{2g} + h_e \quad (3.1)$$

where

Z_1, Z_2 = elevation of the main channel inverts

Y_1, Y_2 = depth of water at cross-sections

V_1, V_2 = average velocities (total discharge/total flow area)

a_1, a_2 = velocity weighting coefficients

g = gravitational acceleration

h_e = energy head loss.

A diagram showing the terms of the energy equation is shown in Figure 3.4. The energy head loss (h_e) is expressed as the following form.

$$h_e = LS_f + C \left| \frac{a_1 v_1^2}{2g} + \frac{a_2 v_2^2}{2g} \right| \quad (3.2)$$

where

L = discharge weighted reach length

S_f = representative friction slope between two sections

C = expansion or contraction loss coefficient.

The distance weighted reach length, L, is calculated as:

$$L = \frac{L_{lob}Q_{lob} + L_{ch}Q_{ch} + L_{rob}Q_{rob}}{Q_{lob} + Q_{ch} + Q_{rob}} \quad (3.3)$$

where

L_{lob}, L_{ch}, L_{rob} = x-section reach length specified for flow in the left overbank, main channel and right overbank respectively

Q_{lob}, Q_{ch}, Q_{rob} = arithmetic average of the flows between sections for the left overbank, main channel and right overbank respectively.

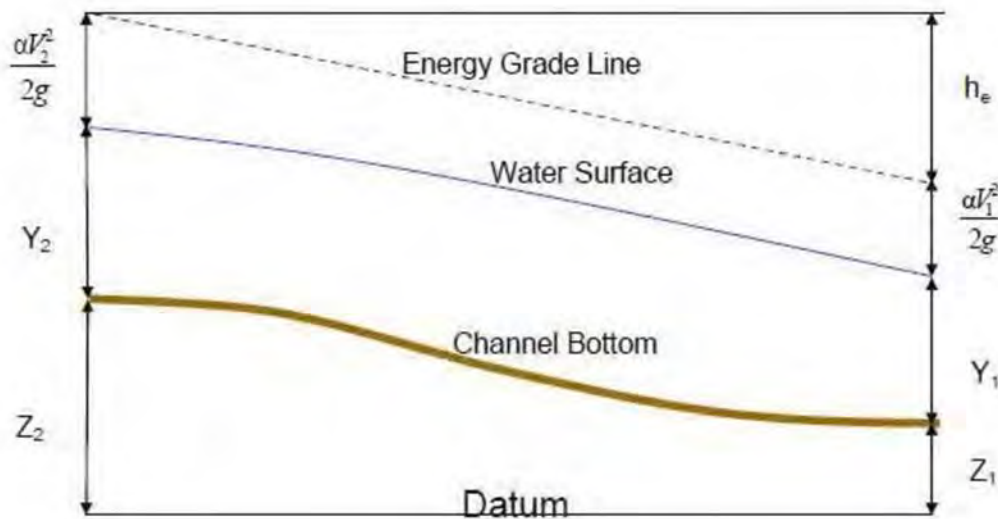


Figure 3.4: Diagram showing the energy equations terms

Calculation of conveyance

The determination of total conveyance and the velocity coefficient for a cross-section requires that it will be sub-divided into units for which the velocity is uniformly distributed. The approach used in HEC-RAS is to sub-divide flow in the overbank areas using the input cross-section n-value

break points as the basis for subdivision. Conveyance is calculated within each subdivision forms in the following form of Manning's equation.

$$Q=KS^{1/2}f \tag{3.4}$$

$$K=\frac{1}{n}AR^{2/3} \tag{3.5}$$

where

K = conveyance for sub-division

n = Manning's roughness coefficient for sub-division

A = Flow area for sub-division

R = hydraulic radius for sub-division.

All the incremental conveyances in the overbank are summed to obtain a conveyance.

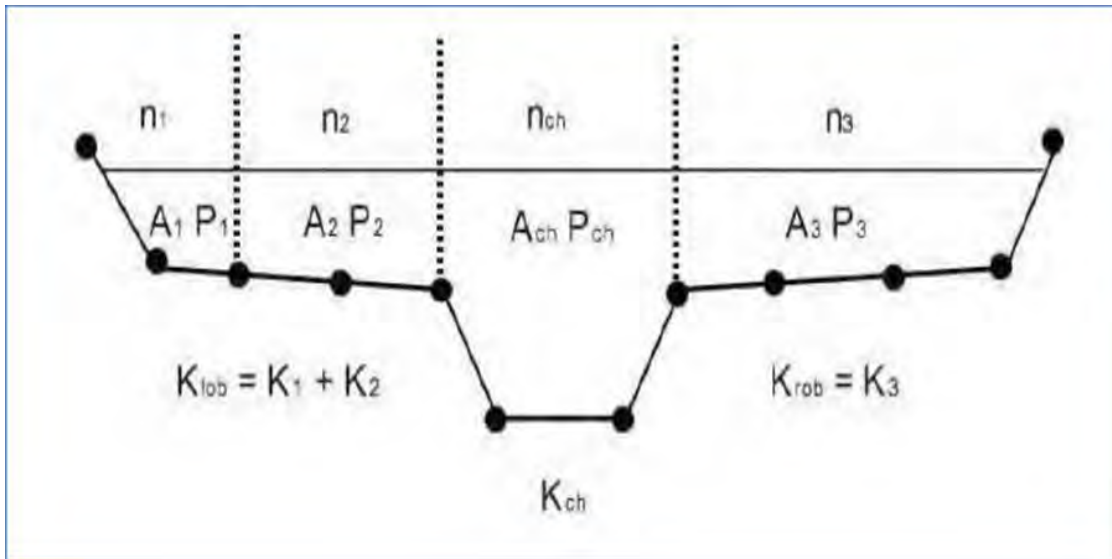


Figure 3.5: HEC-RAS default conveyance subdivision method for the left and the right overbank

Calculation of mean kinetic energy head

Mean kinetic energy head for each cross-section is obtained by computing the flow weighted kinetic energy heads for three sub-sections of the cross-sections. Figure 3.6 illustrates the mean kinetic energy calculation process for a cross-section with a main channel and right bank. To compute the mean kinetic energy, it is necessary to obtain the velocity head.

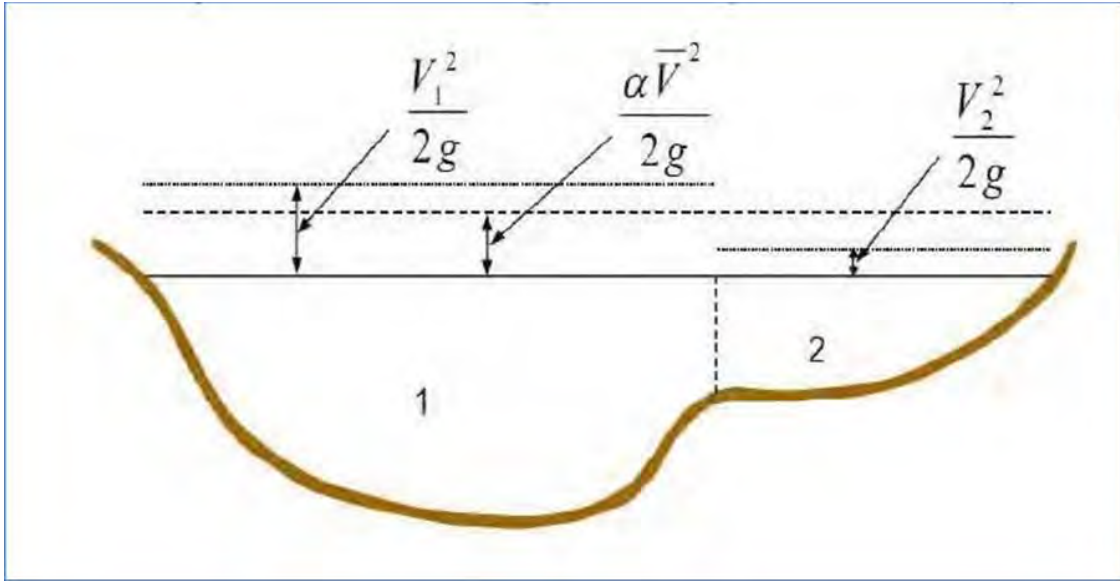


Figure 3.6: Example of how mean energy is obtained weighting coefficient alpha.

Alpha can be calculated by using following equation.

$$\alpha = (A_t)^2 \left(\frac{k_{lob}^2}{A_{lob}^2} + \frac{k_{ch}^2}{A_{ch}^2} + \frac{k_{rob}^2}{A_{rob}^2} \right) / K^3 t \quad (3.6)$$

where

A_t = total flow area of cross-section

A_{lob} , A_{ch} , A_{rob} = flow areas of left bank, main channel and right bank

K_t = total conveyance of cross-section

K_{lob} , K_{ch} , K_{rob} = conveyance of left bank, main channel and right bank.

Saint-Venant equations

HEC-RAS is dependent on finite difference solutions of the Saint-Venant equations shown in equation (3.7) and (3.8):

$$\frac{\partial u}{\partial t} = \frac{\partial Q}{\partial t} \quad (3.7)$$

$$\frac{\partial Q}{\partial t} = \frac{\partial \left(\frac{Q^2}{A} \right)}{\partial x} + gA \frac{\partial H}{\partial x} + gA(S_0 - S_f) \quad (3.8)$$

where

A = cross-sectional area normal to the flow;

Q = discharge;

g = acceleration due to gravity;

H = elevation of the water surface above a specified datum, also called stage;

S_o = bed slope;

S_f = energy slope;

t = temporal coordinate; and

x = longitudinal coordinate.

Equations (3.7) and (3.8) are solved using the well-known four-point implicit box finite difference scheme. This numerical scheme has been shown to be completely non dissipative but marginally stable when run in a semi-implicit form, which corresponds to weighting factor of 0.6 for the unsteady flow simulation.

In HEC-RAS, a default is 1, however, it allows the users to specify any value between 0.6 to 1. The box finite difference scheme is limited to its ability to handle transitions between subcritical and supercritical flow, since a different solution algorithm is required for different flow conditions. The said limitation is overcome in HEC-RAS by employing a mixed flow routine to patch solution in sub reaches.

3.5.2 Unsteady flow equations

A flow, in which quantity of liquid flowing per second is not constant, is called unsteady flow. The physical laws which govern the flow of water in a stream are:

- (1) the principle of conservation of mass or continuity equation, and
- (2) the principle of conservation of momentum or momentum equation.

Continuity equation

Consider the elementary control volume shown in Figure (3.7). In this figure, distance x is measured along the channel, as shown. At the midpoint of the control volume the flow and total

flow area are denoted $Q(x,t)$ and A_T , respectively. The total flow area is the sum of active area A and off channel storage area S .

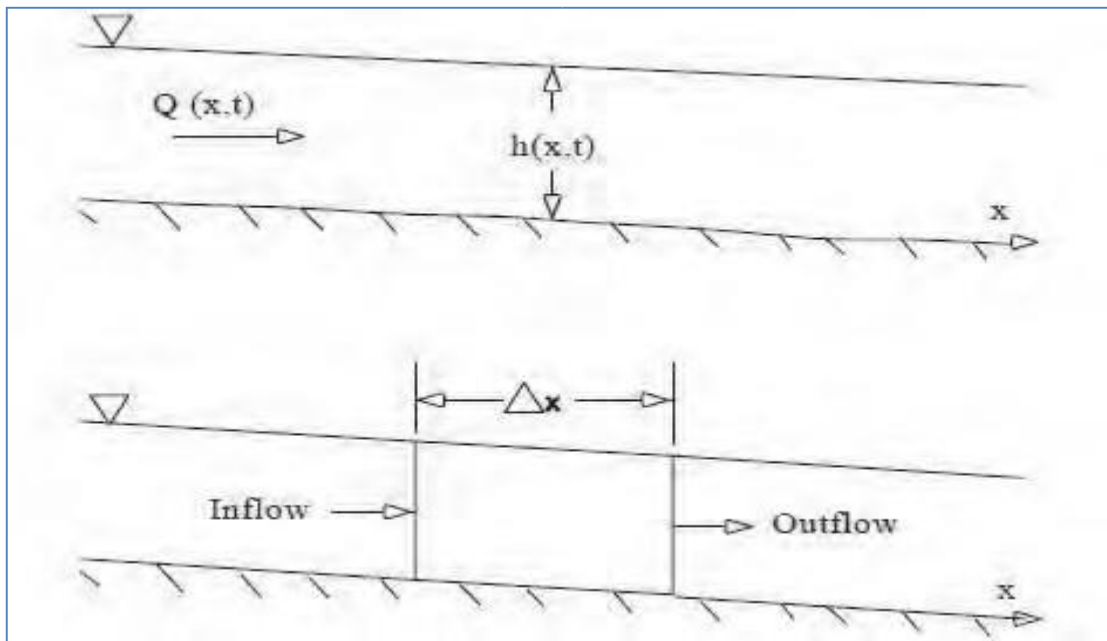


Figure 3.7: Elementary control volume for derivation of continuity and momentum equations

Simplifying form of the continuity equation is shown in equation (3.9) and (3.10).

$$\frac{\partial A_t}{\partial t} + \frac{\partial Q}{\partial x} - q_1 = 0 \quad (3.9)$$

$$\frac{\partial Q}{\partial t} + \frac{\partial Qv}{\partial x} + gA\left(\frac{\partial z}{\partial x} + S_f\right) = 0 \quad (3.10)$$

where

X =distance along the channel

t =time

Q =Flow

A =cross-sectional area

A_T = total flow area

q =lateral inflow per unit distance

g =acceleration due to gravity,

V =velocity

Z = elevation of water surface

S_f =friction slope.

Momentum equation

If F_p is the pressure force in the x direction at the midpoint of the control volume, the force at the upstream end of the control volume may be written as $F_p + \frac{\partial F_p}{\partial t} \frac{\Delta x}{2}$ and at the downstream end as $F_p - \frac{\partial F_p}{\partial t} \frac{\Delta x}{2}$.

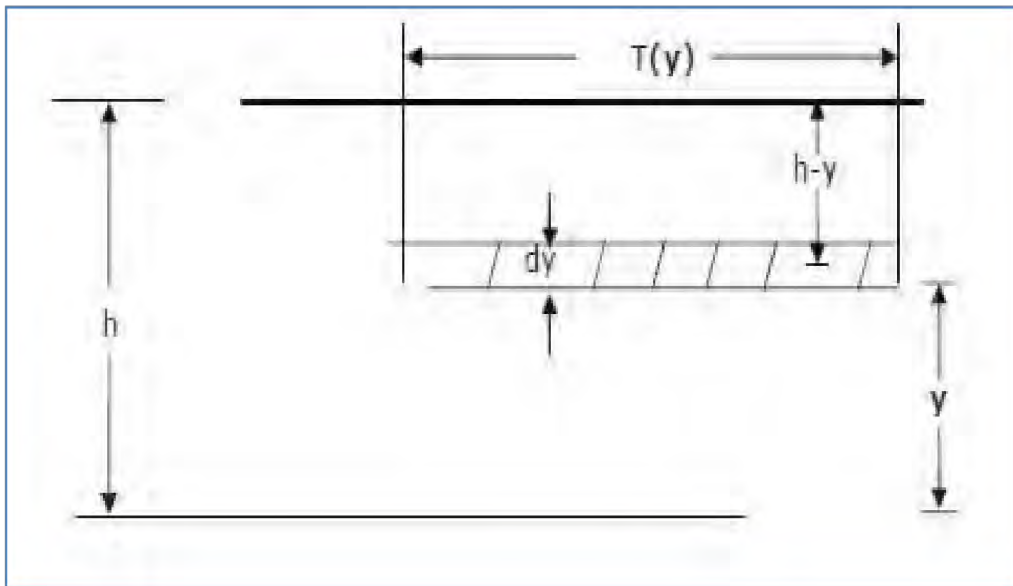


Figure 3.8: Illustration of terms associated with definition of pressure force

The final form of the momentum equation is shown in equation (3.11).

$$\frac{\partial Q}{\partial t} + \frac{\partial QV}{\partial x} + gA \left(\frac{\partial z}{\partial x} + S_f \right) = 0 \quad (3.11)$$

Chapter 4

Data Collection and Methodology

4.1 General

The main objective of this thesis was to prepare the long- and short-reach models for the Atrai River. The process started from data collection and finally the models were set up using HEC-RAS 5.0.3. For some analyses, Google Earth and ArcGIS were used as well. Finally, the water levels were simulated and the results were compared. The whole process is described in this chapter.

4.2 Data Collection

The river bathymetric data and hydrologic data (discharge and water level data) were required for this study. In this study following data was collected:

- i. River cross-sections data
- ii. WL data of Atrai
- iii. Discharge data of Atrai
- iv. DEM of study area

4.2.1 Cross-section data

The cross-section data of the Atrai River at 134 locations were collected from a hydrographic survey data conducted by LGED. Co-ordinates of location of stations and bathymetric data of these different stations were collected in this process and used in this study.

4.2.2 Discharge and water level data

Water level and discharge data of the Atrai River were collected from BWDB from 1985 to 2019. The selected BWDB stations for this study are station 144 (Chak Haripur), station 145 (Mohadebpur), station 147 (Atrai Rly. Bridge) and station 147.5 (Singra). All four of them are non-tidal water level and discharge station. Both discharge and water levels data were collected for all the four stations.

4.2.3 DEM data

The DEM of the Bangladesh was collected from the NASA USGS website. The DEM had a resolution of 30m. The DEM for the study area then was clipped from the DEM of Bangladesh.

4.3 Model Preparation

The short- and long-reach models were prepared in HEC-RAS 5.0.3. For model preparation and information extraction, some steps were followed.

4.3.1 Drawing of the left and right banks in Google Earth

Using Google earth, right bank and left bank of the Atrai river were drawn which covers the study area Patnitola, Mohadebpur, Manda and Atrai. The shapefile was exported as kmz file. The following Figure 4.1 shows the river-banks of the study river.

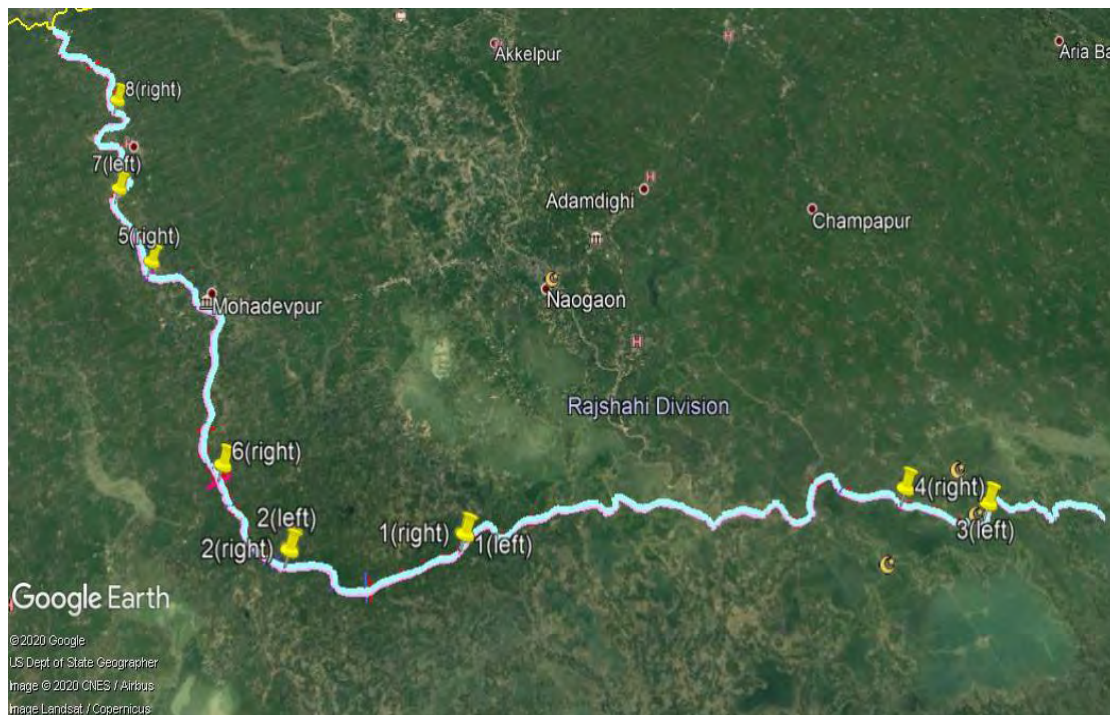


Figure 4.1: River-banks of the Atrai River from Google Earth

4.3.2 Georeferencing of the river-banks using ArcGIS

The study area of the Atrai River was georeferenced using ArcMap 10.2.2 georeferencing tool. The collected co-ordinates of 8 locations in the study area were used as control points for georeferencing. The following Figure 4.2 shows the georeferencing process of ArcGIS.

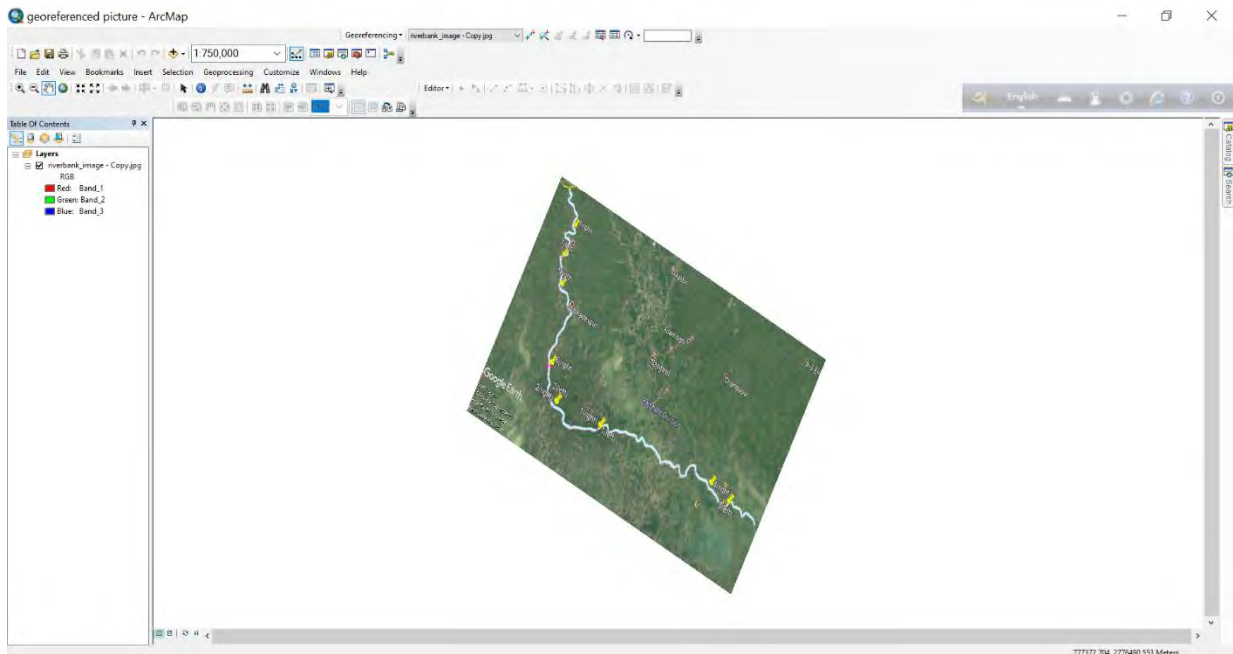


Figure 4.2 : Georeferencing of study area using ArcMap 10.2.2

After georeferencing the shapefile of the Atrai River edge is drawn in ArcGIS. It helped in further analysis and production of the necessary maps of the study area.

4.3.3 Marking of cross-section location from Google Earth

Using google earth, right bank and left bank of the Atrai River were drawn which covers the study area Patnitola, Mohadebpur, Manda and Atrai upazilas. In this study area, the co-ordinates of control points were collected from which the cross-sections were measured. These points were identified from given co-ordinates and were marked at google earth. For Patnitola, Mohadebpur and Manda upazilas, the river bathymetric data or cross-section data were available at 50m, 100m, 200m, 300m, 500m, 1000m, 1500m, 2000m distance for both upstream and downstream from the reference points. For Atrai upazila, the cross-section data were available at 100m, 200m, 300m, 500m, 1000m, 1500m, 2500m, 3000m for both upstream and downstream from the reference point.

4.3.4 Estimation of reach lengths

The consecutive distances of the model cross-sections were estimated from the ruler tool of Google Earth. All the 134 river cross sections were drawn in Google Earth and the distances of LOB, ROB and Channel were calculated.

The stations were named from station 3 to station 136 where station 136 was the first station at upstream and station 3 was the last station at downstream.

4.3.5 River-bank data extraction from AutoCAD

In order to get the bank station data for model, the banks of all 134 river cross sections were identified from the collected AutoCAD files of the study area. After analyzing the files, the river-bank data of all the river cross sections were extracted. The following Table 4.2 represents the river-bank data of the Atrai River.

4.3.6 Slope analysis

For determining the slope of the river for steady flow analysis, the Water Level data of BWDB stations 144, 145, 147 and 147.5 were used. BWDB Water level data from year 1985 to 2014 of these 4 stations were analyzed. The Water level of each simulation year of a particular station was sorted and the corresponding water level of the next station at the same time was identified. The slope between the two stations was defined by the difference between the water levels divided by the linear distance of the two consecutive stations using the Equation 4.1.

$$\text{Slope} = \frac{\text{Water level difference between stations}}{\text{linear distance between stations}} \quad (4.1)$$

For the long-reach model, station 144 and station 147.5 were used. For short-reach model of upstream, station 144 and 145 and for short-reach model of downstream, station 147 and 147.5 were used in the flow data as normal downstream slope.

4.3.7 Rating curve development

The discharge data of BWDB stations 144, 145, 147 and 147.5 were collected earlier. The flow data had some missing entries for each station. So, a rating curve was developed for each station and the value of daily discharge is extracted from daily water level data with the generated rating

curve. The rating curves for stations 144, 145, 147 and 147.5 are shown in the Figures 4.3, 4.4, 4.5, & 4.6.

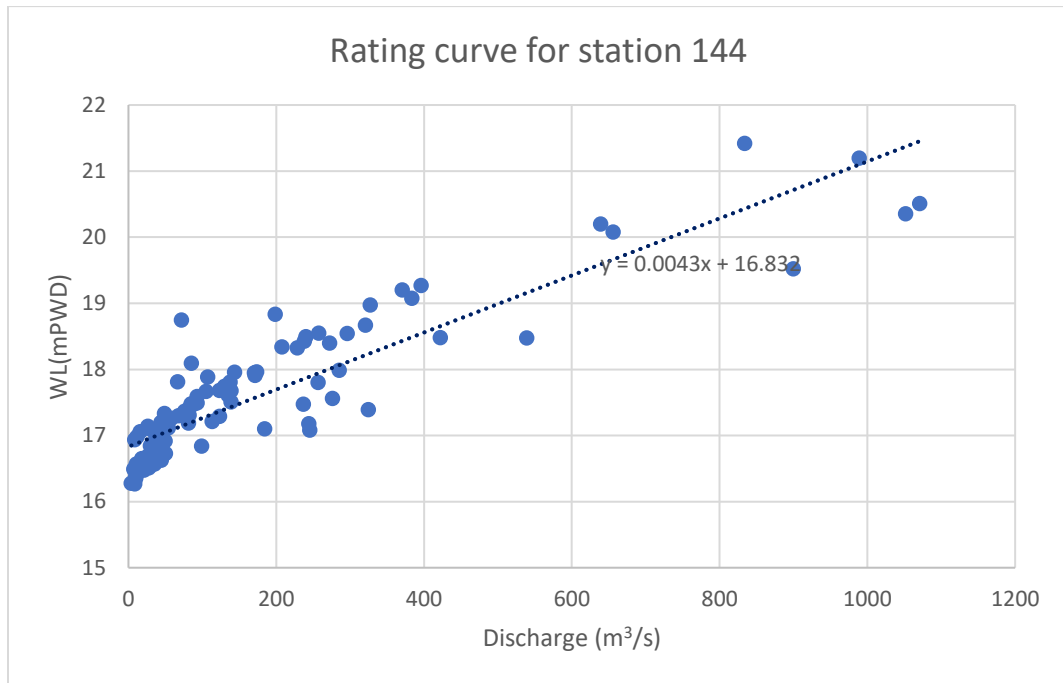


Figure 4.3: Rating curve for station 144

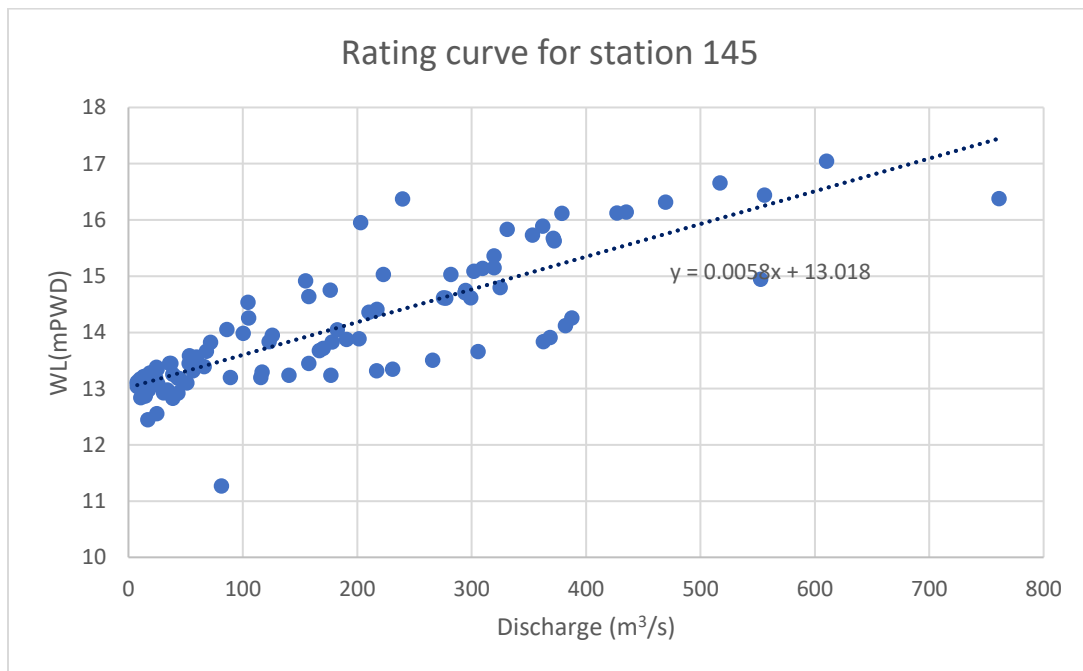


Figure 4.4: Rating Curve for station 145

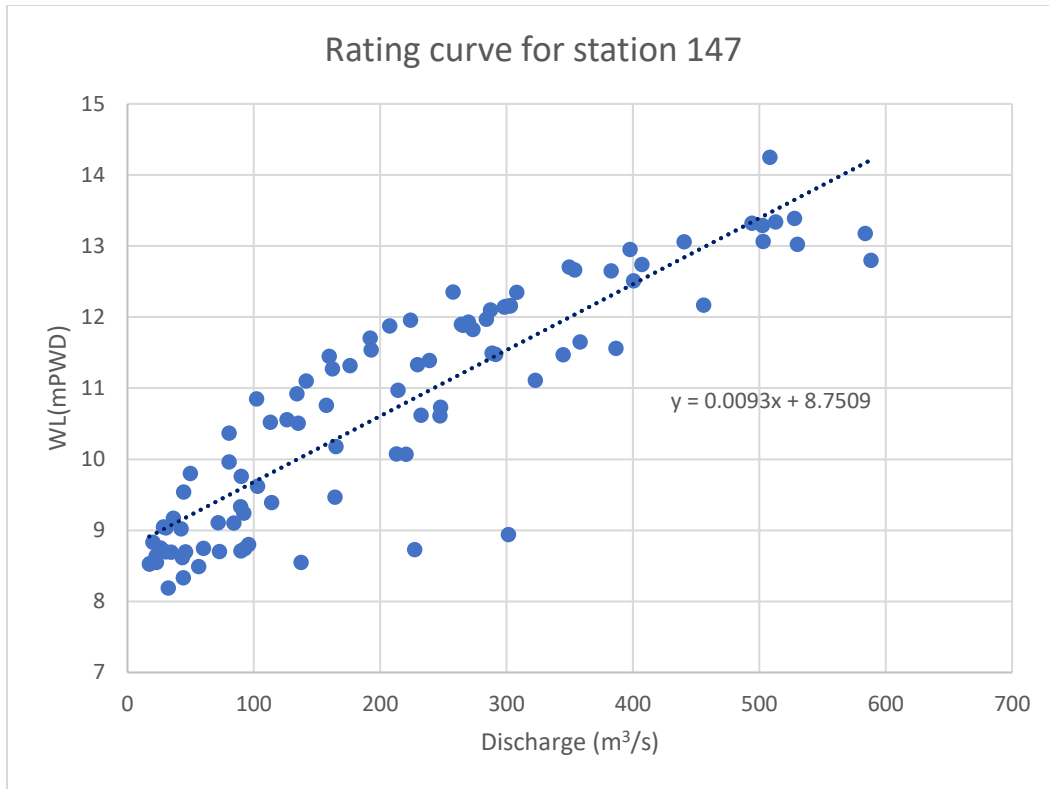


Figure 4.5: Rating Curve for station 147

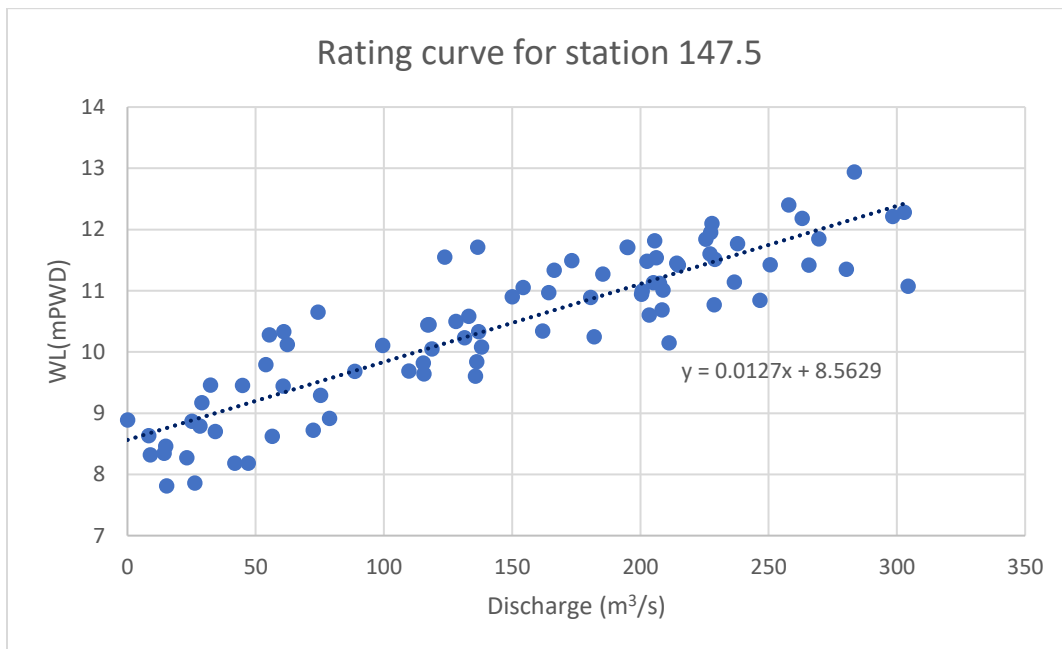


Figure 4.6: Rating Curve for station 147.5

The developed rating curves were kept linear as the data fit in linear form mostly for the stations. Specially for station 144,145 and 147.5 the linear form is quite a good fit for the data set. So, non-linear equations for rating curve weren't developed. Moreover, the missing data were not too significant in numbers. So, the rating curves were mostly kept as linear.

4.3.8. Adjustment of DEM

The DEM of Bangladesh was collected from the USGS website of the Shuttle Radar Topographic Mission of NASA. The Upazilas where the study river flows are extracted and the DEM was clipped according to the study area where the Atrai river reach is situated with the help of "Extraction by Mask" tool of ArcGIS. The DEM of study area comprises of a resolution of 30 m x 30 m. The clipped DEM of the study area is shown in Figure 4.7.

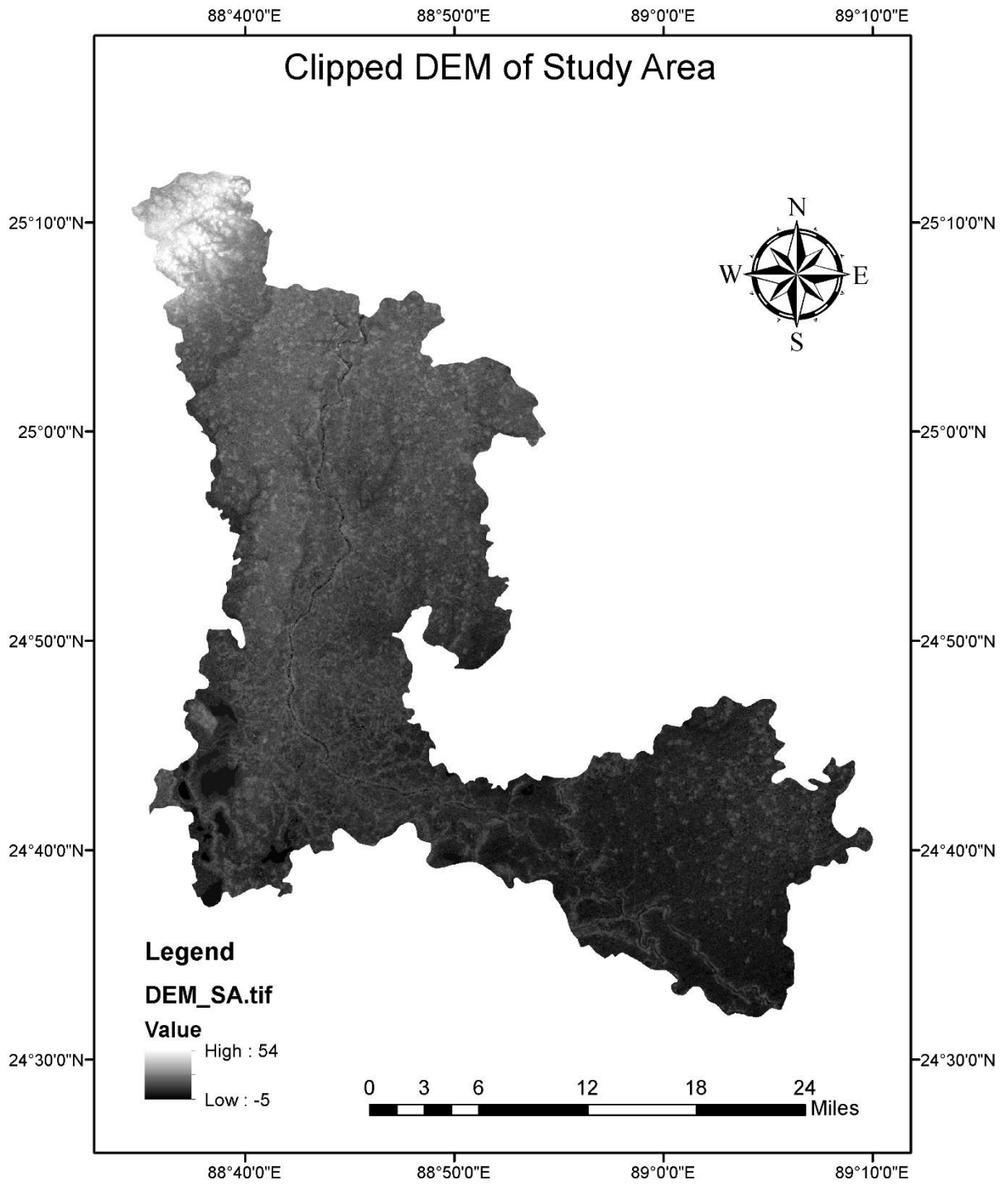


Figure 4.7: DEM of the study area

The elevation of the DEM was measured with respect to the MSL. In this study all the elevations including topography of river cross sections, water surface elevations were considered are measured from Public Works Datum (PWD). PWD is a horizontal datum believed originally to have zero at a determined MSL at Calcutta. PWD is located approximately 1.5 ft (0.46 meter) below the MSL established in India under the British Rule and brought to Bangladesh during the Great Trigonometric Survey. To adjust this difference in elevation, a slight modification of the collected DEM was done using the following equation:

$$\text{Adjusted DEM} = \text{DEM} - 0.46 \text{ (m)} \quad (4.2)$$

One of the limitations of this DEM is it is not calibrated with the measured data. But there has been no specific study in Bangladesh to show that how much deflected the SRTM DEM is from the real data at any specific station. So, it was the best option to adjust the DEM using the above equation where a constant difference of 0.46m was considered for all the stations of Bangladesh.

After this adjustment process, the adjusted or modified DEM was generated using “Raster Calculator” tool of ArcGIS by executing this equation. The modified DEM is shown in Figure 4.8.

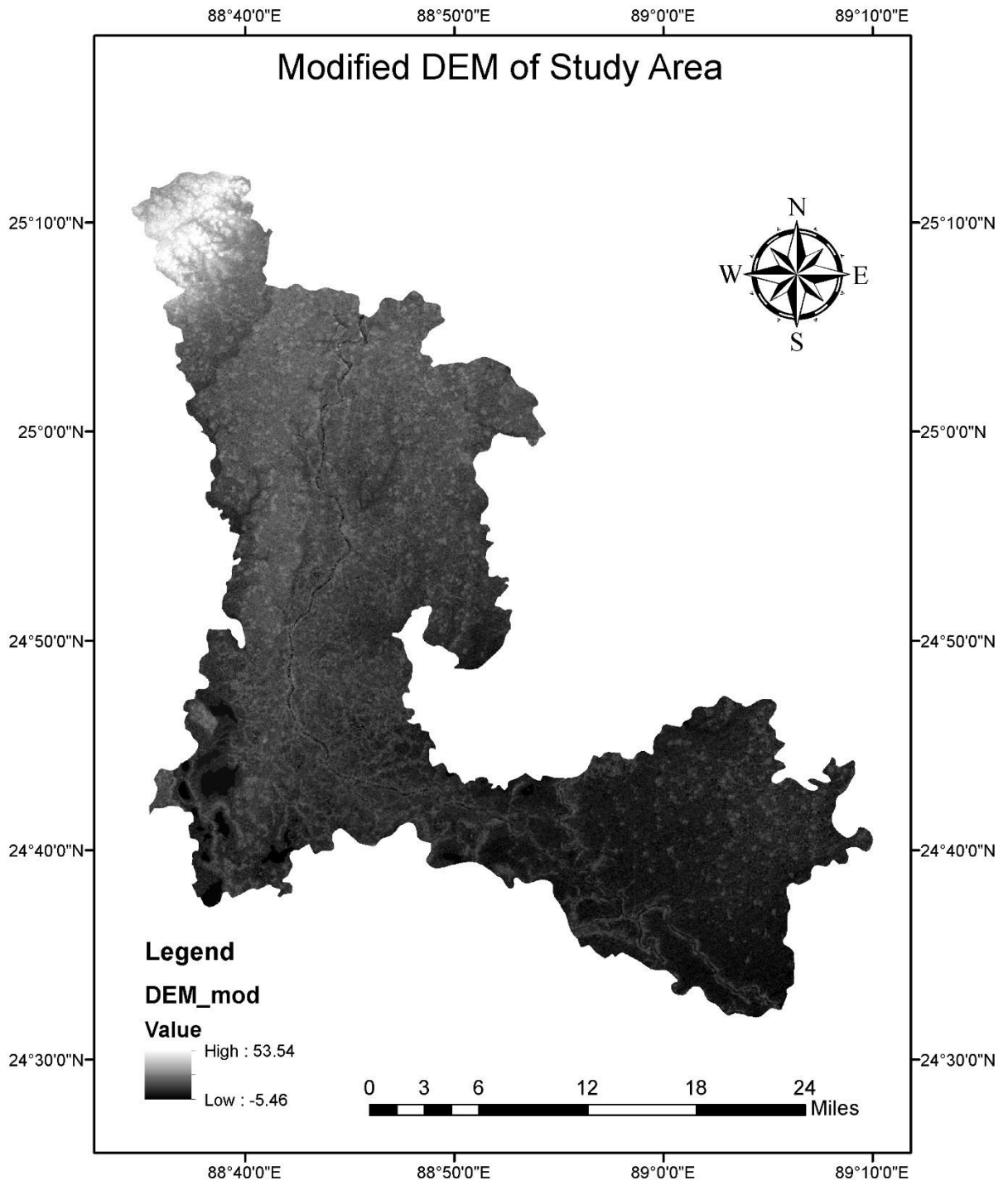


Figure 4.8: Modified DEM of the study area

4.3.9 Conversion of adjusted DEM to Triangulated Irregular Network

The adjusted DEM was converted from raster to a Triangulated Irregular Network. The purpose of the Raster to TIN tool is to create TIN whose surface does not deviate from the input raster by more than a specified Z tolerance. It is used to convert raster from a DEM to a TIN surface model. It is done by using the “Raster to TIN” tool of the ArcToolbox. The TIN of study area is shown in the Figure 4.9.

The purpose of producing the DEM and TIN was to collect the elevation data of the storage areas surrounding the river.

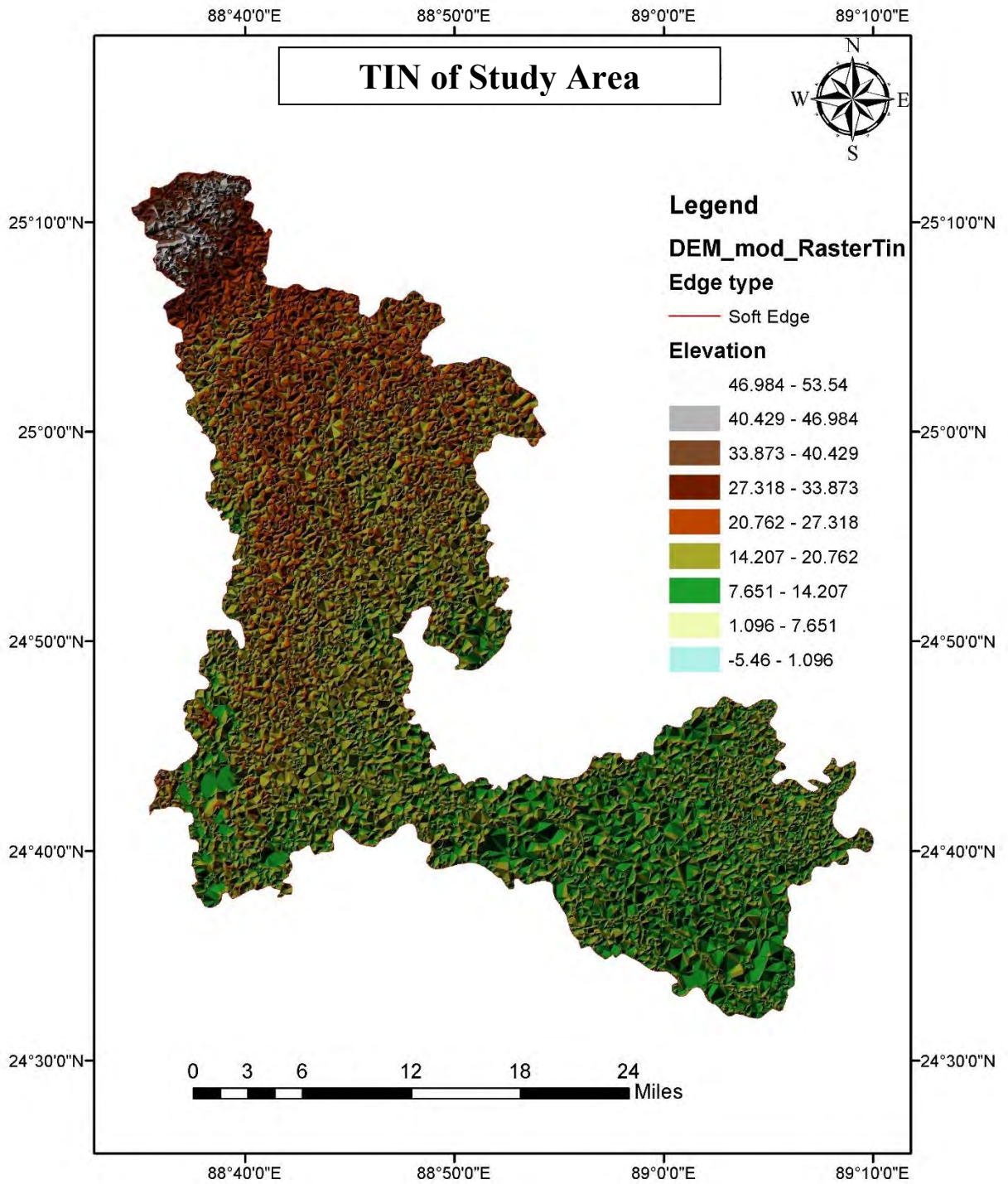


Figure 4.9: TIN of the study area

4.3.10 Storage area identification

The storage areas surrounding the study area were identified from the Google Earth. The area between surrounding road and the river was taken as the storage areas. If there was no road nearby in some places, then area within 100 m distance from the river was taken as the storage areas. Some polygons were drawn in Google earth to identify them. The polygons were drawn on them using “Add polygon” tool and their surface areas were measured using “Ruler” tool of google earth. In Figure 4.10, the blue polygons represent the storage areas in both side of the Atrai River.

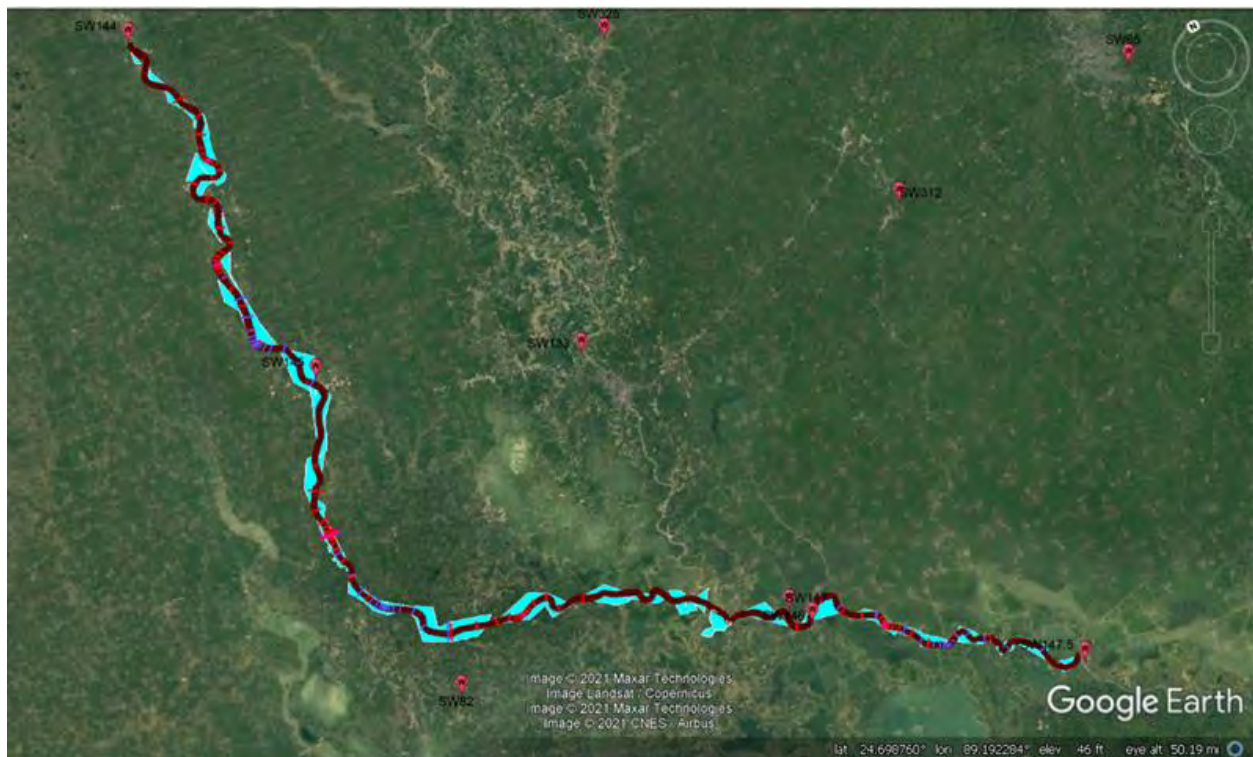


Figure 4.10: Identification of storage areas from Google Earth

4.4 Model Set Up

For setting up the hydrodynamic model in HEC-RAS, geometric data and flow data needs to be given as input.

4.4.1 Geometric data input

Long-reach model:

For long-reach model, geometric data was given as input for 134 stations. The stations were named from station 136 to station 3. The stations were interpolated at a distance of 50 m. HEC-RAS identifies the higher order station as the upstream station and the lower order station as downstream station.

Storage area addition:

Storage areas are lake like regions in which water can be diverted into or from. Storage areas can be located at the beginning of a reach as an upstream boundary to a reach, at the end of a reach as a downstream boundary to a reach, or they can be located laterally to a reach.

In this study, storage areas are added using storage area drawing tool of geometric editor. Then in storage area editor, the information about storage area was given as input. It can be given in two ways:

- Area times depth method
- Elevation vs volume curve

Short-reach model:

For short-reach model at the upstream reach, geometric data was given as input from station 136 to station 124. The stations were interpolated at a distance of 50 m. HEC-RAS identifies the higher order station as the upstream station and the lower order station as downstream station.

On the other hand, for short-reach model at the downstream reach, geometric data was given as input from station 6 to station 3. The stations were interpolated at a distance of 50m. HEC-RAS identifies the higher order station as the upstream station and the lower order station as downstream station.

4.4.2 Flow data input

Flow data needs to be given as input for both steady and unsteady flow simulation of both short- and long-reach models.

Steady flow:

For steady flow simulations, two types of flow data were given as input depending on the boundary conditions. In this study, two boundary conditions were used.

1. Discharge at upstream station and water level at downstream station
2. Discharge at upstream station and slope at downstream station

Unsteady flow:

For unsteady flow simulations, two types of hydrographs were given as input depending on the boundary conditions. In this study, flow hydrograph at upstream station and stage hydrograph at downstream station were used as boundary conditions.

The flow hydrograph and stage hydrograph of 2016 used in this study are showed in Figures 4.11 and 4.12.

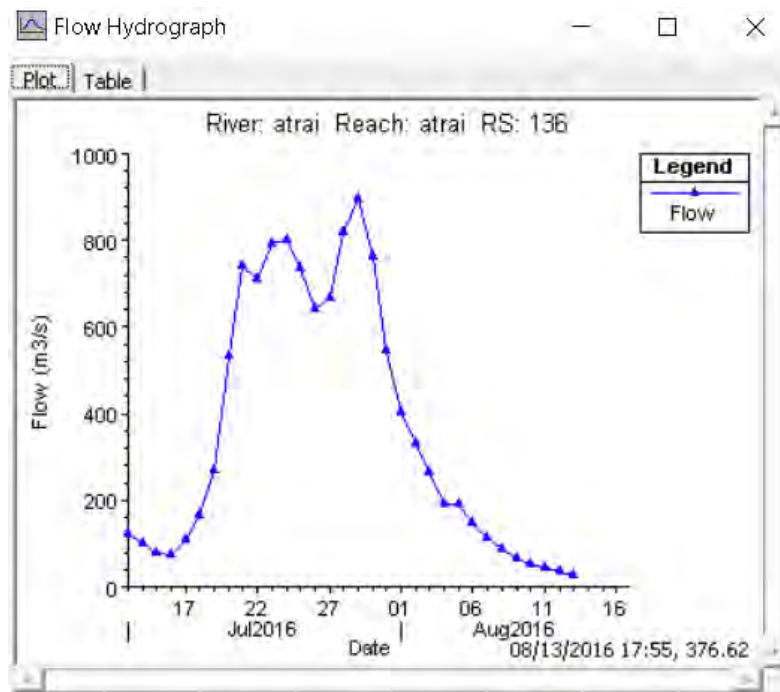


Figure 4.11: Flow hydrograph in unsteady flow simulation for 2016

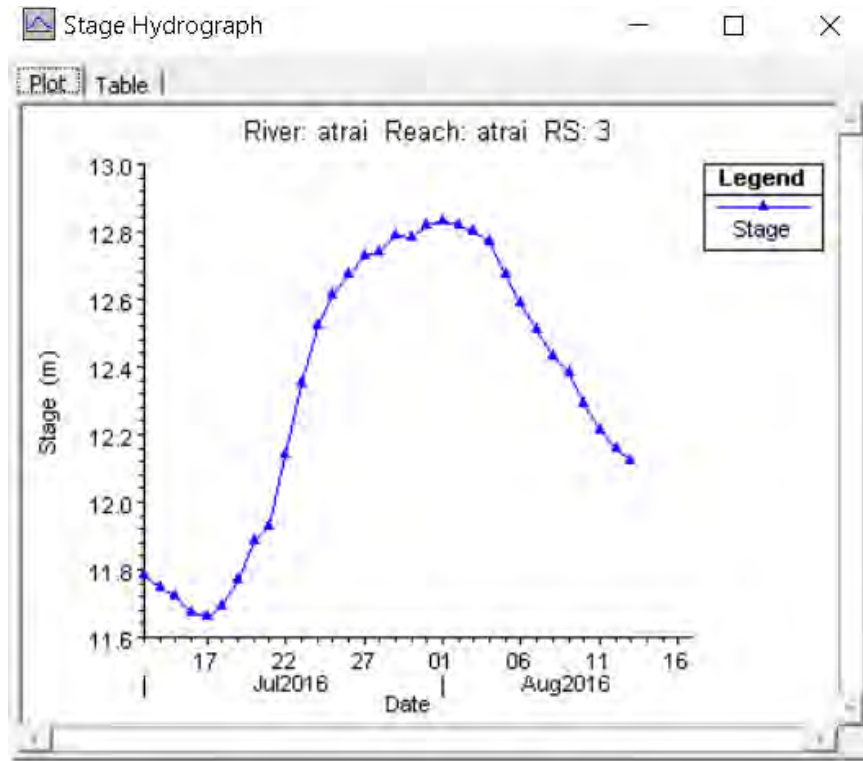


Figure 4.12: Stage hydrograph in unsteady flow simulation of 2016

4.5 Flow Simulation with Model

After setting up all the short- and long-reach hydrodynamic models, the flood levels were simulated for both steady and unsteady flow conditions for the 1998, 2006, 2014 and 2018 flood seasons with different boundary conditions. Model simulated and observed water levels for both steady and unsteady flow were compared.

For flood season 1998, the maximum discharge of the year was observed at 6 September. The one-dimensional model was run for both steady and unsteady flow module for 30 days from 22 August to 20 September so that the peak discharge can be captured. For flood season 2006, the maximum discharge of the year was observed at 17 July. The one-dimensional model was run for both steady and unsteady flow module for 30 days from 16 July to 14 August so that the peak discharge can be captured at starting. For flood season 2014, the maximum discharge of the year was observed at 24 September. The water levels in 1D model were simulated for both steady and unsteady flow module for 30 days from 10 September to 9 October so that the peak discharge can be captured. For flood season 2018, the maximum discharge of the year was observed at 8 July. The water levels in 1D model were simulated for both steady and unsteady flow module for 30 days from 24 June to 23 July so that the peak discharge can be captured.

The model was calibrated and validated by adjusting the manning's roughness co-efficient 'n' using 2016 flood season. The model performance was evaluated based on a number of criteria such as Root Mean Square Error, Mean Absolute Error, Relative Mean Absolute Error, Co-efficient of Determination, Relative Bias, Efficiency Index.

4.6 Model Calibration and Validation

To simulate the water level with base and different flow conditions, it is necessary to test the model's authenticity and performance. This testing provides an impression about the degree of the accuracy of the model in reproducing river processes. This process is known as calibration which is a must for all numerical models before using it for further simulation.

Similarly, for this study, it is important to calibrate the model in order to ascertain the performance of the model. The flood event of 2013 was used for calibration of the one-dimensional HEC-RAS model. The calibration parameter was Manning's roughness co-efficient 'n'. The 'n' value of 0.025 for main channel and 0.030 for Left and Right banks was found to be most effective for this model. The calibration was done for the period of 27 June to 26 July, 2013. The calibration is shown in Figure 4.13 by comparing the observed and simulated water levels for both steady and unsteady flow modules at Mohadebpur station for 2013.

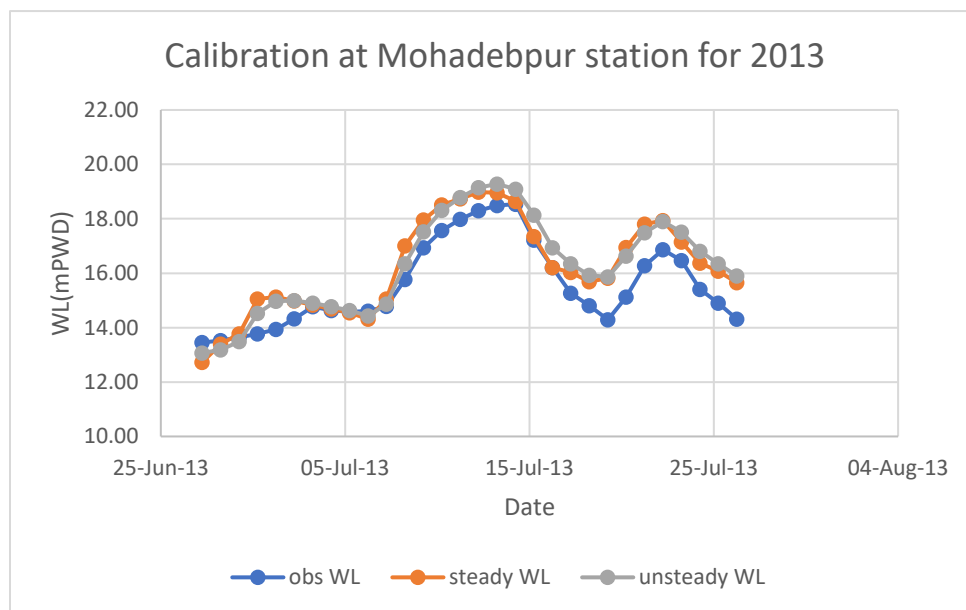


Figure 4.13: Calibration using 2013 flood year

Model validation involves testing of a model with a data set representing ‘observed’ field data. This data set represents an independent source different from the data used to calibrate the model. Due to the uncertainty of prediction, this step is very important prior to widespread application of the model output. The flood event of 2016 was used for validation of this model. The validation of the model was done for the period of 13 July to 11 August, 2016. The validation is shown in Figure 4.14 by comparing the observed and simulated water levels for both steady and unsteady flow modules at Mohadebpur station at this time.

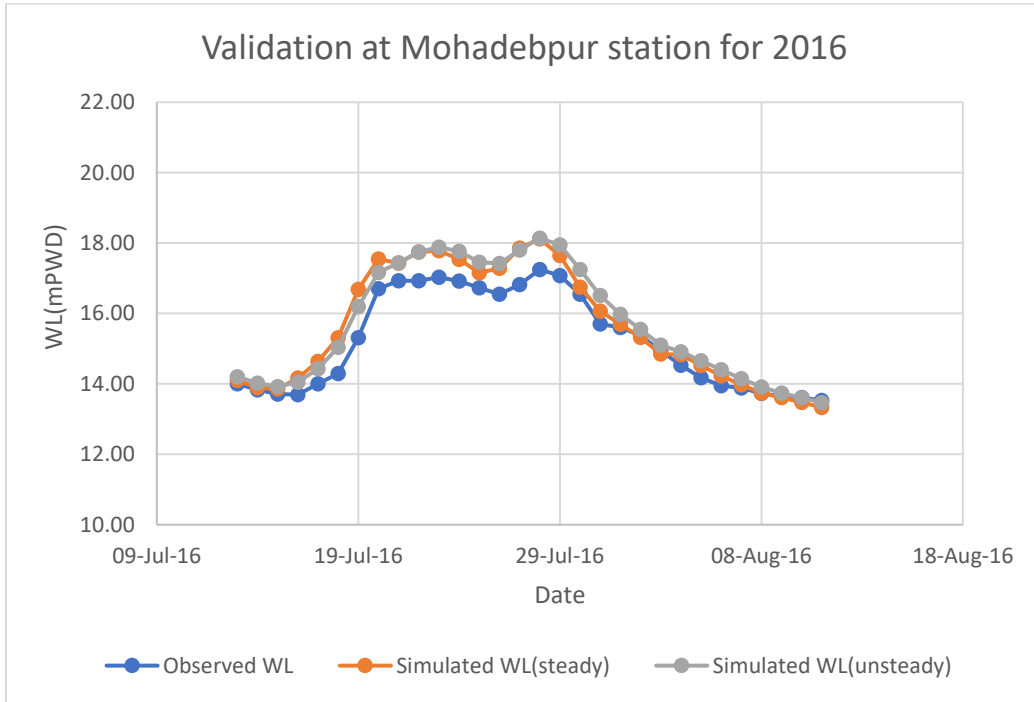


Figure 4.14: Validation using 2016 flood year

Chapter 5: Results and Discussions

5.1 General

In this chapter, the simulation results of the long- and short-reach models are analyzed and discussed.

5.2 Long-Reach Model Simulation Results

In long-reach model, the flood levels were simulated for four flood seasons of 1998, 2006, 2014 and 2018. The results of the model simulation are shown in this section.

5.2.1 Long-reach model result for 1998

After setting up the long-reach model in HEC-RAS 5.0.3, the model was run for 1998. This year was selected as it was a big flood year. The water levels were simulated for both steady and unsteady flow conditions. The upstream discharge of station 144 and the interpolated water level of station 147 and 147.5 was used as boundary conditions. In 1998, the maximum flow was observed on 06 September. The water levels were simulated in unsteady flow module for 1 month starting from 15 days before the peak flood means from 22 August to 20 September 1998. For comparing it with steady flow module in the same timeframe, steady flow run was done 30 times separately with observed discharge and water level data of the same time.

The comparison among observed, steady and unsteady water levels of 22August-20 September 1998 for stations 144, 145, 147 are shown in Figures 5.1, 5.2, 5.3.

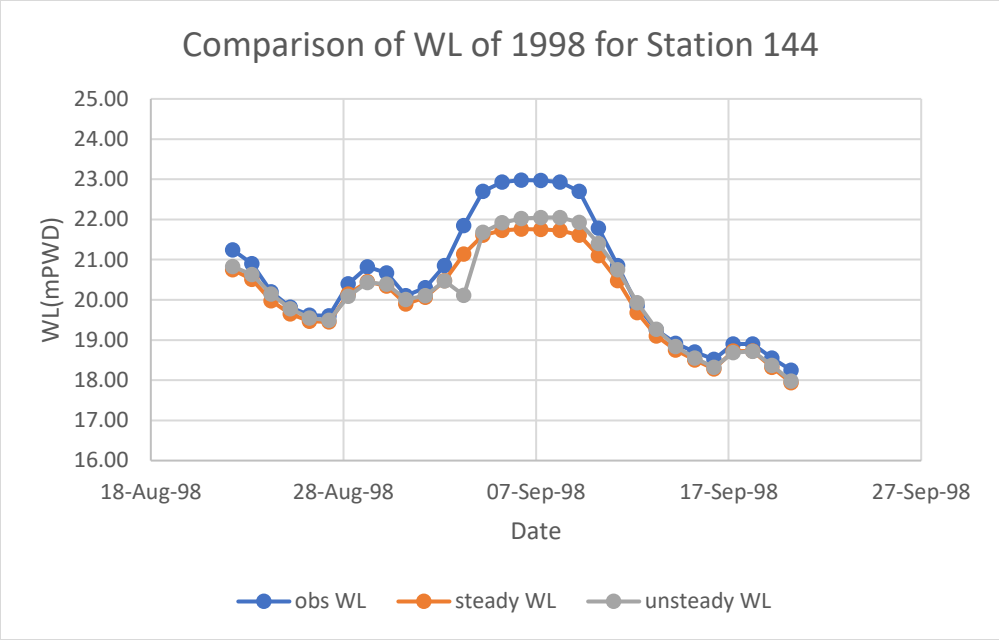


Figure 5.1: Comparison of WL of 1998 for station 144

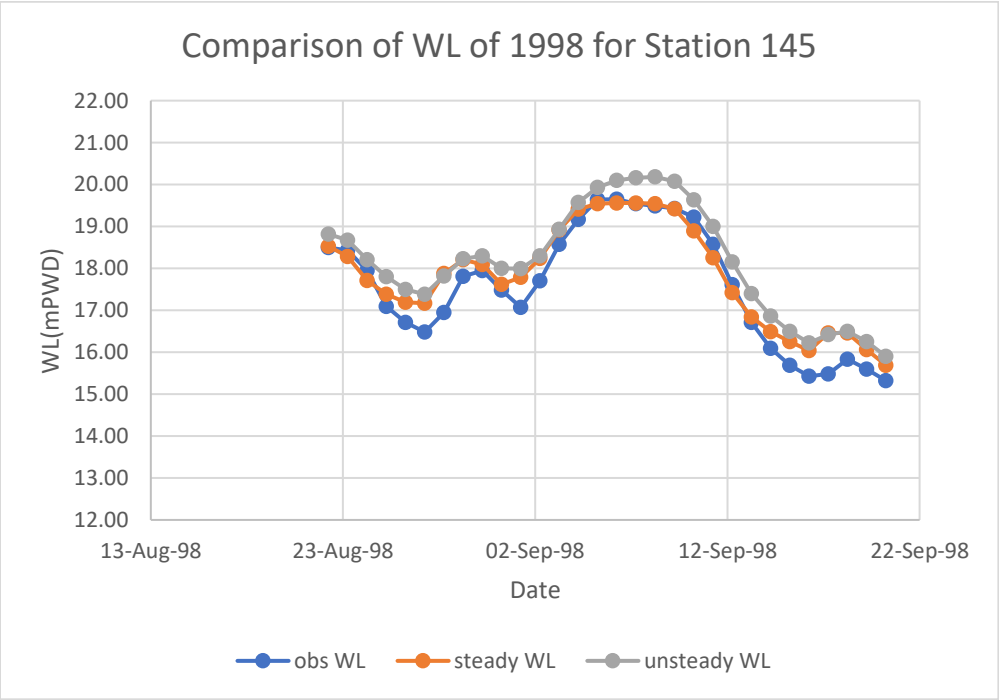


Figure 5.2: Comparison of WL of 1998 for station 145

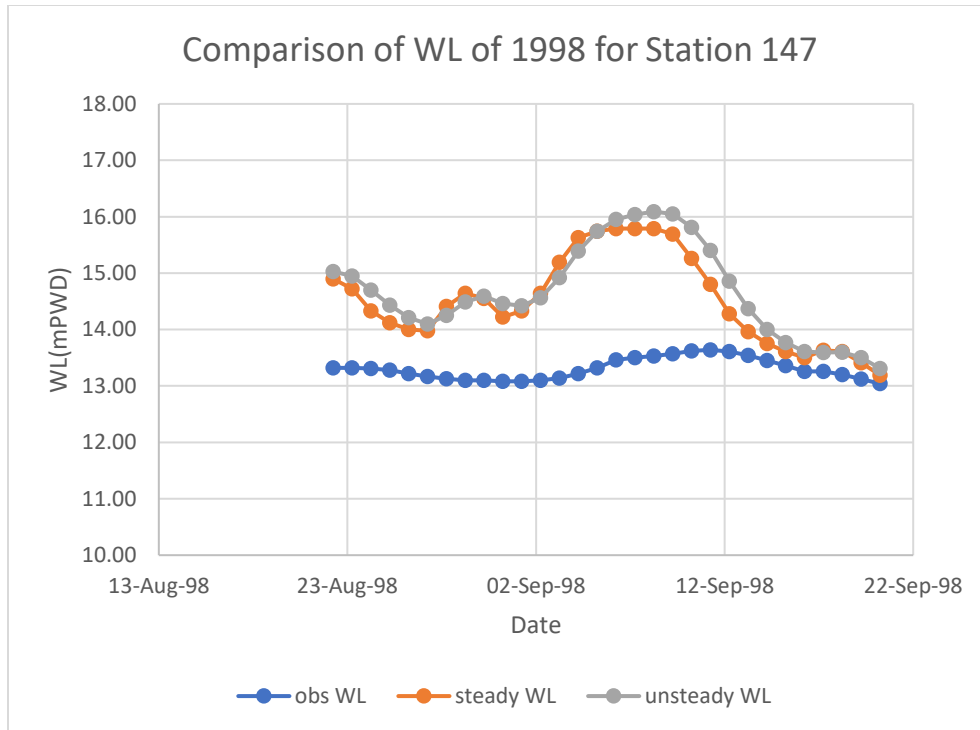


Figure 5.3: Comparison of WL of 1998 for station 147

For 1998, except for station 147 all the other stations could capture the overall trend of the observed data. For station 144, the falling phases of flood was quite well captured but the rising phase was estimated a bit lower in both steady and unsteady flow module. For station 145, both the rising and falling phase were very well captured. A bit different scenario was observed in station 147 where both the modules showed higher results in comparison to the observed water level. It can be interpreted that there can be a role of storage surrounding this station.

5.2.2 Long-reach model result for 2006

2006 flood event was used in this study as there was a moderate flood in this year. Thus, the water levels were simulated for both steady and unsteady flow conditions keeping the same boundary condition for 2006. From the observed data, the maximum water level was found at 17 July. The steady and unsteady flow simulation was done for 1 month that includes the peak value. Thus, the water levels were simulated from 16 July to 14 August 2006.

The comparison among observed, steady and unsteady water levels of 16 July-14 August 2006 for stations 144, 145, 147 are shown in Figures 5.4, 5.5, 5.6.

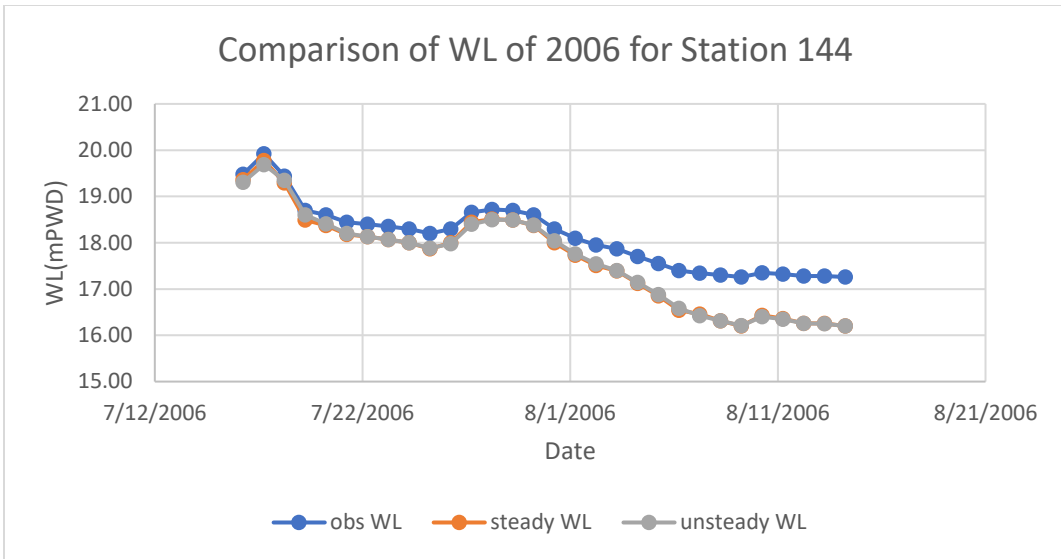


Figure 5.4: Comparison of WL of 2006 for station 144

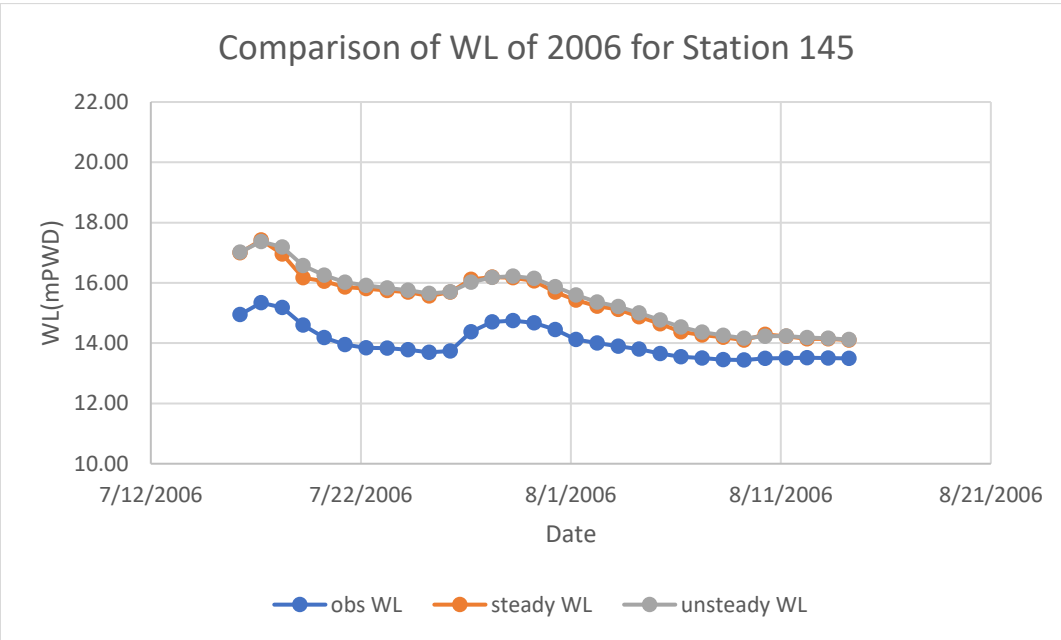


Figure 5.5: Comparison of WL of 2006 for station 145

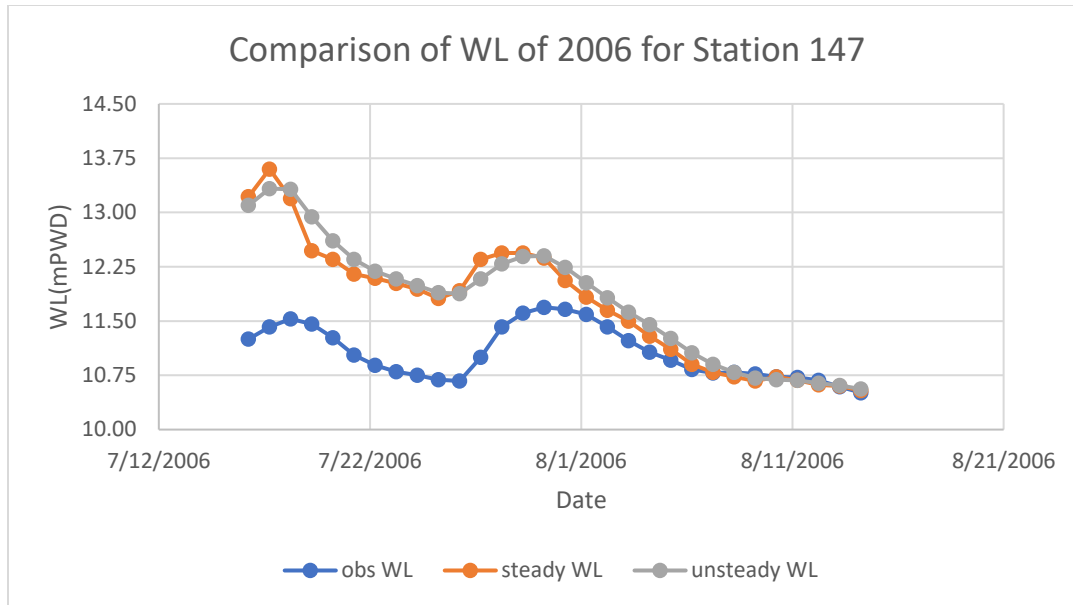


Figure 5.6: Comparison of WL of 2006 for station 147

For the flood year of 2006, the model could capture the overall trend better than 1998. In station 144, the rising phase was very well captured but slightly deviation was observed in the falling phase. For station 145, the trend was captured well but the model slightly overestimated the water levels. For station 147, the trend was captured better in comparison to the year of 1998 specially the falling phase was well captured but in the rising phase the model overestimated the water levels. It again indicates the effect of storage areas surrounding this station.

5.2.3 Long-reach model result for 2014

After analysis with 1998 and 2006, the water levels were simulated for 2014. The water levels were simulated for both steady and unsteady flow conditions by keeping the same boundary conditions. In 2014, the maximum flow was observed at 24 September. The water level was simulated for 1 month starting from 15 days before the peak flood means from 10 September to 09 October 2014.

The comparison among observed, steady and unsteady water levels of 10 September-09 October 2014 for stations 144, 145, 147 are shown in Figures 5.7, 5.8, 5.9.

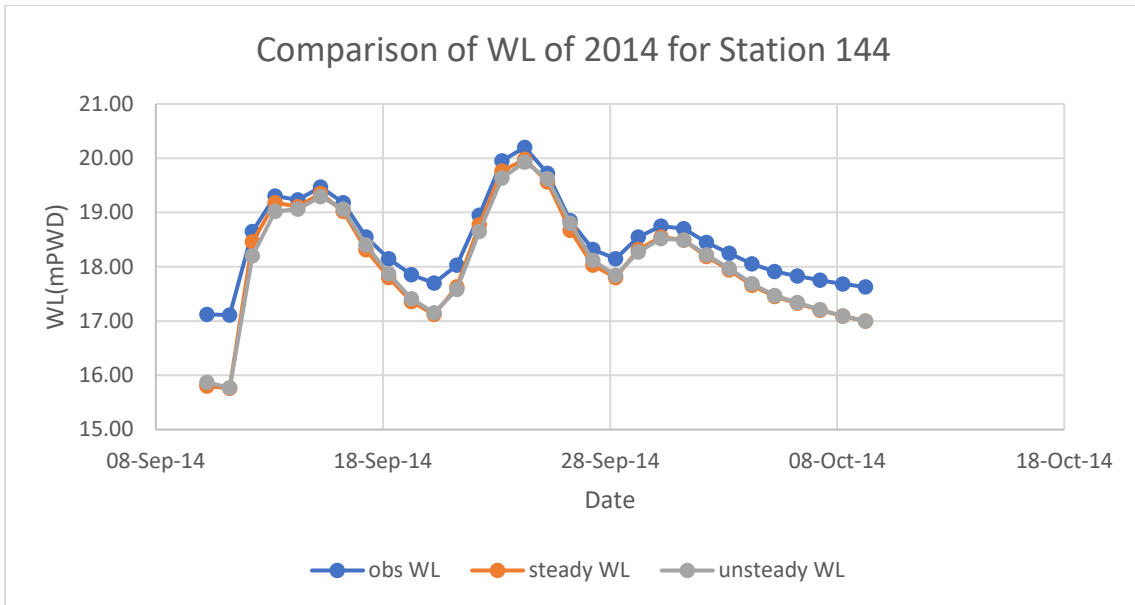


Figure 5.7: Comparison of WL of 2014 for station 144

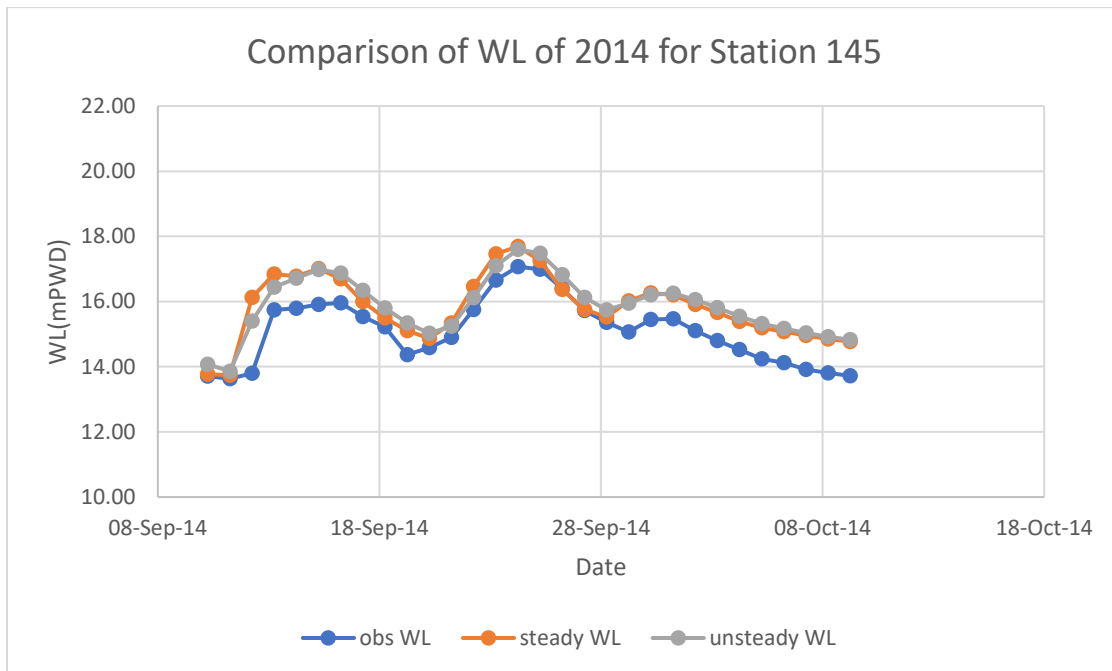


Figure 5.8: Comparison of WL of 2014 for station 145

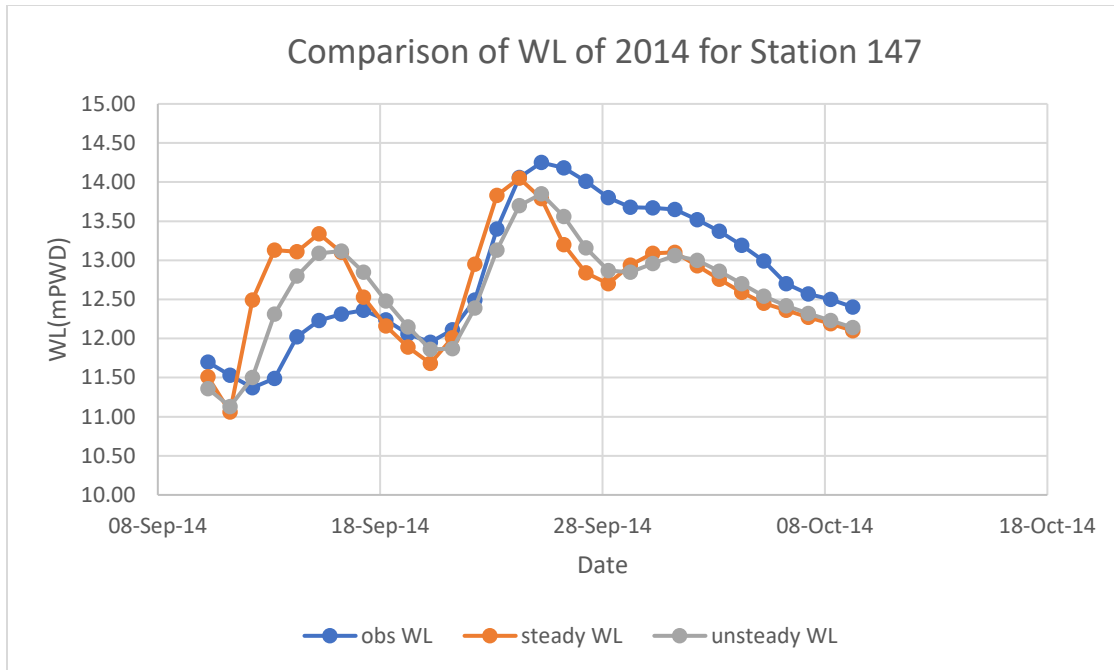


Figure 5.9: Comparison of WL of 2014 for station 147

For 2014, all the stations showed better results in comparison with all the other flood years. The overall trend of water levels matched with the observed data quite well. Station 144, 145 showed consistent better results. Specially there was significant improvement in the prediction of station 147 as well. It was observed that the storage areas surrounding this station was less in this year in comparison to the previous years because of human settlements. Thus, the influence of storage area was less in water level for this year. So, in long-reach model even without storage areas, the water level elevations matched with the observed data to a good extent.

5.2.4 Long-reach model result for 2018

At last the water levels were simulated for 2018. This year of 2018 is taken because the bathymetry data used in this study were also taken in this year. The water levels were simulated for both steady and unsteady flow conditions by keeping the same boundary conditions. In 2018, the maximum flow is observed at 8 July. The model is run for 1 month starting from 15 days before the peak flood means from 24 June to 23 July 2018.

The comparison among observed, steady and unsteady water levels of 24 June-23 July 2018 for stations 144, 145, 147 are shown in Figures 5.10, 5.11, 5.12.

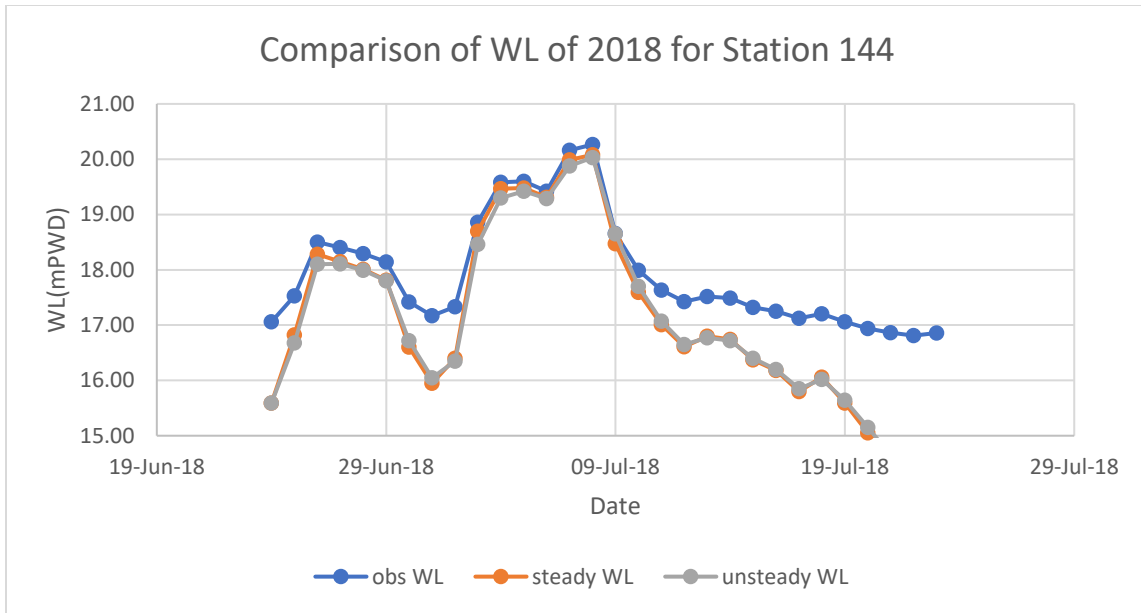


Figure 5.10: Comparison of WL of 2018 for station 144

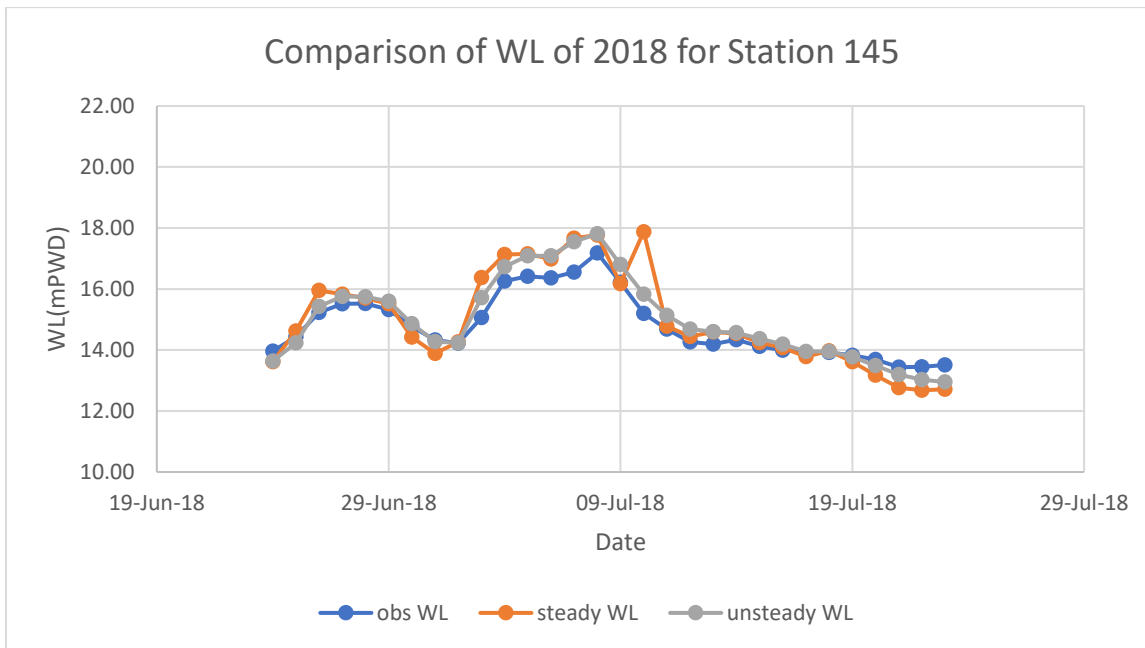


Figure 5.11: Comparison of WL of 2018 for station 145

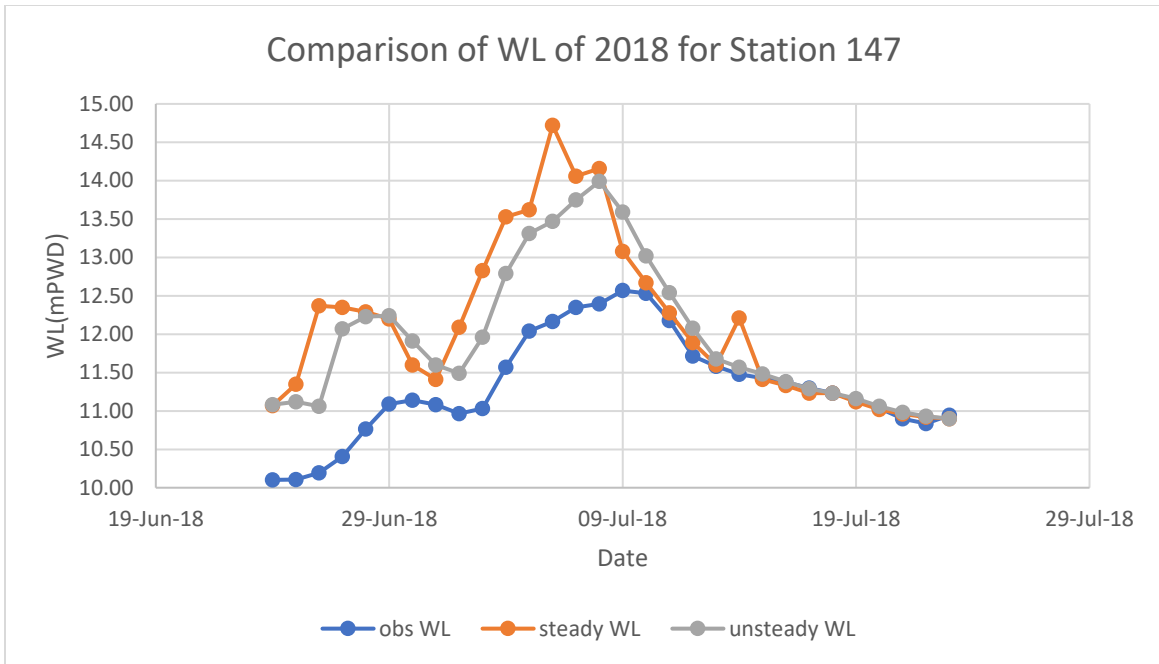


Figure 5.12: Comparison of WL of 2018 for station 147

For 2018, the results showed that for all the stations, the overall water level trend matched with the observed water level data. For station 144, the rising phase was well captured but in falling phase, the model estimated a bit lower value where in station 147 the rising phase was overestimated by the model but the falling trend was captured in a good manner. For station 145, both the rising and falling phase was quite well captured.

5.2.5 Long-reach model performance evaluation

Though there were several studies available for performance evaluation of model such as by Aitken (1973) and Fleming (1975), the method given by Nash and Sutcliffe (1970) is widely used in the area of hydrology and water resources for the detection of systematic errors with respect to long-term simulation. The long-reach model is evaluated by the following 6 criteria:

- i. Root Mean Square Error (RMSE)
- ii. Mean Absolute Error (MAE)
- iii. Relative Mean Absolute Error (RMAE)
- iv. Co-efficient of Determination or R^2
- v. Relative Bias
- vi. Efficiency Index (EI)

The RMSE, MAE, RMAE, Relative bias, Efficiency Index is given by the following equations:

$$\text{RMSE} = \sqrt{\frac{\sum_{i=0}^n (q_s - q_i)^2}{n}} \quad (5.1)$$

$$\text{MAE} = \frac{1}{n} \sum_{i=0}^n |q_s - q_i| \quad (5.2)$$

$$\text{RMAE} = \frac{\text{MAE}}{\frac{1}{n} \sum_{i=0}^n q_i} \quad (5.3)$$

$$\text{Relative Bias} = \frac{\frac{1}{n} \sum_{i=0}^n (q_s - q_i)}{\frac{1}{n} \sum_{i=0}^n q_i} \quad (5.4)$$

$$\text{EI} = \frac{\sum_{i=0}^n (q_i - \bar{q})^2 - \sum_{i=0}^n (q_i - q_s)^2}{\sum_{i=0}^n (q_i - \bar{q})^2} \quad (5.5)$$

where

q_i =observed WL at time i ;

\bar{q} =mean value of observed WL;

q_s =simulated WL at time i ;

and n =number of data points.

The model evaluation was done for both the steady and unsteady flow simulations of all four years 1998, 2006, 2014 and 2018.

At first the model was evaluated for 1998 by steady and unsteady flow simulations using all six criteria. The results are shown in the following tables:

Table 5.1: Model evaluation for 1998 using RMSE value (m)			
Station	Steady	Unsteady	Expected Value
144	0.59	0.56	0
145	0.43	0.62	0
147	1.41	1.55	0

Table 5.2: Model evaluation for 1998 using MAE value (m)			
Station	Steady	Unsteady	Expected Value
144	0.46	0.39	0
145	0.35	0.58	0
147	1.21	1.37	0

Table 5.3: Model evaluation for 1998 using RMAE value (m)			
Station	Steady	Unsteady	Expected Value
144	0.02	0.01	0
145	0.02	0.03	0
147	0.09	0.10	0

Table 5.4: Model evaluation for 1998 using R² value			
Station	Steady	Unsteady	Expected Value
144	0.98	0.95	1
145	0.95	0.98	1
147	0.16	0.35	1

Table 5.5: Model evaluation for 1998 using Relative Bias value			
Station	Steady	Unsteady	Expected Value
144	-0.68	-0.56	0
145	0.44	1.00	0
147	2.51	2.83	0

Table 5.6: Model evaluation for 1998 using Efficiency Index value			
Station	Steady	Unsteady	Expected Value
144	0.84	0.85	1
145	0.90	0.80	1
147	0.04	-0.14	1

Then the model was evaluated for 2006 for steady and unsteady flow simulations using all six criteria. The results are shown in the following tables:

Table 5.7: Model evaluation for 2006 using RMSE value (m)			
Station	Steady	Unsteady	Expected Value
144	0.60	0.60	0
145	1.43	1.52	0
147	0.93	0.96	0

Table 5.8: Model evaluation for 2006 using MAE value (m)			
Station	Steady	Unsteady	Expected Value
144	0.50	0.49	0
145	1.34	1.43	0
147	0.69	0.74	0

Table 5.9: Model evaluation for 2006 using RMAE value (m)			
Station	Steady	Unsteady	Expected Value
144	0.027	0.027	0
145	0.09	0.10	0
147	0.06	0.06	0

Table 5.10: Model evaluation for 2006 using R² value			
Station	Steady	Unsteady	Expected Value
144	0.98	0.97	1
145	0.82	0.81	1
147	0.47	0.52	1

Table 5.11: Model evaluation for 2006 using Relative Bias value			
Station	Steady	Unsteady	Expected Value
144	-0.82	-0.83	0
145	2.88	3.06	0
147	1.73	1.88	0

Table 5.12: Model evaluation for 2006 using Efficiency Index value			
Station	Steady	Unsteady	Expected Value
144	0.29	0.29	1
145	-5.48	-6.69	1
147	0.25	0.20	1

Then the long-reach model was evaluated for 2014 for steady and unsteady flow simulations using all six criteria. The results are shown in the following tables:

Table 5.13: Model evaluation for 2014 using RMSE value (m)			
Station	Steady	Unsteady	Expected Value
144	0.48	0.47	0
145	0.84	0.82	0
147	0.69	0.53	0

Table 5.14: Model evaluation for 2014 using MAE value (m)			
Station	Steady	Unsteady	Expected Value
144	0.37	0.38	0
145	0.71	0.76	0
147	0.57	0.46	0

Table 5.15: Model evaluation for 2014 using RMAE value (m)			
Station	Steady	Unsteady	Expected Value
144	0.02	0.02	0
145	0.04	0.05	0
147	0.04	0.03	0

Table 5.16: Model evaluation for 2014 using R² value			
Station	Steady	Unsteady	Expected Value
144	0.96	0.95	1
145	0.78	0.89	1
147	0.39	0.66	1

Table 5.17: Model evaluation for 2014 using Relative Bias value			
Station	Steady	Unsteady	Expected Value
144	-0.61	-0.62	0
145	1.41	1.51	0
147	-0.29	-0.44	0

Table 5.18: Model evaluation for 2014 using Efficiency Index value			
Station	Steady	Unsteady	Expected Value
144	0.61	0.62	1
145	0.26	0.29	1
147	-0.03	0.39	1

Then the model was evaluated for 2018 for steady and unsteady flow simulations using all six criteria. The results are shown in the following tables:

Table 5.19: Model evaluation for 2018 using RMSE value (m)			
Station	Steady	Unsteady	Expected Value
144	1.10	1.08	0
145	0.72	0.42	0
147	1.14	0.85	0

Table 5.20: Model evaluation for 2018 using MAE value (m)			
Station	Steady	Unsteady	Expected Value
144	0.85	0.85	0
145	0.49	0.34	0
147	0.80	0.64	0

Table 5.21: Model evaluation for 2018 using RMAE value (m)			
Station	Steady	Unsteady	Expected Value
144	0.04	0.04	0
145	0.03	0.02	0
147	0.07	0.05	0

Table 5.22: Model evaluation for 2018 using R² value			
Station	Steady	Unsteady	Expected Value
144	0.93	0.92	1
145	0.86	0.97	1
147	0.38	0.63	1

Table 5.23: Model evaluation for 2018 using Relative Bias value			
Station	Steady	Unsteady	Expected Value
144	-1.43	-1.44	0
145	0.43	0.43	0
147	1.97	1.59	0

Table 5.24: Model evaluation for 2018 using Efficiency Index value			
Station	Steady	Unsteady	Expected Value
144	0.06	0.10	1
145	0.56	0.84	1
147	0.16	0.52	1

From the standard criteria, it was found that for the year of 2014, the long-reach model result was better in comparison to other years. For both modules, the year of 2014 results were found as the best. On the other hand, between the comparison of steady and unsteady flow modules, the standard criteria show that unsteady flow module of the model was better than the steady flow module. The reason is quite obvious because the assumptions of velocity, density, discharge, etc. are considered constant with time in a steady flow module, whereas in an unsteady flow module there is no such assumption.

5.3 Comparison of Downstream Short-Reach Model and Long-Reach Model Using WL as Downstream Boundary Condition

The downstream short-reach model of 6 km was developed from station 147. The water levels were simulated for both steady and unsteady flow conditions using discharge of station 147 and interpolated water level of stations 147 and 147.5 as boundary conditions. The water levels were simulated for the years of 1998, 2006, 2014 and 2018, and compared with the long-reach model's results.

5.3.1 Comparison for 1998

The comparison of short- and long-reach model was done at first for the large flood year of 1998. The comparison is shown from 22 August to 20 September 1998. The downstream short-reach model's water levels were simulated for both steady and unsteady flows and the results were compared with the long-reach model's steady and unsteady flow simulation results at station 147 using the same boundary conditions.

The results showed that the short-reach model's unsteady flow module produces the best result in this scenario. The most deviated result was found for the long-reach unsteady flow module.

5.3.2 Comparison for 2006

Similarly, for 2006 the comparison between the downstream short-reach model and the long-reach model is shown from 16 July to 14 August 2006. The short-reach model water levels were simulated for both steady and unsteady flows and the results were compared with the long-reach model's steady and unsteady flow simulation results at station 147 using the same boundary conditions.

Like the year of 1998, the short-reach model performed better than the long-reach model and the unsteady flow module of the short-reach model performed the best.

5.3.3 Comparison for 2014

For the year of 2014, the comparison between the downstream short-reach model and the long-reach model was done for 10 September to 9 October. The short-reach model downstream water levels were simulated for both steady and unsteady flows and the results were compared with the long-reach model's steady and unsteady flow simulation results at station 147.

In this year, both long- and short-reach model's results were close, but the short-reach model performed better than the long-reach model. The unsteady flow module of the short-reach model was the best performed model among all.

5.3.4 Comparison for 2018

For 2018, the comparison between both the model types was shown from 24 June to 23 July. The short-reach model downstream water levels were simulated for both steady and unsteady flows and the results were compared with the long-reach model's steady and unsteady flow simulation results at station 147 using the same boundary conditions.

In this year, the short-reach model performed better than the long-reach model, and the unsteady flow module of the short-reach model performed the best.

The following Figures 5.13, 5.14, 5.15 and 5.16 show the comparisons of WL (mPWD) between the long- and short-reach downstream models at station 147 using WL as the downstream boundary condition for 1998, 2006, 2014 and 2018 respectively.

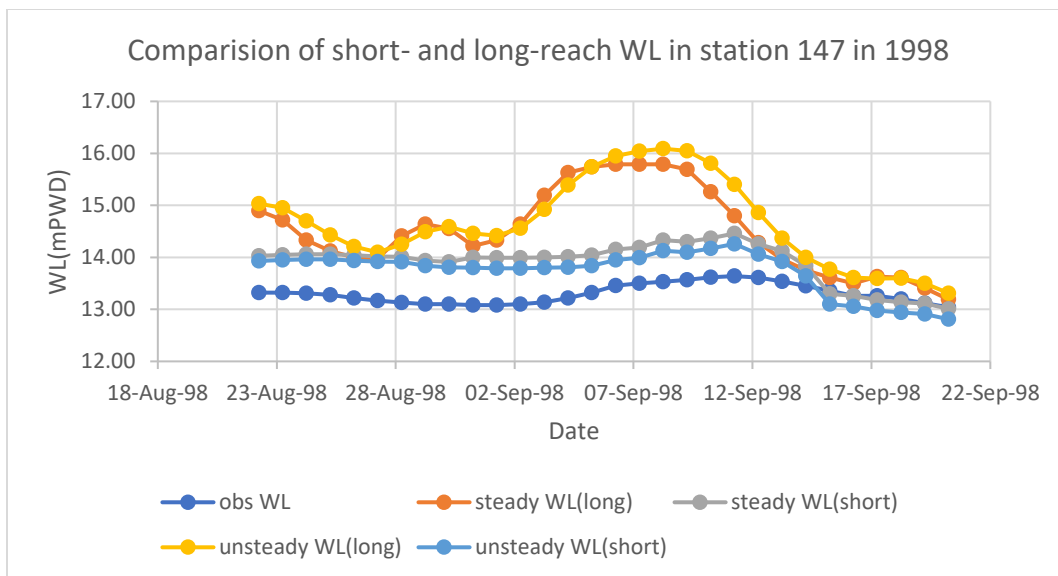


Figure 5.13: Comparison of WL of short- and long-reach model at station 147 for 1998 using downstream WL as boundary condition

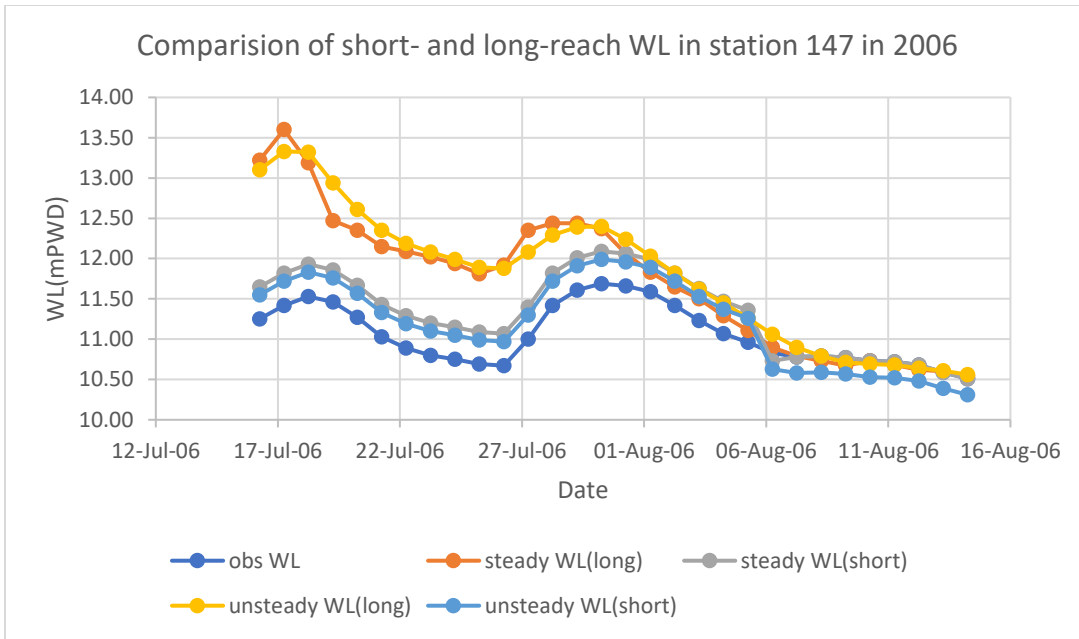


Figure 5.14: Comparison of WL of short- and long-reach model at station 147 for 2006 using downstream WL as boundary condition

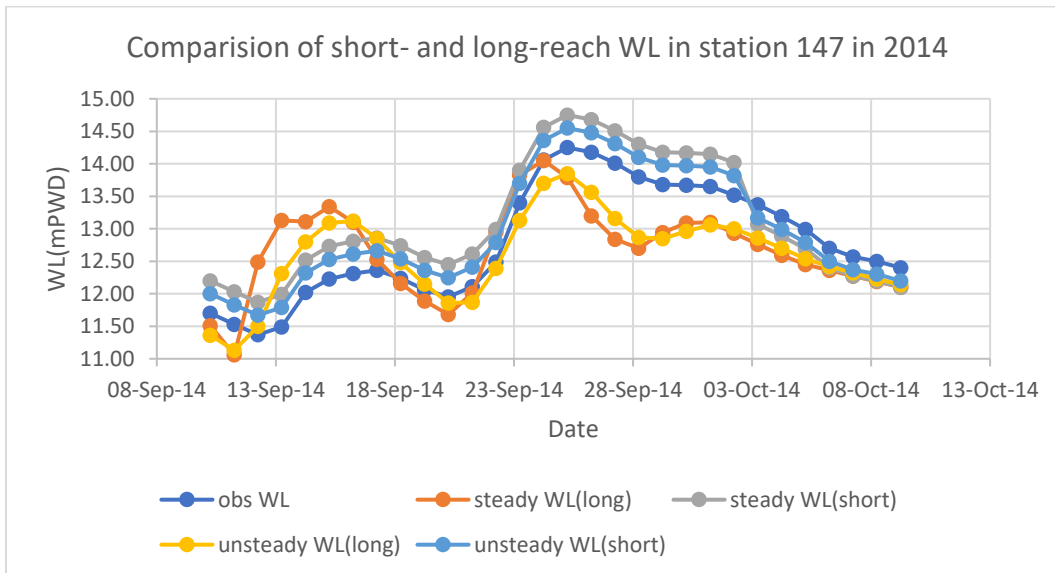


Figure 5.15: Comparison of WL of short- and long-reach model at station 147 for 2014 using downstream WL as boundary condition

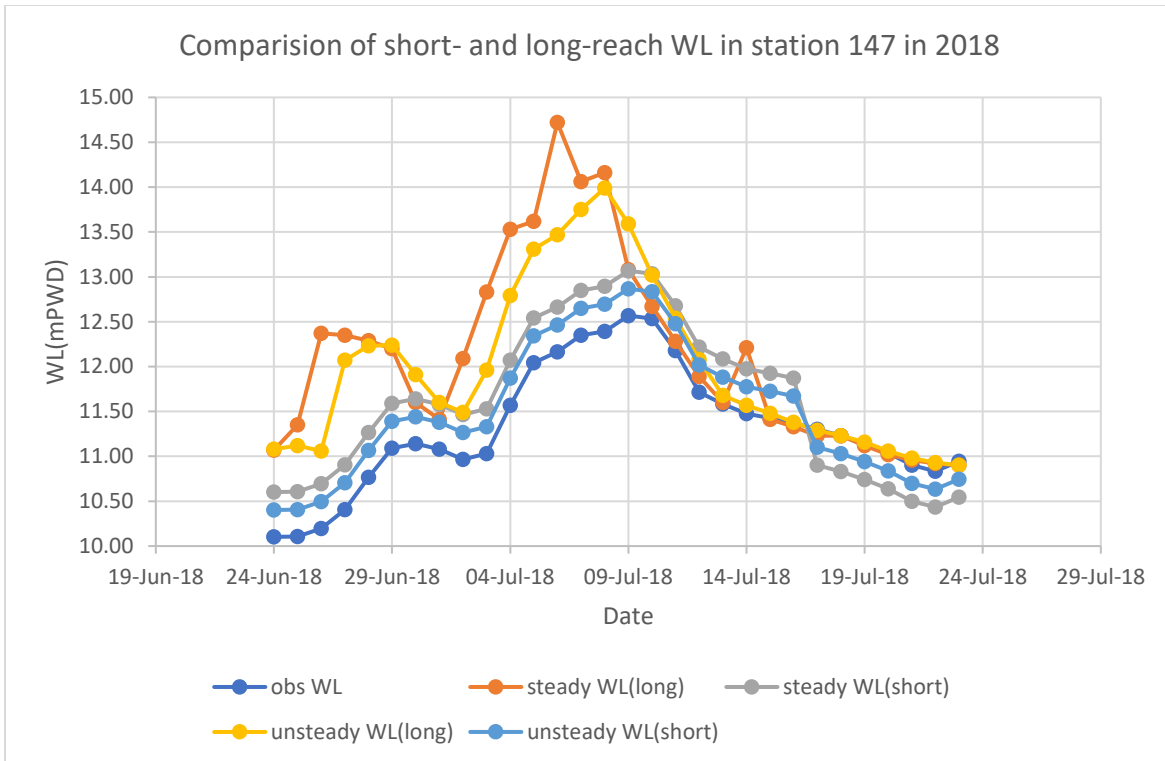


Figure 5.16: Comparison of WL of short- and long-reach model at station 147 for 2018 using downstream WL as boundary condition

5.4 Comparison of Upstream Short-Reach Model and Long-Reach Model Using WL as Downstream Boundary Condition

After comparing the downstream portion, a short-reach upstream model of 6 km was developed at the upstream portion of the study area in order to compare the water levels of upstream stations as well. The water levels were simulated for both steady and unsteady flow simulations using discharge of station 144 and interpolated water level from station 144 and 145 as boundary conditions. The short-reach model's water levels were simulated for year of 1998, 2006, 2014, 2018 and compared with the long-reach model's results for station 144.

5.4.1 Comparison for 1998

For the year of 1998, the water level value was interpolated for downstream water level data from 22 August to 20 September 1998 and used as downstream boundary condition. For upstream boundary condition the discharge of station 144 of the same timeline was used. Then the short-

reach upstream water levels were simulated for both steady and unsteady flow and the results were compared with the long-reach model's steady and unsteady flow simulation results at 144 station using same boundary conditions.

The results predicted that all the models predicted the falling phase of the year quite well but the rising phase was best predicted by the short-reach model's unsteady flow module. So, in that sense the short-reach model was better than the long-reach model for the year of 1998.

5.4.2 Comparison for 2006

Similarly, from 16 July to 14 August 2006 the short-reach upstream water levels were simulated for both steady and unsteady flow and the results were compared with the long-reach model's steady and unsteady flow simulation results at 144 station using same boundary conditions.

The result of this year was found a bit different than the other years. In this year, long reach model's unsteady flow module showed better performance than the short-reach model in the rising phase of flood but in the falling phase, short-reach model's results were better. The potential cause behind this phenomenon can be the effect of change in storage throughout this year.

5.4.3 Comparison for 2014

For 2014, the short-reach upstream water levels were simulated for both steady and unsteady flow from 10 September to 9 October 2014 and the results were compared with the long-reach model's steady and unsteady flow simulation results at 144 station using same boundary conditions.

For the year of 2014, the short-reach model performed better clearly than the long-reach model. In this year, long-reach model's result was quite deviated in the falling phase of the flood where in short-reach model the water levels were predicted quite well.

5.4.4 Comparison for 2018

From 24 June to 23 July 2018 the short-reach upstream water levels were simulated for both steady and unsteady flow and the results were compared with the long-reach model's steady and unsteady flow simulation results at 144 station using same boundary conditions.

In this year, both the short- and long-reach model predicted almost similar results in the rising phase of the flood but the falling phase of the flood year was not well captured by the long-reach model. The short-reach model's unsteady flow module could produce closest result with the observed data. So, in this year as well, short-reach model performed better than long-reach model.

Figures 5.17, 5.18, 5.19, 5.20 show the comparison of WL between long- and short-reach upstream model at station 144 using downstream WL as boundary condition for 1998, 2006, 2014, 2018.

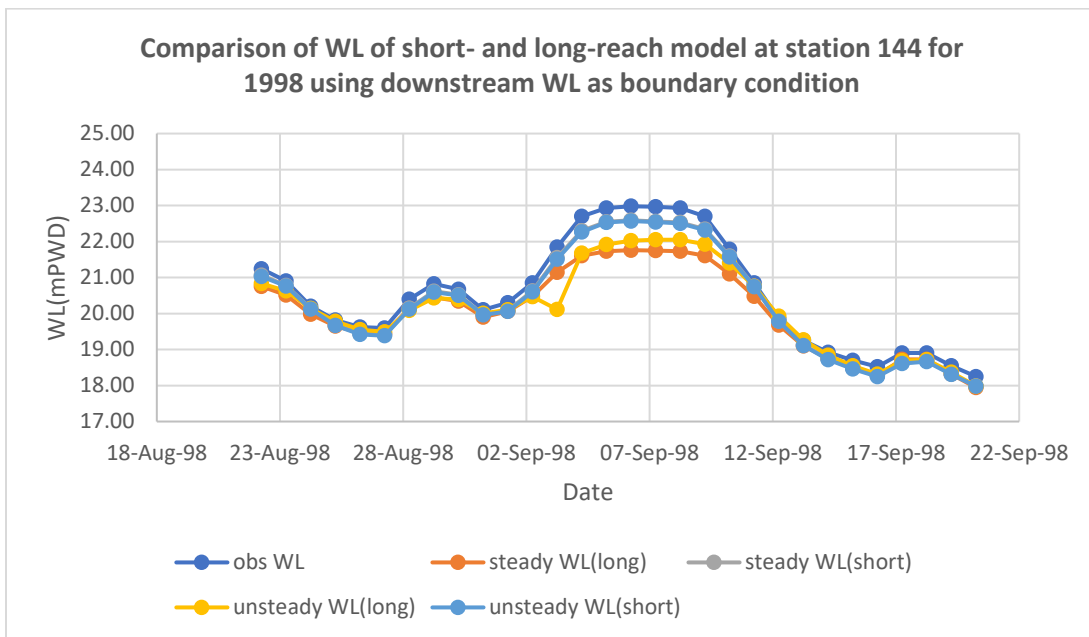


Figure 5.17: Comparison of WL of short- and long-reach model at station 144 for 1998 using downstream WL as boundary condition

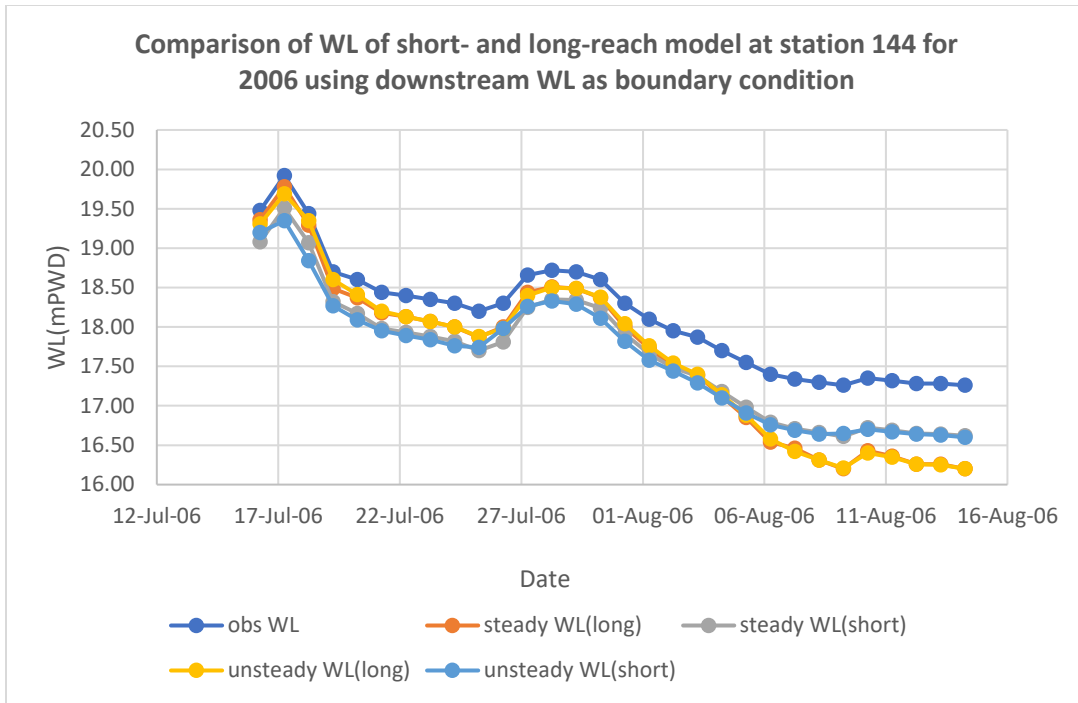


Figure 5.18: Comparison of WL of short- and long-reach model at station 144 for 2006 using downstream WL as boundary condition

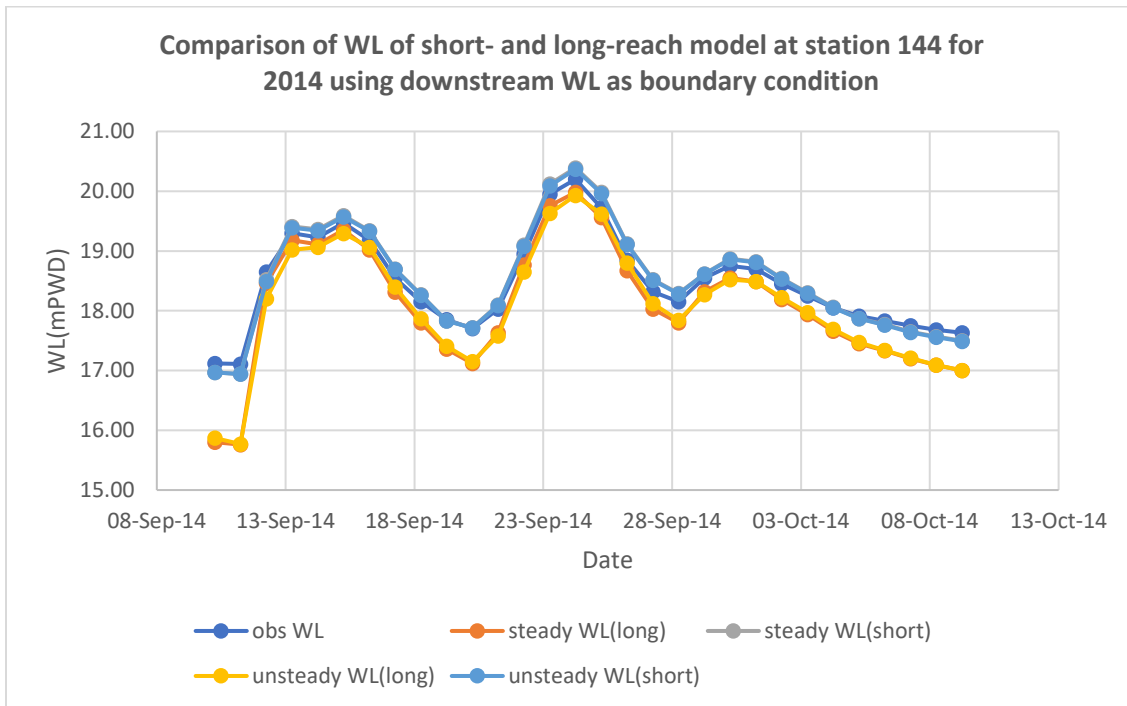


Figure 5.19: Comparison of WL of short- and long-reach model at station 144 for 2014 using downstream WL as boundary condition

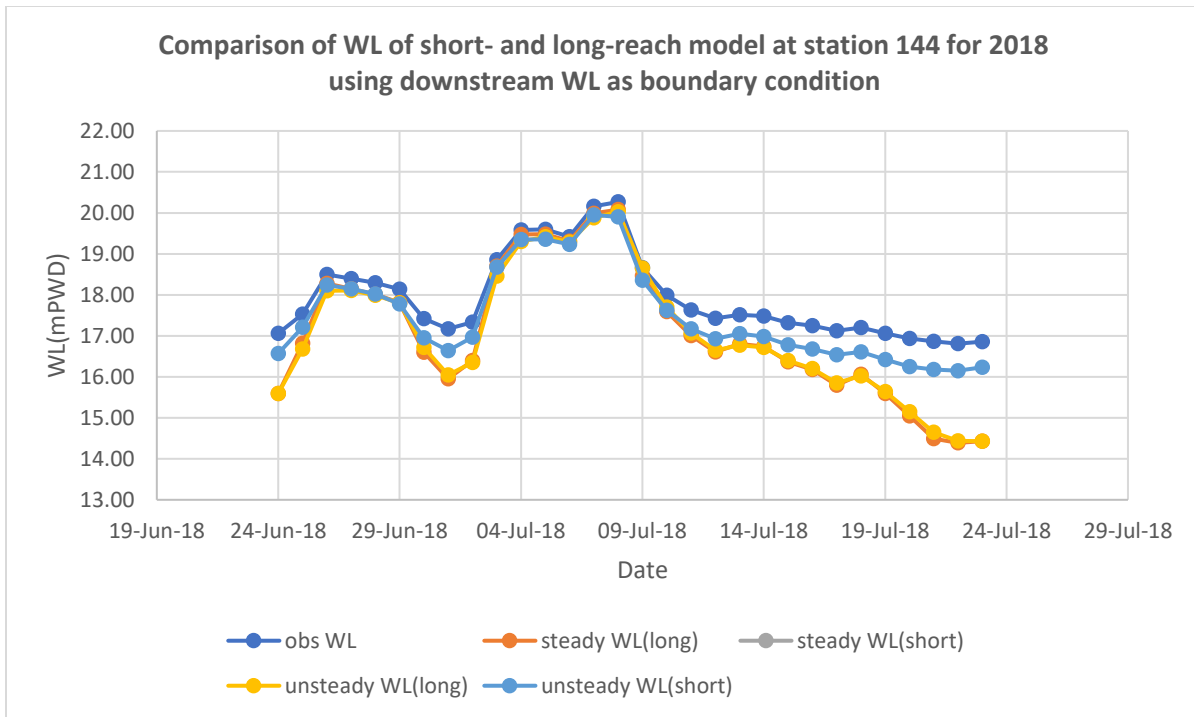


Figure 5.20: Comparison of WL of short- and long-reach model at station 144 for 2018 using downstream WL as boundary condition

5.5 Comparison of Downstream Short-Reach Model and Long-Reach Model Using Normal Depth as Boundary Condition

The water levels of the downstream short-reach model were simulated for steady flow simulations using discharge of station 147 and normal depth of its downstream station as boundary conditions. The water levels were simulated for year of 1998, 2006, 2014, 2018 and compared with the long-reach model's results of station 147.

5.5.1 Comparison for 1998

For this comparison, the normal depth was used as boundary condition. For giving input of normal depth, the downstream slope was required. The slope was calculated using the observed water level data of station 147 and 147.5 from 22 August to 20 September 1998. The slope value was calculated from the difference in observed water level between two stations at a particular time divided by the distance of the two stations. Then the short-reach downstream water levels were simulated for steady flow and the results are compared with the long-reach model's steady flow simulation results at 147 station using same boundary conditions.

The results showed that both the short- and long-reach models overestimated the water levels for this year. But the short-reach model's result was closer to the observed value. So, the short-reach model performed better.

5.5.2 Comparison for 2006

Similarly like 1998, the discharge and slope were calculated using the observed water level data of station 147 and 147.5 from 16 July to 14 August 2006. Then the short-reach downstream water levels were simulated for steady flow and the results were compared with the long-reach model's steady flow simulation results at 147 station using same boundary conditions.

The results of 2006 were quite similar with the year of 1998. In this year, both the short- and long-reach models also overestimated the water levels but the short-reach model's result was closer to the observed value. So, the short-reach model performed better.

5.5.3 Comparison for 2014

Like the previous two years, the discharge and slope were calculated using the observed water level data of station 147 and 147.5 from 10 September to 9 October 2014. Then the short-reach downstream water levels were simulated for steady flow and the results were compared with the long-reach model's steady flow simulation results at 147 station using same boundary conditions.

The result of 2014 was also similar like the other two years. The short-reach model performed better in this year as well.

5.5.4 Comparison for 2018

For 2018, the discharge and slope were calculated using the observed water level data of station 147 and 147.5 from 24 June to 23 July. Then the short-reach downstream water levels were simulated for steady flow and the results were compared with the long-reach model's steady flow simulation results at 147 station using same boundary conditions.

The year of 2018 showed similar results like the other years. The short-reach model performed better than the long-reach model in this year as well.

Figures 5.21, 5.22, 5.23, 5.24 show the comparison of WL (mPWD) between long- and downstream short-reach model at station 147 using normal depth as boundary condition for 1998, 2006, 2014, 2018.

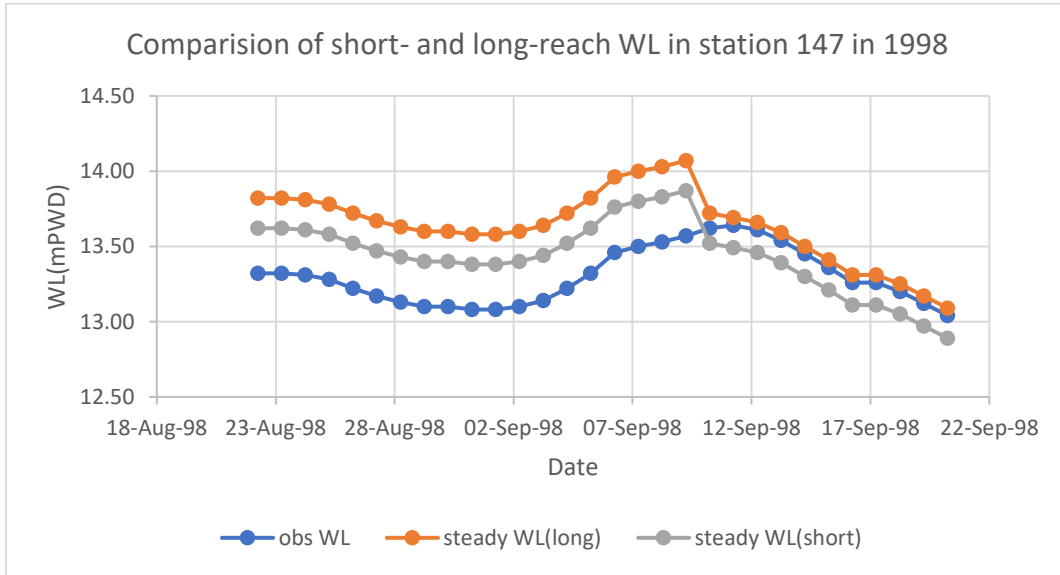


Figure 5.21: Comparison of WL of short- and long-reach model at station 147 for 1998 using normal depth as boundary condition

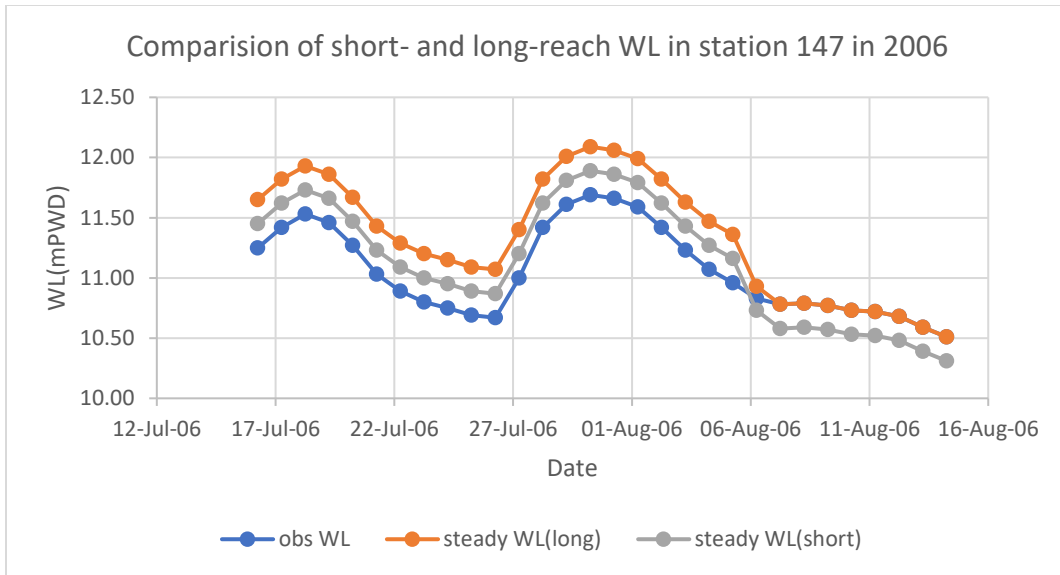


Figure 5.22: Comparison of WL of short- and long-reach model at station 147 for 2006 using normal depth as boundary condition

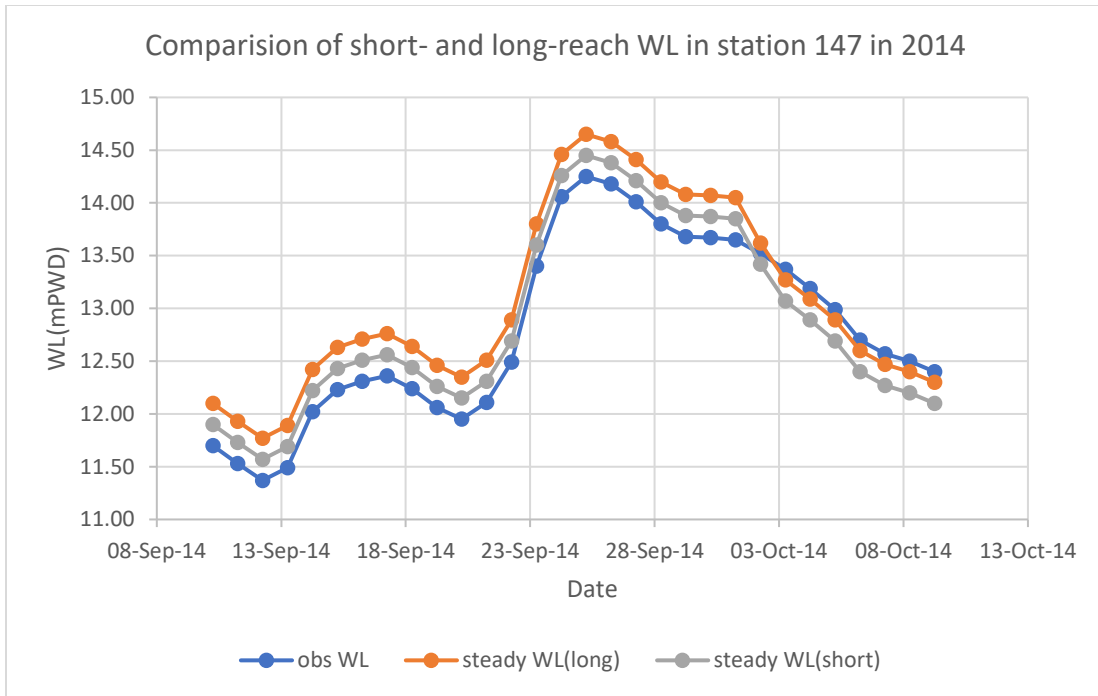


Figure 5.23: Comparison of WL of short- and long-reach model at station 147 for 2014 using normal depth as boundary condition

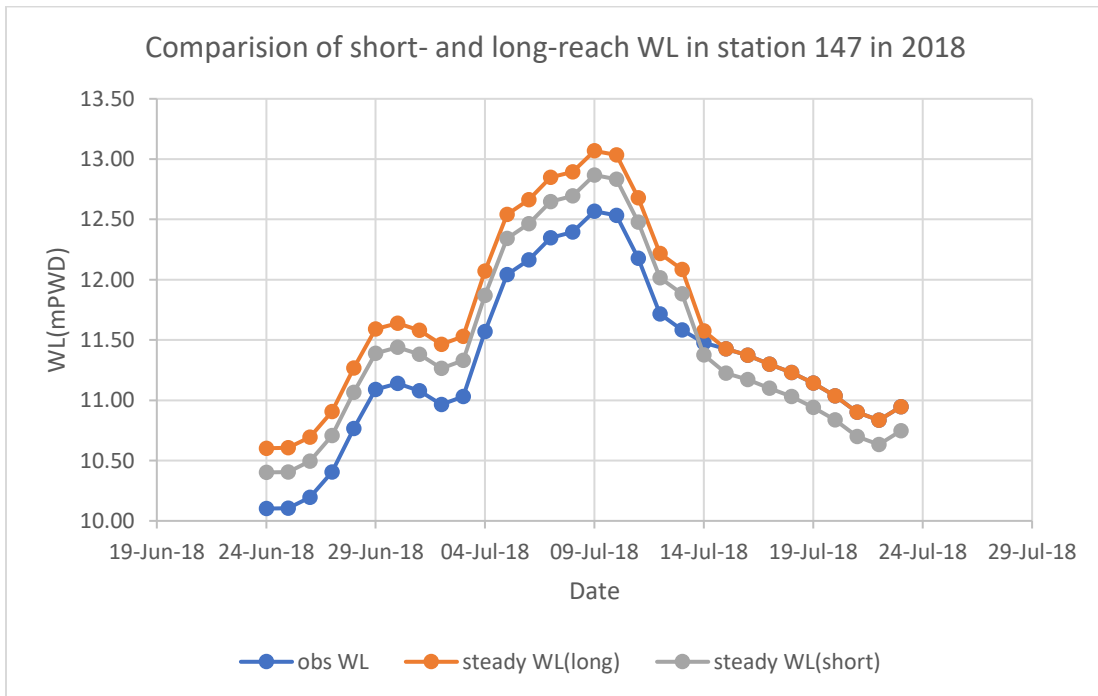


Figure 5.24: Comparison of WL of short- and long-reach model at station 147 for 2018 using normal depth as boundary condition

Overall, in this analysis, it was observed that the short-reach model performed better than the long-reach model.

5.6 Comparison of Upstream Short-Reach Model and Long-Reach Model Using Normal Depth as Downstream Boundary Condition

The water levels of short-reach upstream model were simulated with steady flow in order to compare the water levels of upstream stations as well with normal depth as boundary condition. The water levels were simulated for steady flow using discharge of upstream station and normal depth at downstream station as boundary conditions. The water levels were simulated for year of 1998, 2006, 2014, 2018 and compared with the long-reach model's results.

5.6.1 Comparison for 1998

At this point, the normal depth was used as boundary condition for comparing upstream short-reach and long-reach model. For giving input of normal depth, the downstream slope was required like previous one. The slope was calculated using the observed water level data of stations 144 and 145 from 22 August to 20 September 1998. The slope value was calculated from the difference in observed water level between two stations at a particular time divided by the distance of the two stations. For upstream boundary condition the discharge of station 144 was used. Then the short-reach upstream water levels were simulated for steady flow and the results were compared with the long-reach model's steady flow simulation results at 144 station using same boundary conditions.

5.6.2 Comparison for 2006

Similarly, the slope was calculated using the observed water level data of stations 144 and 145 from 16 July to 14 August 2006. For upstream boundary condition the discharge of station 144 was used. Then the water levels of short-reach upstream model were simulated for steady flow and the results were compared with the long-reach model's steady flow simulation results at 144 station using same boundary conditions.

5.6.3 Comparison for 2014

Like the previous years at 2014, the slope was calculated using the observed water level data of stations 144 and 145 from 10 September to 9 October. For upstream boundary condition the

discharge of station 144 was used. Then the water levels of short-reach upstream model were simulated for steady flow and the results were compared with the long-reach model's steady flow simulation results at 144 station using same boundary conditions.

5.6.4 Comparison for 2018

For 2018, the slope was calculated using the observed water level data of stations 144 and 145 from 24 June to 23 July. For upstream boundary condition the discharge of station 144 was used. Then the water levels of short-reach upstream model were simulated for steady flow and the results were compared with the long-reach model's steady flow simulation results at 144 station using same boundary conditions.

Figures 5.25, 5.26, 5.27, 5.28 show the comparison of WL between long and short-reach upstream model at station 144 using normal depth as boundary condition for 1998, 2006, 2014, 2018.

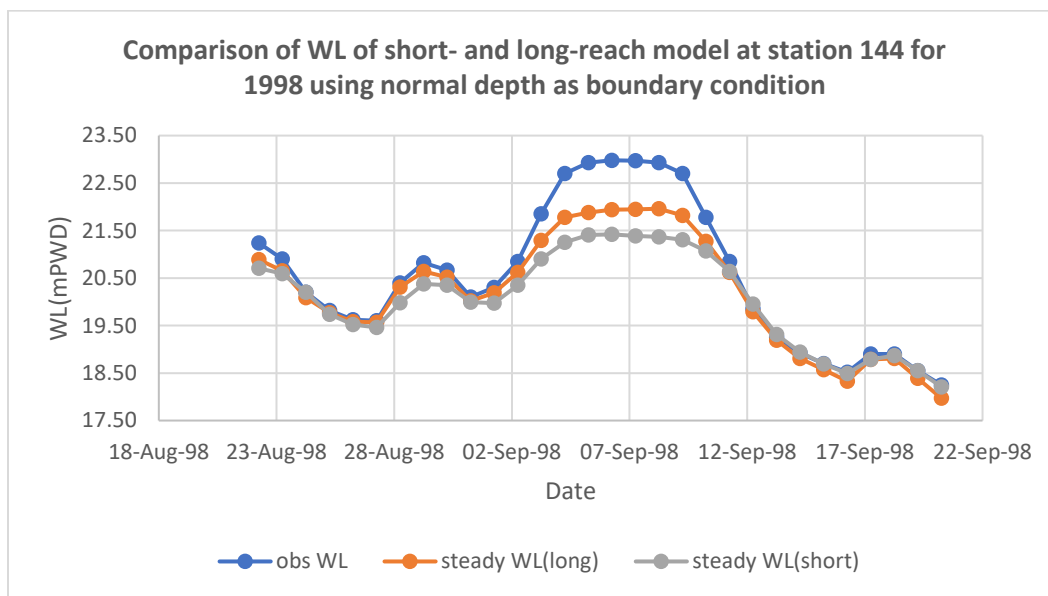


Figure 5.25: Comparison of WL of short- and long-reach model at station 144 for 1998 using normal depth as boundary condition

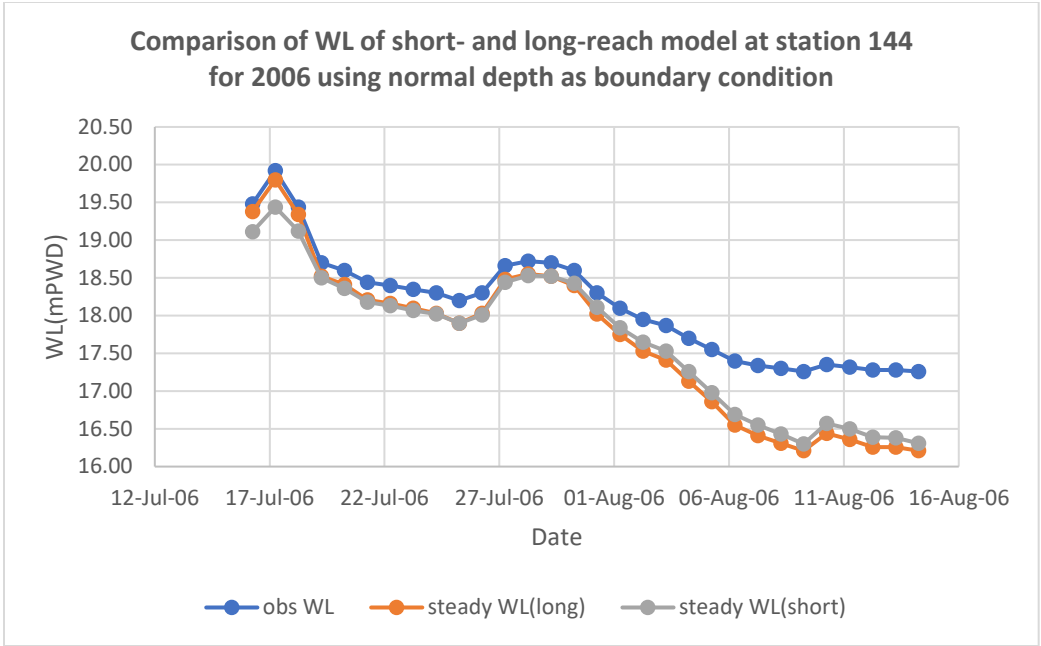


Figure 5.26: Comparison of WL of short- and long-reach model at station 144 for 2006 using normal depth as boundary condition

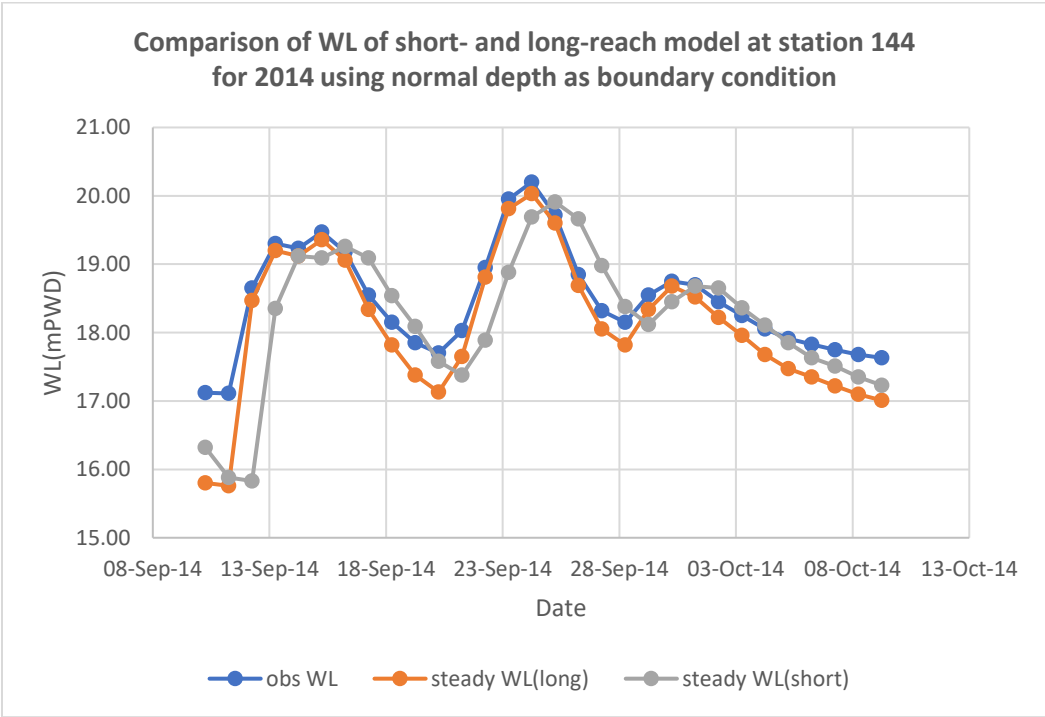


Figure 5.27: Comparison of WL of short- and long-reach model at station 144 for 2014 using normal depth as boundary condition

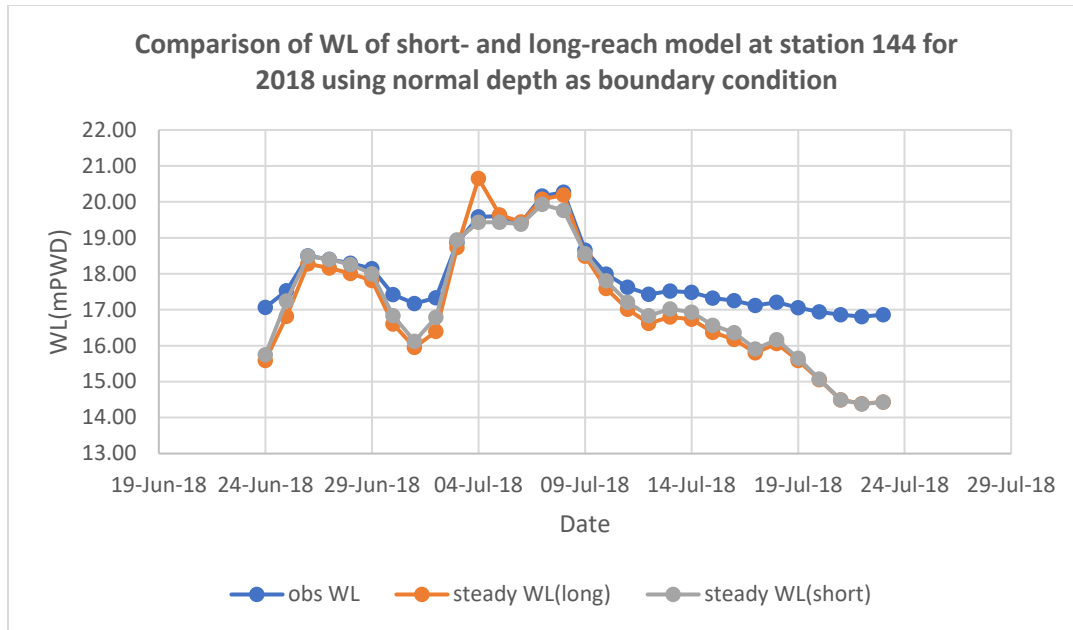


Figure 5.28: Comparison of WL of short- and long-reach model at station 144 for 2018 using normal depth as boundary condition

For both of the boundary conditions, it can be concluded that the short-reach model performs better than the long-reach model. The reason behind this phenomenon can be explained with following three reasons:

- i. River-floodplain interaction is very prominent in the Atrai River floodplain. The river loses water to floodplain when it overflows and it gains water from floodplain when the flow of the river is less. This interaction and change in water level are significant in the long-reach model. But in short-reach model this interaction is not that significant as the model is associated with a small portion of floodplain area. That's why short-reach model performs better than long-reach model.
- ii. The second reason can be the rainfall contribution from hydrologic runoff model. Along with 1D hydrodynamic model, FFWC uses hydrologic runoff model to forecast the flood condition of the country that are quite accurate. In this model, the contribution of rain was not taken into account. Though for both short- and long-reach models the contribution is equally important but the effect of it is higher in long-reach model than the short-reach model. So, the short-reach model result will deviate less in comparison to long-reach model.
- iii. The third reason is the boundary of the model. In long-reach model, the boundaries are quite far. Many interventions can be happened within the long distance thus the water level can deviate in the field level where models can't capture this. But in short-reach models, the

boundaries are relatively close and the chances of such interventions are less which helps to make better prediction of water level of the stations.

5.7 Comparison of Model Results with and without Storage Areas

The water levels of long-reach model were simulated both with and without storage areas. The comparison was done for 1998, 2006, 2014 and 2018 for unsteady flow module.

5.7.1 Comparison for 1998

For 1998, the water levels of long-reach model were simulated after adding the storage areas and the simulated water levels of station 144, 145, 147 and 147.5 were compared. It was observed that the simulated water level of the model with storage area of station 145 was a bit better suited with the observed water level. For the other stations, the results were pretty close.

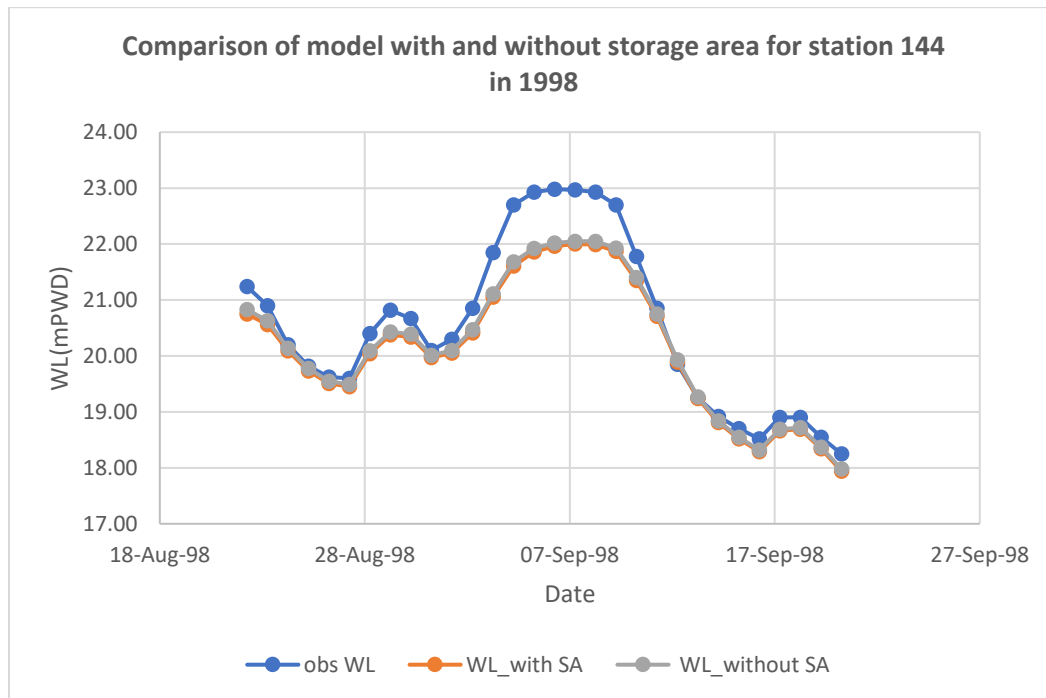


Figure 5.29: Comparison of model with and without storage area for station 144 in 1998

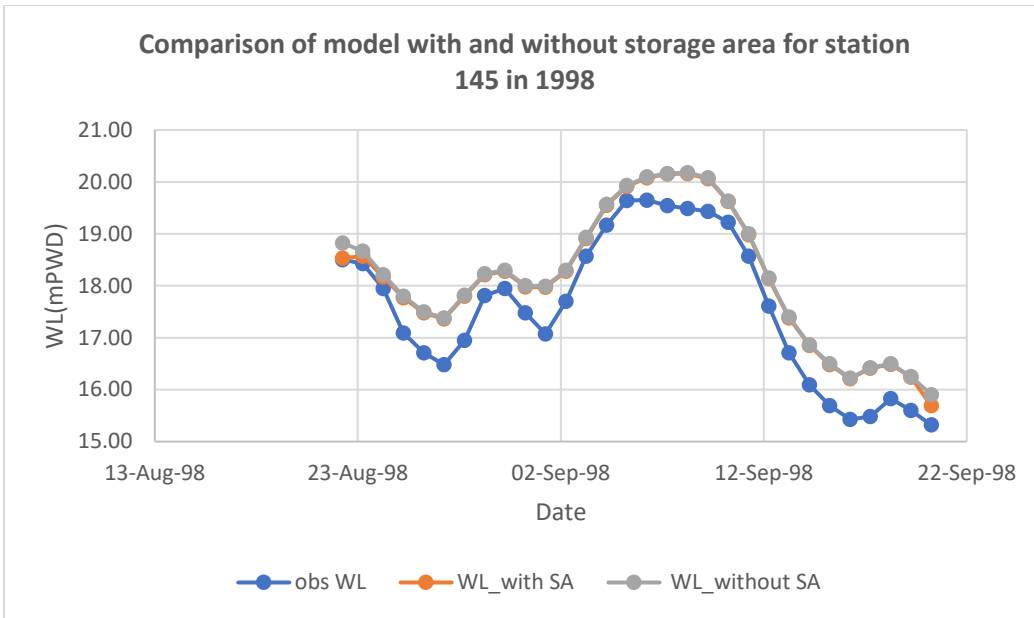


Figure 5.30: Comparison of model with and without storage area for station 145 in 1998

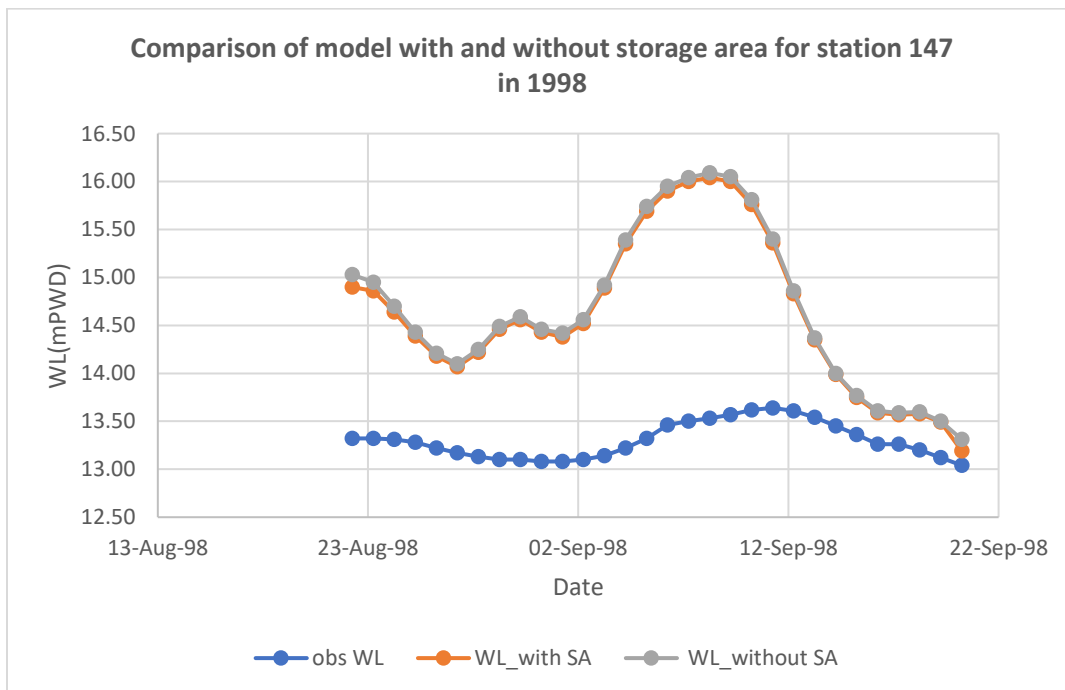


Figure 5.31: Comparison of model with and without storage area for station 147 in 1998

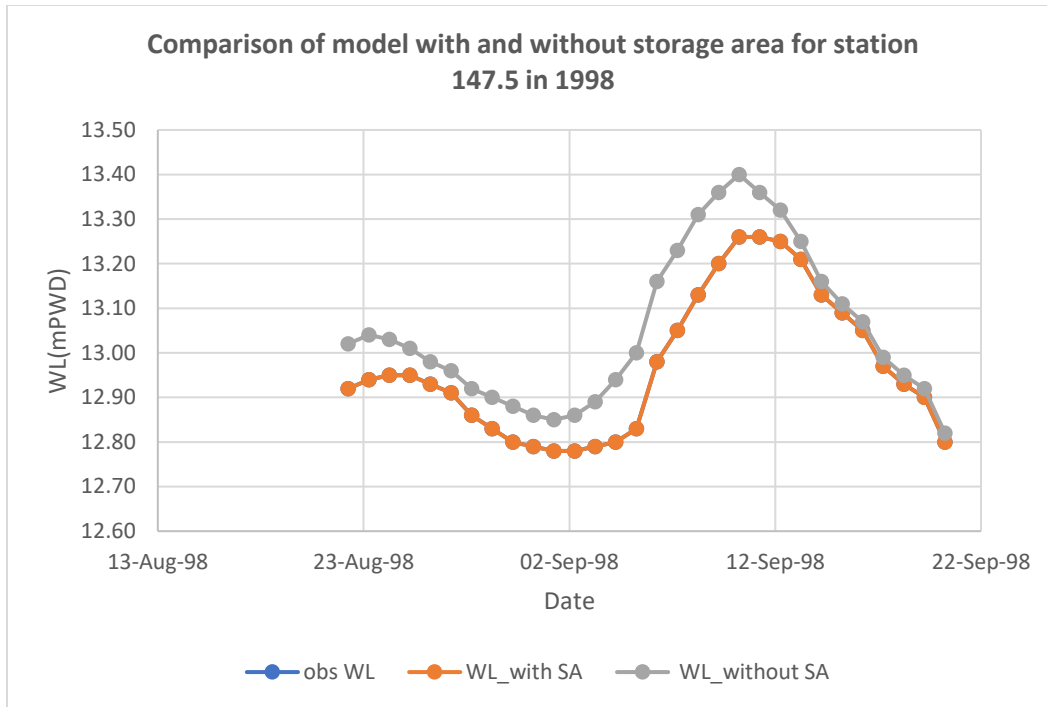


Figure 5.32: Comparison of model with and without storage area for station 147.5 in 1998

5.7.2 Comparison for 2006

Similarly for 2006, the water levels of the long-reach model were simulated after adding the storage areas and the simulated water levels of station 144, 145, 147 and 147.5 were compared. Though the other station results were quite similar but for station 147, some significant changes in results were observed for without and with storage areas. The model with storage areas showed closer result with the observed data in this station.

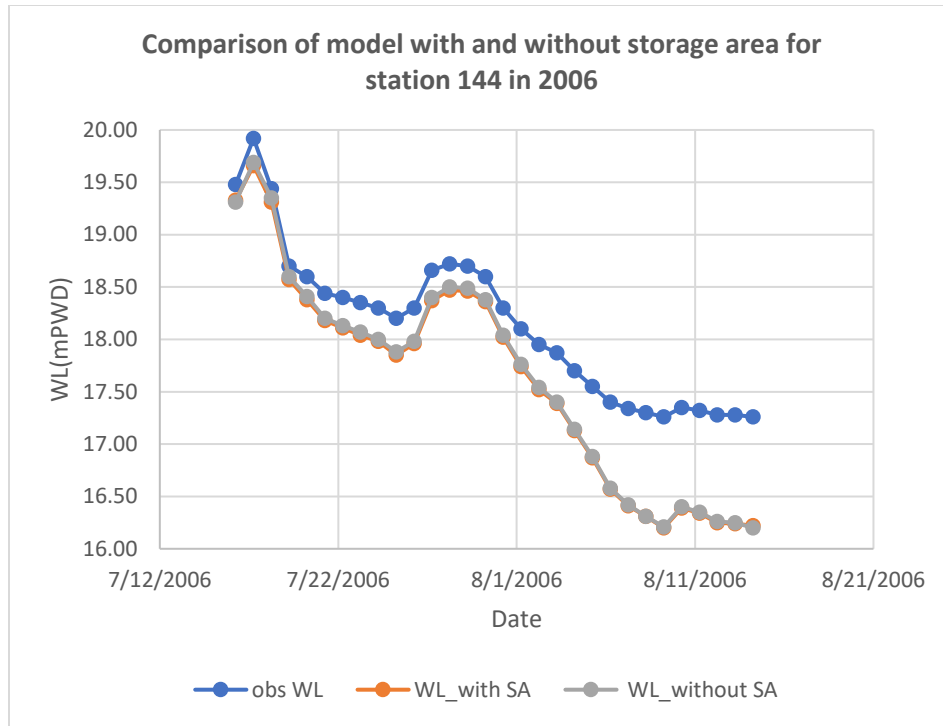


Figure 5.33: Comparison of model with and without storage area for station 144 in 2006

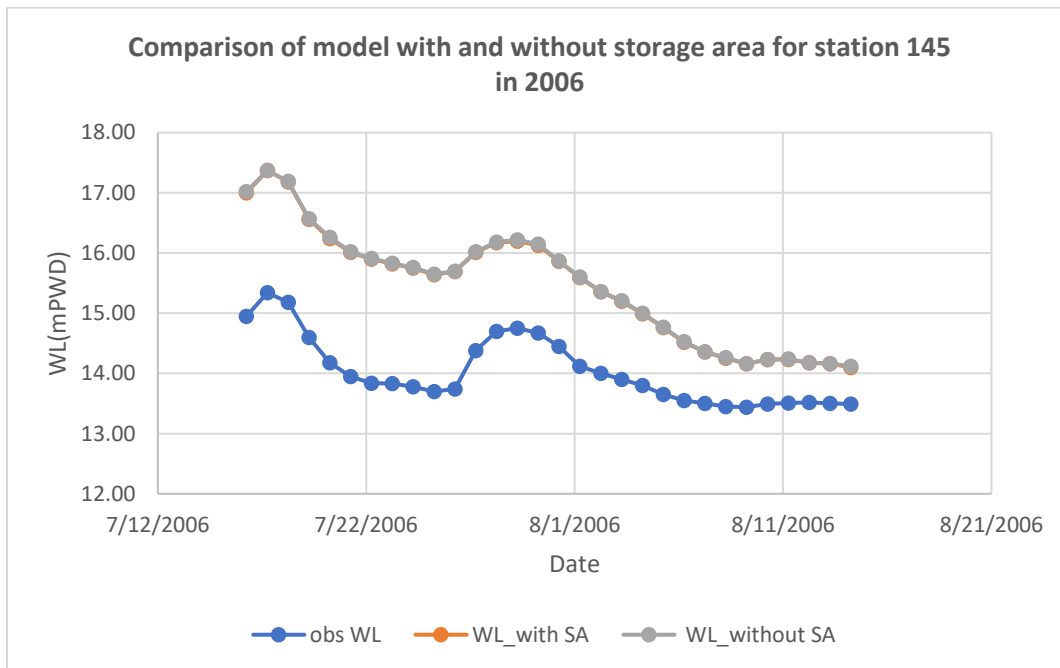


Figure 5.34: Comparison of model with and without storage area for station 145 in 2006

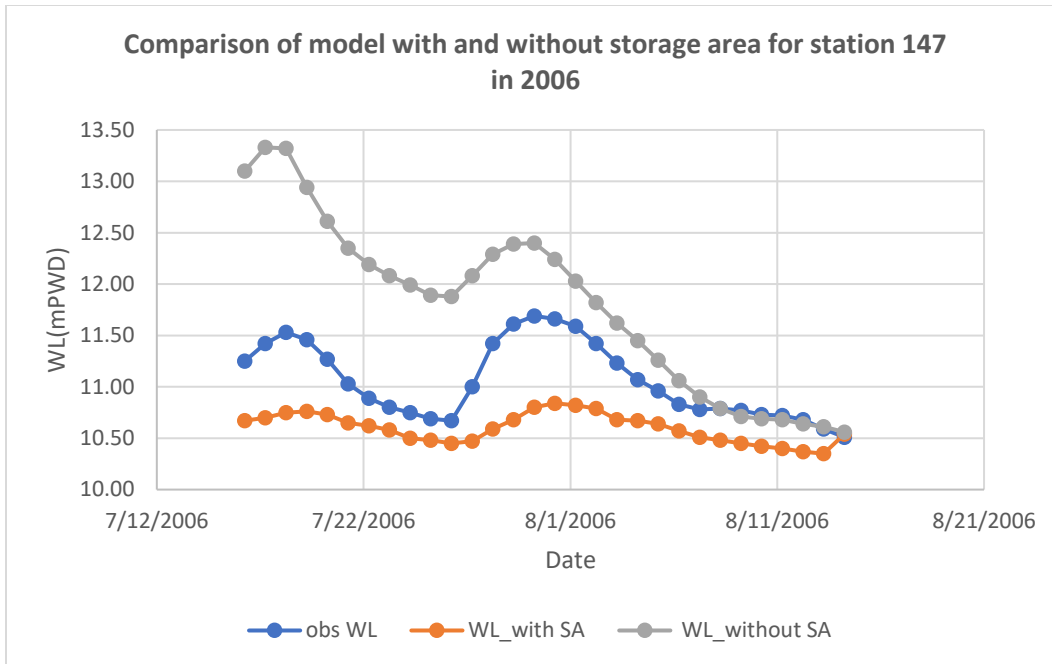


Figure 5.35: Comparison of model with and without storage area for station 147 in 2006

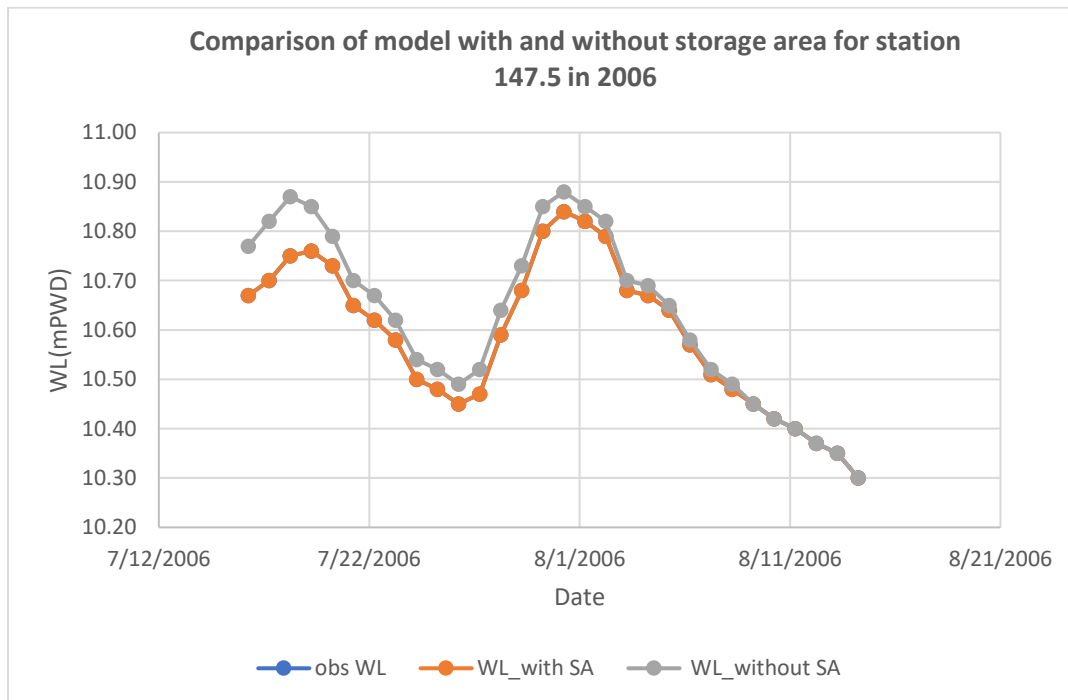


Figure 5.36: Comparison of model with and without storage area for station 147.5 in 2006

5.7.3 Comparison for 2014

Similarly like the previous years in the year of 2014, the water levels of the long-reach model were simulated after adding the storage areas. Then the simulated water levels of station 144, 145, 147 and 147.5 were compared. It was observed that the simulated water level of the model with storage area of station 147.5, the model with storage areas fluctuates a bit more where for station 147, the results were better for the model with storage areas. For the other stations, the results were quite similar.

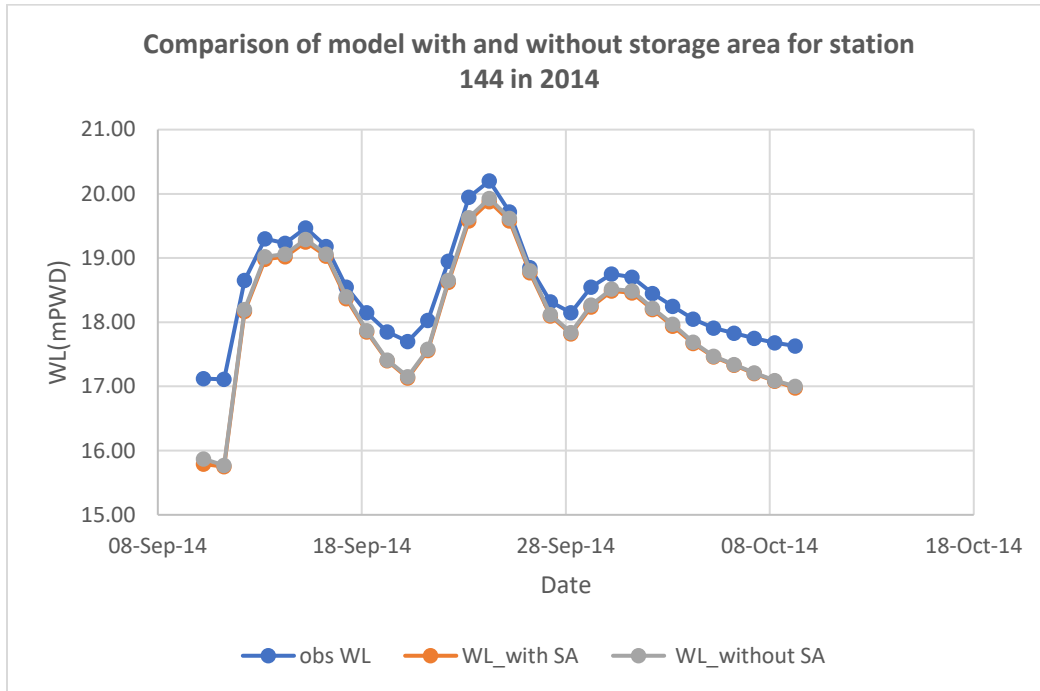


Figure 5.37: Comparison of model with and without storage area for station 144 in 2014

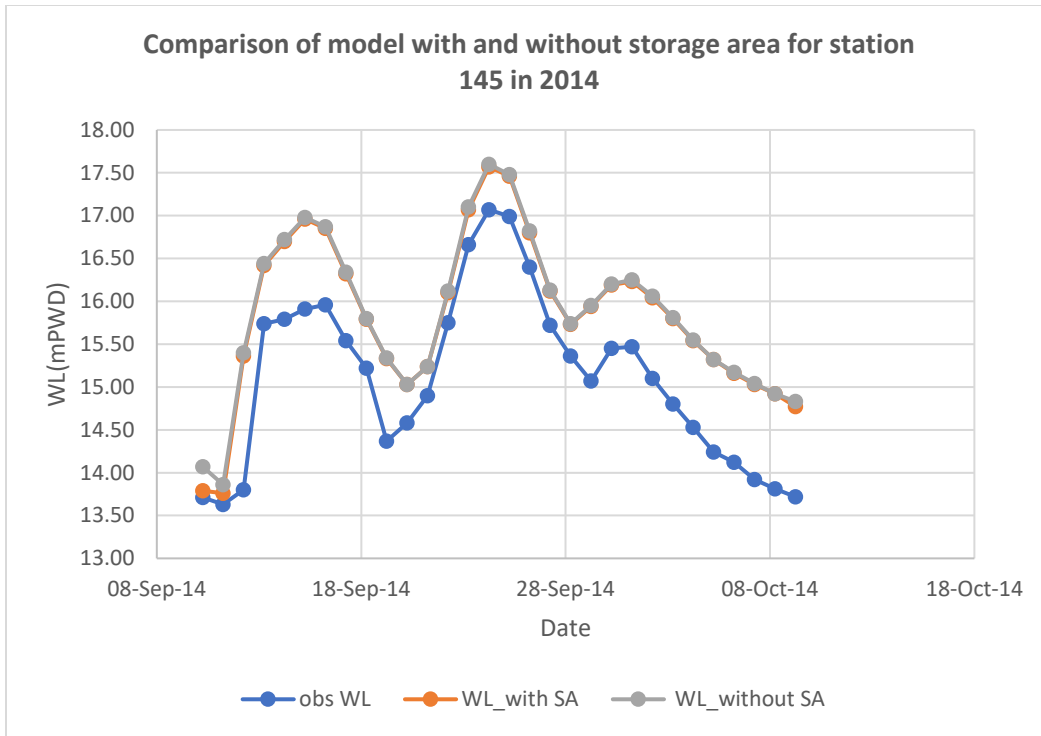


Figure 5.38: Comparison of model with and without storage area for station 145 in 2014

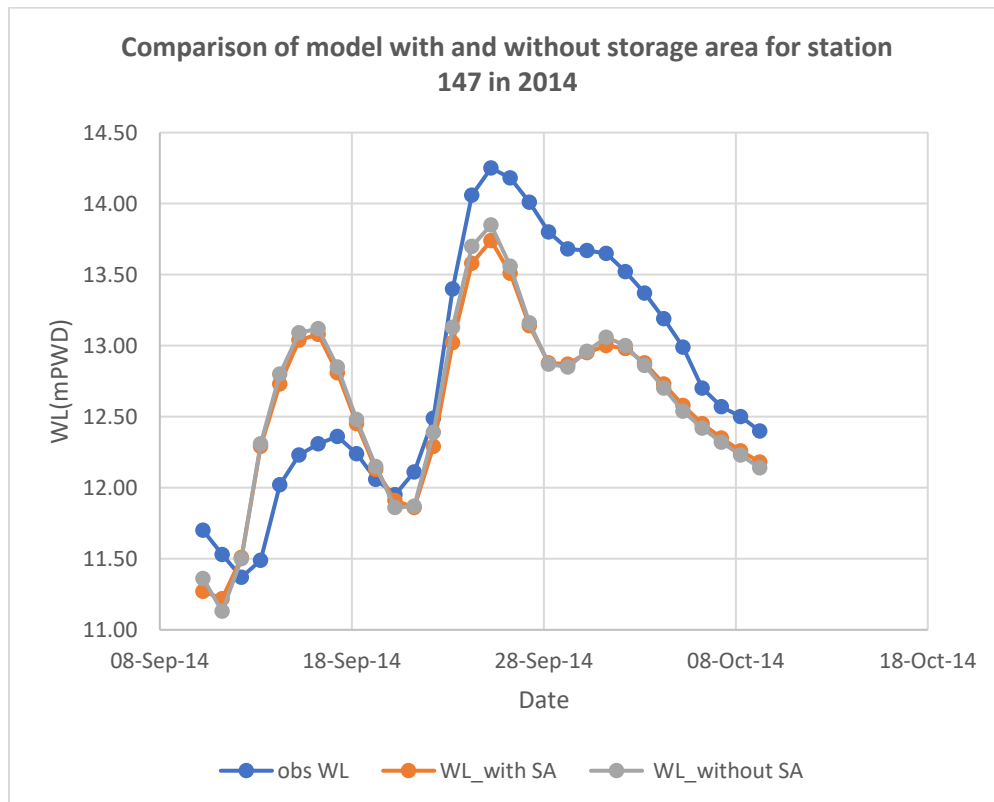


Figure 5.39: Comparison of model with and without storage area for station 147 in 2014

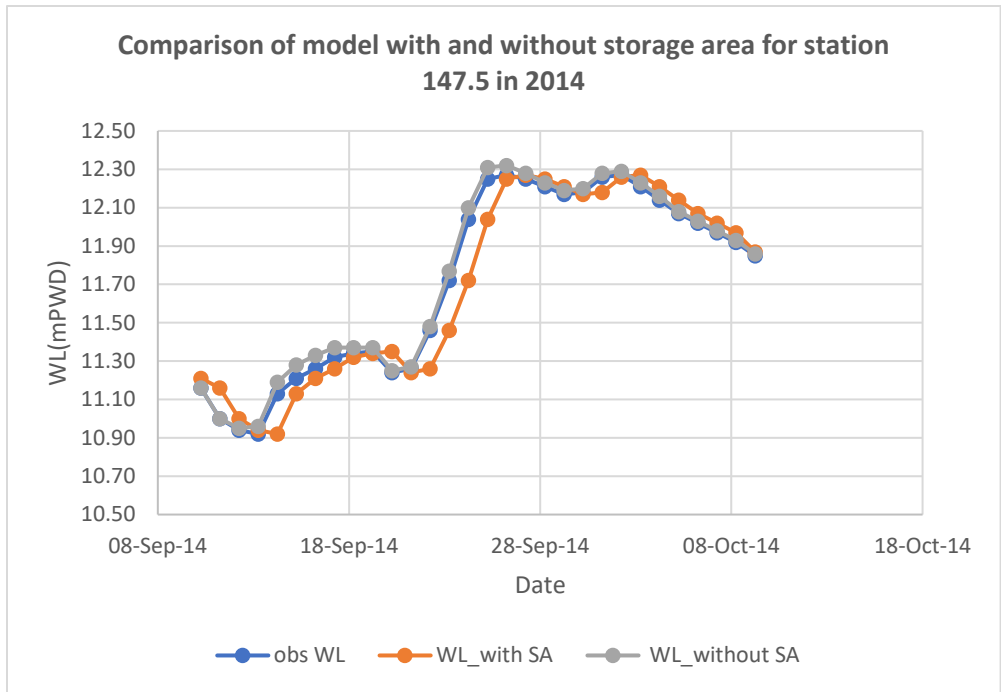


Figure 5.40: Comparison of model with and without storage area for station 147.5 in 2014

5.7.4 Comparison for 2018

After the above mentioned three years, the water levels of the long-reach model were simulated after adding the storage areas for the year of 2018. Then the simulated water levels of station 144, 145, 147 and 147.5 were compared. In this year, no significant changes were observed for the model with and without storage areas in all the stations.

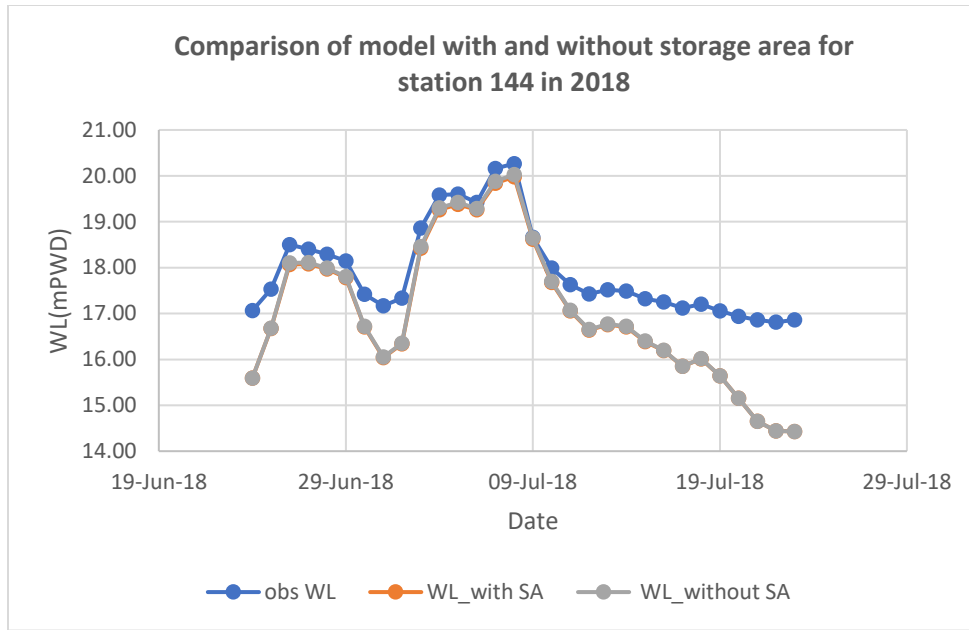


Figure 5.41: Comparison of model with and without storage area for station 144 in 2018

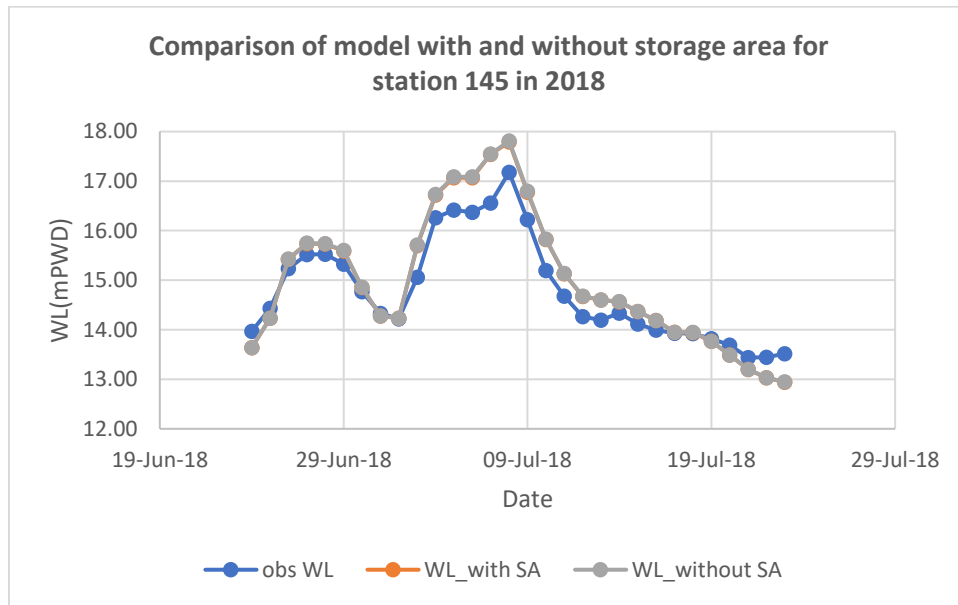


Figure 5.42: Comparison of model with and without storage area for station 145 in 2018

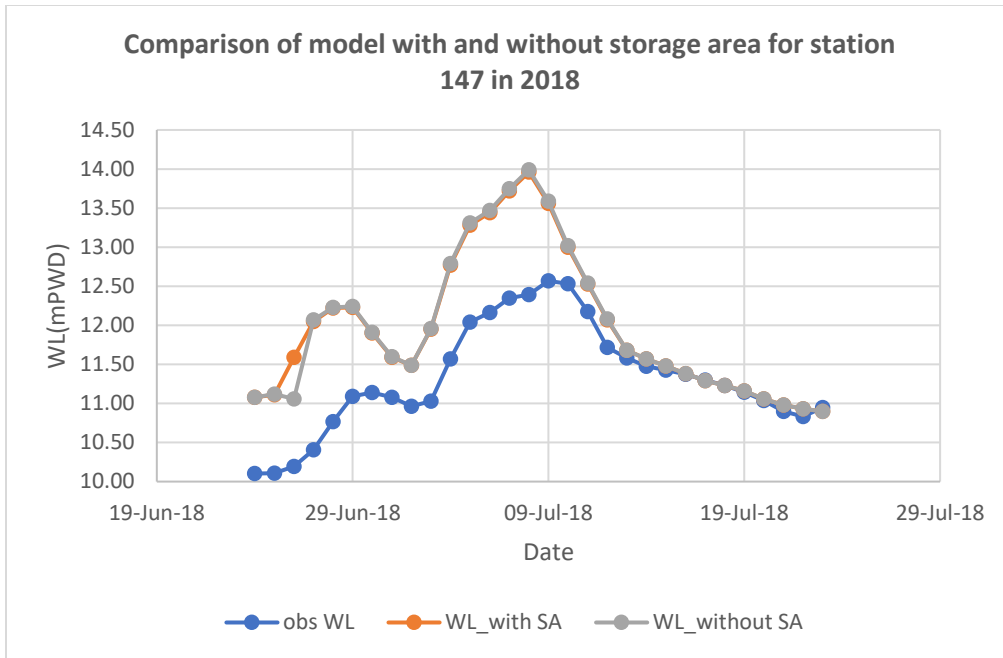


Figure 5.43: Comparison of model with and without storage area for station 147 in 2018

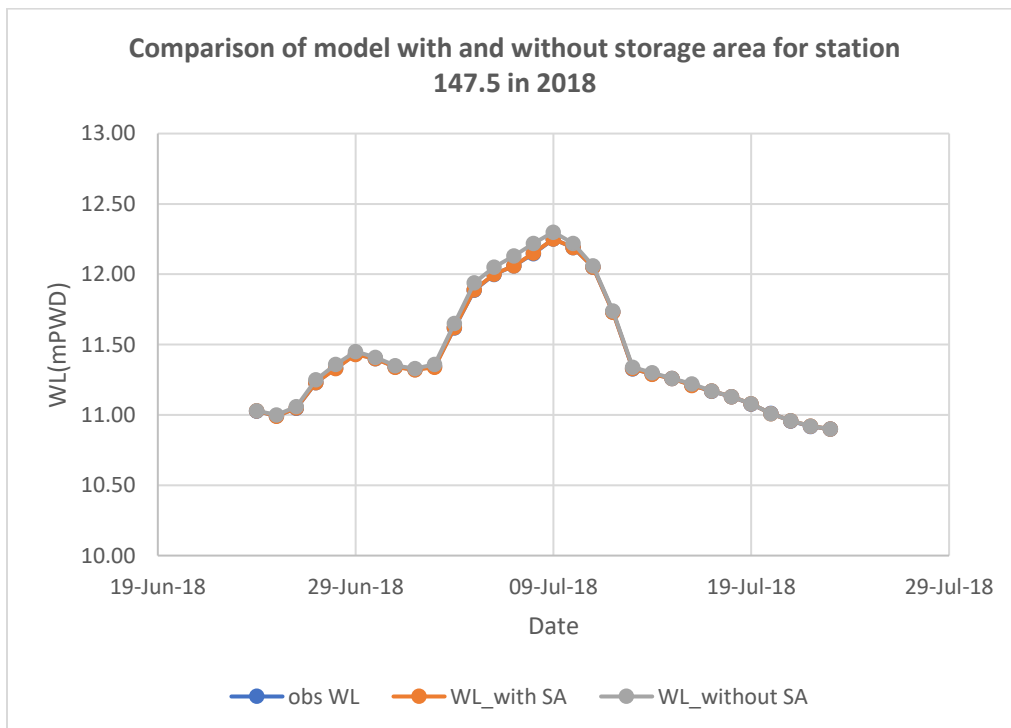


Figure 5.44: Comparison of model with and without storage area for station 147.5 in 2018

Chapter 6: Conclusions and Recommendations

6.1 General

As a floodplain dominated country, analysis of hydrodynamic behavior of rivers is really important in the context of Bangladesh. Thus, understanding the importance, in total three short- and long-reach models were developed in this study for the Atrai River using the HEC-RAS one-dimensional model and a number of simulations were conducted using different boundary conditions and flow modules. Finally, the simulation results of the models were compared to get a clear understanding of better suited model for the Atrai River reach.

6.2 Conclusions

The water levels of the long- and short-reach models were simulated for four flood seasons, which were 1998, 2006, 2014 and 2018. From the study, the following conclusions are drawn:

- i. The long-reach model was calibrated with Manning's roughness coefficient ' n '=0.025 for main channel and ' n '=0.030 for floodplain. The calibrated model could efficiently simulate the water level of 1998, 2006, 2014 and 2018 flood events.
- ii. There were six model evaluating criteria in this study to understand the performance of the long-reach model. Among them, RMSE is the most used one. The RMSE value of the steady flow module of stations 144,145 and 147 for the flood of 2006 are 0.6, 1.4 and 0.9 m, respectively. The RMSE value of the unsteady flow module of these stations are 0.6, 0.5 and 0.9 m respectively. According to the RMSE value, the unsteady flow module is better than the steady flow module for 2006. Similar results were also found for the years of 2014 and 2018. Only exception was found for 1998 where the steady flow module performed better.
- iii. While water level was used as downstream boundary condition for the downstream short-reach model and long-reach models, it was found that in 1998, 2006 and 2018 clearly the unsteady short-reach model performed better than the long-reach model. In 2014 the results of the long- and short-reach models were close, but the short-reach model results were little better. So, using water level as boundary condition, the downstream short-reach model performed better than the long-reach model.

- iv. For the same downstream boundary condition in the upstream short-reach and long-reach models, it was found that in all the years the unsteady short-reach model performed better than the long-reach model. Though in 1998 and 2014, both the models' results were close; in 2006 and 2018, the long-reach model could not capture the falling phase of the hydrograph where the short-reach model could successfully do it. So, using water level as downstream boundary condition, the upstream short-reach model performed better than the long-reach model.
- v. When normal depth was used as the downstream boundary condition for the downstream short-reach and long-reach models, it was found that in every year the short-reach model predicted better result than the long-reach model. So, it can be said that using normal depth as the boundary condition, the downstream short-reach model performed better than the long-reach model.
- vi. For similar downstream boundary condition in the upstream short-reach model and long-reach model, it was found that in 2006, 2014 and 2018, the upstream short-reach model predicted better result than the long-reach model. Only in 1998, the long-reach model performed little better in the rising phase of the hydrograph than the short-reach model. Overall discarding the little exception, it can be said that using normal depth as the boundary condition, the upstream short-reach model performed better than the long-reach model.
- vii. Overall, from the comparison results of both the long- and short-reach models with different boundary conditions, it can be concluded that in the floodplain environments like the Atrai River, the short-reach model performs better than the long-reach model. This could be due to the fact that the river-floodplain interaction effects are more pronounced in a long-reach model due to its large reach, which cannot be captured in a one-dimensional model with distant boundary conditions. Thus, a short-reach model may be a better choice in floodplain environment if boundary data are available.
- viii. The model with storage areas showed better results at some stations than the model without storage areas. The results were prominent for the years of 1998 and 2006 than for 2014 and 2018. The possible reason behind that could be the settlements and residences surrounding the river in recent years.

6.3 Recommendations

Some recommendations can be made from the results and analyses of this study. These are stated in following:

- i. Short-reach models are better suited for the rivers in floodplain environment like the Atrai River. So, while preparing models in such river floodplain dominated areas, it is better to use a short-reach model.
- ii. This comparative study between short- and long-reach models was done using the HEC-RAS one-dimensional model. Similar study can be done using other models. Then it will be easier to verify whether the short-reach model performs better with other models as well.
- iii. Bathymetry data of the year 2018 was used in this study, whereas the simulation year data can be applied for better assessment, which will improve the reliability of the model results for future work.
- iv. The contribution of rain from hydrologic rainfall-runoff model was not considered in this study. It can be taken into account to increase the accuracy of the model in future research. It will be interesting to include the contribution of rainfall in this type of model.
- v. This study only focuses on the technical aspect of the floodplain environment of the Atrai River. Some future works may also focus on social and inter-disciplinary aspects in the study area.

Reference

- Akonda, A. W. Wetlands of Bangladesh. Gland, Switzerland: International Union for the Conservation of Nature, Worldwide Fund for Nature, International Council for Bird Preservation, International Waterfowl and Wetlands Research Bureau. *A directory of Asian wetlands*, 541–581. (1989).
- Ali, M.M., Anik, M.S.B.M. and Khan, A.H.N. Flood inundation mapping of Jamuna basin floodplain using HEC-RAS 1D/2D coupled model. *3rd International Conference on Advances in Civil Engineering 2016 (ICACE 2016), 21 –23 December 2016, CUET, Chittagong, Bangladesh* (2016).
- Aitken, A. P. Assessing systematic errors in rainfall-runoff models. *Journal of Hydrology*, 20, 121–136 (1973).
- Bagnold, R. A. An approach to the sediment transport problem from general physics. *USGS Numbered Series*, 422(I) (1966).
<https://doi.org/10.3133/pp422I>
- Bárcena, J. F., García-Alba, J., García, A. and Álvarez, C. Analysis of stratification patterns in river-influenced mesotidal and macrotidal estuaries using 3D hydrodynamic modelling and K-means clustering, *Estuarine, Coastal and Shelf Science*, 181, 1-13, ISSN 0272-7714 (2016).
<https://doi.org/10.1016/j.ecss.2016.08.005>.
- Bose, I. and Navera, U.K. Flood Mapping for Dharla River in Bangladesh using HECRAS 1D/2D Coupled Model. *International journal of science and research*, 7(9), 2319-7064 (2018).
- Brammer, H. Floods in Bangladesh: Geographical background to the 1987 and 1988 floods. *Geographic Journal*, 156(1), 12–22 (1990).
- Costabile, P., Costanzo, C., Ferraro, D., Macchione, F. and Petaccia, G. Performances of the New HEC-RAS Version 5 for 2-D Hydrodynamic-Based Rainfall-Runoff Simulations at Basin Scale: Comparison with a State-of-the Art Model. *Water*, 12(9), 2326 (2020).
<https://doi.org/10.3390/w12092326>
- FFWC, BWDB. *Annual flood report 2017*. Flood Forecasting and Warning Centre, Processing and Flood Forecasting Centre, Bangladesh Water Development Board, Dhaka.
<http://www.ffwc.gov.bd>. (2018).
- FFWC, BWDB. *Flood Inundation Map of Bangladesh 2020*. Flood Forecasting and Warning Centre, Processing and Flood Forecasting Centre, Bangladesh Water Development Board, Dhaka.
<http://www.ffwc.gov.bd/index.php/map/inundation-map/bangladesh-today> (2020).
- Fleming, G. *Computer simulation techniques in hydrology*, Elsevier, New York, 18–53, 239–252

- (1975).
- Garde, R. J. and Ranga Raju, K. G. Mechanics of sediment transportation and alluvial stream problems New Delhi, Wiley Eastern Ltd. (1980).
<https://doi.org/10.1177/030913338000400111>
- Halcrow. Jamuna-Meghna River Erosion Mitigation Project. *Draft Inception Report, Vol.1*. Options assessment Halcrow (2002).
- HEC-RAS, Wikipedia, (2021). <https://en.wikipedia.org/wiki/HEC-RAS>
- HEC-RAS user manual, US Army Corps of Engineers (2016).
<https://www.hec.usace.army.mil/software/hec-ras/documentation/HEC-RAS%205.0%20Users%20Manual.pdf>
- Heimann, D. C., Weilert, T. E., Kelly, B. P. and Studley, S. E. Flood Inundation Mapping for the Blue River and Selected Tributaries in Kansas City, Missouri, and Vicinity. *US Geological Survey*, 2015-3008 (2012).
<https://doi.org/10.3133/fs20153008>
- Hicks, F.E. and Peacock, T. Suitability of HEC-RAS for Flood Forecasting. *Canadian Water Resources Journal*, 30(2), 159–174 (2005).
<https://doi.org/10.4296/cwrj3002159>
- Humanitarian Response. *NAWG Monsoon Flood Preliminary Impact and KIN Assessment*, <https://www.humanitarianresponse.info/en/operations/bangladesh/document/nawg-monsoon-flood-pliminary-impact-and-kin20200725> (2020).
- Islam, M.D. and Sado, K. Development of Flood Hazard Maps of Bangladesh Using NOAA-AVHRR Images with GIS. *Hydrological Sciences Journal*, 45(3) (2000).
- Islam, R. Hydrodynamic modeling of Dhaleswari River for dry period flow augmentation, B.Sc. thesis, Submitted to the Department of Water Resources Engineering, Bangladesh University of Engineering & Technology (BUET), Dhaka, Bangladesh (2016).
- Islam, S. *Flooding worsens in Naogaon, dams at risk*. bdnews24.
<https://bdnews24.com/bangladesh/2017/08/17/flooding-worsens-in-naogaon-dams-at-risk#:~:text=Dams%20in%20Naogaon%20have%20given,250%2C000%20people%20in%20the%20district.&text=Floods%20damaged%20at%20least%2050%2C000,fish%20in%20almost%201%2C000%20ponds> (2017).
- Jagers, H. R. A. Modelling Planform Changes of Braided Rivers, ISBN 90-9016879-6 (2003).
- Jahandideh-Tehrani, M., Helfer, F., Zhang, H., Jenkins, G., and Yu, Y.. Hydrodynamic modelling of a flood-prone tidal river using the 1D model MIKE HYDRO River: calibration and sensitivity analysis. *Journal of Environmental Monitoring and Assessment* **192**, 97 (2020).
<https://doi.org/10.1007/s10661-019-8049-0>

- Jarihani, A. A., Callow J. N., McVicar, T.R., Niel, T. G.V. and Larsen, J. R. Satellite-derived Digital Elevation Model (DEM) selection, preparation and correction for hydrodynamic modelling in large, low-gradient and data-sparse catchments. *Journal of Hydrology*, 524, 489-506 (2015).
<https://doi.org/10.1016/j.jhydrol.2015.02.049>
- Kalra, A. and Ahmed, S. Estimating annual precipitation for the Colorado River Basin using oceanic-atmospheric oscillations.. *Water Resources Research*, 48 (6) (2012).
<https://doi.org/10.1029/2011WR010667>
- Khan, D. M. S. M. & Das, P. Assessment of Hydro-Morphological Change of Surma-Kushiyara River System. *Journal of Modern Science and Technology*, 6(1), 113-123 (2018).
- Khattak, M.S., Anwar, F., Saeed, T.U., Sharif, M., Sheraz, K. and Ahmed, A. Floodplain mapping using HECRAS and ArcGIS: a case study of Kabul River. *Arab Journal of Science & Engineering*, 41, 1375–1390 (2016).
<https://doi.org/10.1007/s13369-015-1915-3>
- Kumbier, K., Carvalho, R.C., Vafeidis, A. T. and Woodroffe, C. D. Investigating compound flooding in an estuary using hydrodynamic modelling: a case study from the Shoalhaven River, Australia. *Natural Hazards and Earth System Science*, 18, 463–477 (2018).
<https://doi.org/10.5194/nhess-18-463-2018>
- Leopold, L.B., Wolman, M.G. and Miller, V.P. *Fluvial Processes in Geomorphology*, Freeman and Company, Sanfrancisco, California, U.S.A. (1964)
- Leopold, L.B. and Wolman, M.G. River Channel Patterns: Braided, Meandering and Straight. *U.S. Geological Survey*, Prof. Paper 282-B (1957).
- Logah, F. Y., Amisigo, A. B., Obuobie, E. and Kankam-Yeboah, K. Floodplain hydrodynamic modelling of the Lower Volta River in Ghana. *Journal of Hydrology: Regional Studies*, 14, 1-9, ISSN 2214-5818 (2017).
<https://doi.org/10.1016/j.ejrh.2017.09.002>.
- Mamun, M. The Braiding Indices of the Brahmaputra-Jamuna River. M. Engg. thesis, Submitted to the Department of Water Resources Engineering, Bangladesh University of Engineering & Technology (BUET), Dhaka, Bangladesh (1997).
- Masood, M. and Takeuchi, K. Assessment of flood hazard, vulnerability and risk of mid-eastern Dhaka using DEM and 1D hydrodynamic model. *Natural Hazards*, 61, 757–770 (2012).
<https://doi.org/10.1007/s11069-011-0060-x>
- Mondal, I., Bandyopadhyay, J. and Paul, A.K. Estimation of hydrodynamic pattern change of Ichamati River using HEC RAS model, West Bengal, India. *Modeling Earth System and Environment*. 2, 125 (2016).

<https://doi.org/10.1007/s40808-016-0138-2>

- Mukharjee, M.M. A study on Morphological Behaviors of Brahmaputra-Jamuna River. M.Sc. thesis, Submitted to the Department of Water Resources Engineering, Bangladesh University of Engineering & Technology (BUET), Dhaka, Bangladesh (1995).
- Nash, J. E., and Sutcliffe, J. V. River flow forecasting through conceptual models, part 1: A discussion on principals. *Journal of Hydrology*, 10, 282–290(1970).
- Othman, F., Heydari, M., Sadeghian, M.S., Rashidi, M. and Shahiri Parsa, M. The necessity of systematic and integrated approach in water resources problems and evaluation methods, a review. *Advances in Environmental Biology*, 8(8): 307–315 (2014).
- Parhi, P.K., Sankhua, R.N. & Roy, G.P. Calibration of Channel Roughness for Mahanadi River, (India) using HEC-RAS Model. *Journal of Water Resource and Protection*, 4, 847-850 (2012).
- Parsapour-Moghaddam, P. and Rennie, C.D. Hydrostatic versus nonhydrostatic hydrodynamic modelling of secondary flow in a tortuously meandering river: Application of Delft3D. *Journal of River Research and Applications*, 33(9), 1400-1410 (2017).
<https://doi.org/10.1002/rra.3214>
- Patel, D.P., Ramirez, J.A. and Srivastava, P.K. Assessment of flood inundation mapping of Surat city by coupled 1D/2D hydrodynamic modeling: a case application of the new HEC-RAS 5. *Natural Hazards*, 89, 93–130 (2017).
<https://doi.org/10.1007/s11069-017-2956-6>
- Pathan, A.I. and Agnihotri, P.G. Application of new HEC-RAS version 5 for 1D hydrodynamic flood modeling with special reference through geospatial techniques: a case of River Purna at Navsari, Gujarat, India. *Modeling Earth System and Environment* (2020).
<https://doi.org/10.1007/s40808-020-00961-0>
- Patro, S., Chatterjee, C., Singh, R. and Raghuwanshi, N. S. Hydrodynamic modelling of a large flood-prone river system in India with limited data. *Journal of Hydrological Process*, 23 (19), 2774-2791 (2009).
<https://doi.org/10.1002/hyp.7375>
- Quiroga, V.M., Kure, S., Udo, K. and Mano, A. Application of 2D numerical simulation for the analysis of the February 2014 Bolivian Amazonia flood: Application of the new HEC-RAS version 5. *RIBAGUA Revista Iberoamericana del Agua*, 3, 25–33 (2016).
- Rahman, M. *Bangladesh Needs to Shore up its Flood Defence*. Inter press service.
<http://www.ipsnews.net/2017/09/bangladesh-needs-shore-flood-defence/> (2017).

- Rahman. Modeling Flood Inundation of the Jamuna River. B.Sc. Thesis. Submitted to the Department of Water Resources Engineering, Bangladesh University of Engineering & Technology (BUET), Dhaka, Bangladesh (2015).
- Rahman, A., Zafor, M.A., and Kar, S. Analysis and comparison of surface water quality parameters in and around Dhaka City. *International journal*, 3(2), 7-15 (2012).
- Sabol, G.V. and Nordin, C.F. Dispersion in rivers as related to storage zones, *Journal of the Hydraulics Division* (1978)
- Sandbach, S.D., Nicholas, A.P., Ashworth, P.J., Best, J.L., Keevil, C.E., Parsons, D.R., Prokocki, E.W. and Simpson, C.J. Hydrodynamic modelling of tidal-fluvial flows in a large river estuary, *Estuarine, Coastal and Shelf Science*, 212, 176-188, ISSN 0272-7714 (2018). <https://doi.org/10.1016/j.ecss.2018.06.023>.
- Schumm, S.A. and Khan H.R. Experimental Study of Channel Patterns, *Geological Society of American Bulletin*, 83, 1755-1770 (1977).
- Shaad, K., Ninsalam, Y., Padawangi, R., and Burlando, P. Towards high resolution and cost-effective terrain mapping for urban hydrodynamic modelling in densely settled river-corridors, *Sustainable Cities and Society*, 20, 168-179, ISSN 2210-6707 (2016). <https://doi.org/10.1016/j.scs.2015.09.005>.
- ShahiriParsa, A., Noori, M., Heydari, M. and Rashidi, M. Floodplain zoning simulation by using HEC-RAS and CCHE2D models in the Sungai Maka River. *Air, Soil Water Research* , 9, 55 (2016). <https://doi.org/10.4137/ASWR.S36089>
- Shampa. Dynamics of Bar in the Braided River Jamuna. M.Sc. thesis, Submitted to the Department of Water Resources Engineering, Bangladesh University of Engineering & Technology (BUET), Dhaka, Bangladesh (2015).
- Simons, D.B. and Senturk, F. Sediment Transport Technology. Water Resources Publications Fort Collins, Colorado, 80522, U.S.A., 24-72 (1971).
- Sultana, P. and Thompson, P. Livelihoods in Bangladesh Floodplains *Oxford Research Encyclopedias*. Oxford University Press (2017).
- Timbadiya, P.V., Patel, P.L. and Porey, P.D. Calibration of HEC-RAS Model on Prediction of Flood for Lower Tapi River, India. *Journal of Water Resource and Protection*, 3, 805-811 (2011). [10.4236/jwarp.2012.410098](https://doi.org/10.4236/jwarp.2012.410098)
- Timbadiya, P. V., Patel, P. L. and Porey, P. D. One-dimensional hydrodynamic modelling of flooding and stage hydrographs in the lower Tapi River in India. *Journal of Current Science*, 106(5), 708-716 (2014).
- Tran Anh, D., Hoang, L.P., Bui, M.D. and Rutschmann, P. Simulating Future Flows and Salinity Intrusion Using Combined One- and Two-Dimensional Hydrodynamic Modelling—The Case of Hau River, Vietnamese Mekong Delta. *Water*, 10(7), 897 (2018).

<https://doi.org/10.3390/w10070897>

UKessays. The Importance Of Flood Inundation Modeling Environmental Sciences Essay. <https://www.ukessays.com/essays/environmental-sciences/the-importance-of-flood-inundation-modeling-environmental-sciences-essay.php> (2018)

Vu, T. T., Nguyen, P. K. T., Chua, L. H. C. and Law, A. W. K. Two-dimensional hydrodynamic modelling of flood inundation for a part of the Mekong River with TELEMAC-2D. *British Journal of Environment and Climate Change*, 5(2), 162-175 (2015).

Wester, S. J., Grimson, R., Minotti, P. G., Booij, M. J. and Brugnach, M. Hydrodynamic modelling of a tidal delta wetland using an enhanced quasi-2D model. *Journal of Hydrology*, 559, 315-326, ISSN 0022-1694 (2018).
<https://doi.org/10.1016/j.jhydrol.2018.02.014>.

Wikipedia. *Atrai River*. https://en.wikipedia.org/wiki/Atrai_River (2021)

Worldometer. *World Population Prospects: The 2019 Revision. United Nations*, <https://www.worldometers.info/world-population/bangladesh-population/#:~:text=Bangladesh%20population%20is%20equivalent%20to,3%2C277%20people%20per%20mi2> (2020).

WWAP. *UN world water development report*. World Water Assessment Programme WWAP. Paris (2006).

Xia, X., Liang, Q. and Ming, X. A full-scale fluvial flood modelling framework based on a high-performance integrated hydrodynamic modelling system (HiPIMS), *Advances in Water Resources*, 132, 103392, ISSN 0309-1708 (2019)
<https://doi.org/10.1016/j.advwatres.2019.103392>.

Zainalfikry, M.K., Ab Ghani, A., Zakaria, N.A., Chan, N.W. HEC-RAS One-Dimensional Hydrodynamic Modelling for Recent Major Flood Events in Pahang River. *Mohamed Nazri F. (eds) Proceedings of AICCE'19. AICCE 2019. Lecture Notes in Civil Engineering, vol 53. Springer, Cham* (2020).
https://doi.org/10.1007/978-3-030-32816-0_83